NUREG/CR-3426
EPRI NP-3802
Creare TN-384
Vol. 1

Thermal and Fluid Mixing in 1/2-Scale Test Facility

Facility and Test Design Report

Prepared by F. X. Dolan, J. A. Valenzuela

Creare Incorporated

Prepared for
U.S. Nuclear Regulatory Commission

and
Electric Power Research Institute

and
Creare Incorporated

NUREG/CR-3426
EPRI NP-3802
Creare TN-384
Vol. 1
R4

Thermal and Fluid Mixing in 1/2-Scale Test Facility

Facility and Test Design Report

Manuscript Completed: January 1985
Date Published: September 1985

Prepared by
F. X. Dolan, J. A. Valenzuela

Creare Incorporated
Etna Road
Hanover, NH 03755

Prepared for
Division of Accident Evaluation
Office of Nuclear Regulatory Research
U.S. Nuclear Regulatory Commission
Washington, D.C. 20555
NRC FIN A4070

and
Electric Power Research Institute
3412 Hillview Avenue
Palo Alto, CA 94303

and
Creare Incorporated
Etna Road
Hanover, NH 03755

Title Page

ABSTRACT

This report describes the test facility and program designed to measure fluid mixing and heat transfer in a 1/2-scale model of the cold leg downcomer and lower plenum of a pressurized water reactor under conditions of interest to the issue of pressurized thermal shock. Several cold leg assemblies are modeled and the downcomer arrangement can be altered to match vendor-specific configurations. The facility can be operated to model flow rates based on Froude number of the injected flow in the cold leg and with steady or transient inlet boundary conditions. Extensive instrumentation is provided to measure flow rates, temperatures and pressure at the facility boundaries and for detailed measurements of temperature, velocity and heat transfer data in the cold leg and downcomer models. The test data are monitored and recorded by a computer data acquisition system that is also used for post-test data reduction and plotting.

The planned test matrix includes 75 tests with variations in cold leg and downcomer geometries, loop and HPI flow rates, cold leg Froude number and loop to HPI density difference. Test results will be reported in a series of quick look reports.

ACKNOWLEDGEMENTS

The authors of this report acknowledge the valuable contributions made to the design of this test project by the plant owners and vendors through their input to EPRI, and by the technical consultants of the NRC Advanced Code Review Group. The several scaling and design reviews conducted by Dr. Jean-Pierre Sursock of EPRI and Dr. Novak Zuber of NRC were extremely effective in achieving wide input and verification of the approaches taken in this project. We are also grateful to Dr. Jose Reyes and Dr. Avtar Singh for their effective project management and their technical support in reviewing the data.

Much of the basis of this facility and project design is derived from small scale flow visualization studies sponsored by EPRI during 1981 and 1982; we acknowledge the foresight and technical contributions of Dr. Bill K. H. Sun, Project Manager, in establishing this essential early data base.

Many people at Creare also made significant contributions to the overall experimental program. Mike Hall was responsible for the test facility design with major design and construction support from Frank LeBlanc, Harold Clark, Mario Langsten and John White. Instrumentation system design and development were carried out by Tom Tantillo. Norm Williams fabricated many of the special purpose instruments and Bob Eccher designed and built the data acquisition system. Computer programming for data acquisition and data reduction and reporting was done by Judy Durant. Becky Cummings performed the data reduction. This report was prepared by Beverly Brooks and Leann Cushman with figures drafted by John Wickman. Their efforts are greatly appreciated.

CONTENTS

TABLE OF CONTENTS (CONTS.)

LIST OF TABLES

LIST OF FIGURES

NOMENCLATURE

A	area, m^2
a	coefficient in Eq. 5.1
D	diameter, m
E	error term
F_{CL}	HPI Froude number (dimensionless), Equation 4.1
g	acceleration due to gravity, m/s^2
g_c	dimensional proportionality constant, $kg\text{-}m/N\text{-}s^2$
H	head (pressure), m
h	heat transfer coefficient $W/m^2\text{-}°c$ or specific enthalpy, J/k_g
j	superficial velocity, m/s
k	thermal conductivity, $W/m\text{-}°c$
K	velocity probe pressure coefficient
L	length, m
P	pressure, Pa
q''	wall heat flux, W/m^2
Q	volumetric flow rate, m^3/s
t	time, s
T	temperature, °c
V	velocity, m/s or voltage, v
X	distance, m
α	thermal diffusivity, m^2/s
Δ	differential
Γ	sum of system component volumes, m^3
$\Delta\rho/\rho$	dimensionless density ratio $(\rho_H\text{-}\rho_L/\rho_H)$
ρ	density, kg/m^3
τ	mixing time, s
ν	kinematic viscosity, m^2/s
λ_n	eigen values, Eq. 5.14

SUBSCRIPTS

a	see Eq. 3.6
CL	refers to cold leg
c	see Eq. 3.6
DC	refers to downcomer
f	fluid or final (in context)
H	HPI flow
i	index
L	loop flow
lm	see Eq. 3.6
m	mixed-mean
o	initial value
p	see Eq. 3.6
pm	see Eq. 3.6
q	quench front
r	see Eq. 3.6
s	static, steady-state or surface (in context)
sp	see Eq. 3.6

T	total
TS	refers to thermal shield
V	vent flow
w	wall
ΔT	temperature differential
ΔX	wall thickness

SUMMARY

This report describes the test facility and program designed to measure fluid and thermal mixing of high pressure injection (HPI) water in 1/2-scale models of the cold leg, downcomer and lower plenum of a pressurized water reactor. A companion report (Volume 2) discusses data from two transient cool down tests conducted in this facility during May 1984. This experimental project is being carried out at Creare under the joint sponsorship of U.S. Nuclear Regulatory Commission (NRC) and the Electric Power Research Institute (EPRI).

The test facility is designed for operation at 1.38 MPa (200 psia) with loop and HPI flows covering ranges of interest to the issue of pressurized thermal shock. Several different cold leg assemblies and safety injection lines are modeled, to simulate configurations for Westinghouse, Combustion Engineering and Babcock & Wilcox. The downcomer has thick metal walls to provide data on wall to fluid heat transfer. A thermal shield can be installed in the downcomer for some tests and the downcomer has ports to simulate vent flow for tests of the Babcock & Wilcox configuration. A lower plenum is attached to the bottom of the downcomer, replicating the reactor geometry. The support facility includes water storage tanks, heating and cooling systems, pumps, flow meters and control valves needed to establish the required initial conditions and to run tests of sufficient duration to achieve steady fluid temperature throughout the test vessel. Prescribed loop flow rate transients can also be simulated.

Test measurements include flow rates, temperatures and pressures at the boundaries of the 1/2-scale model facility to characterize the test conditions, plus over 300 local measurements of temperature, flow velocity and wall-to-fluid heat transfer within the cold legs, downcomer and lower plenum. Test data are recorded from all instruments simultaneously on a computer-based data acquistion system for the duration of each test.

The planned test matrix includes 75 tests - 66 with steady inlet boundary conditions, and 9 with transient inlet boundary conditions. Variables in the test matrix are the cold leg and downcomer geometry combinations, loop, vent and HPI flow rates, HPI Froude number and initial loop to HPI density difference.

Results of the tests will be reported in quick look reports that will describe the geometry and instrumentation for that test and will display the data in tabular and graphical formats.

The test program is being conducted under Quality Assurance procedures which make the data available for use in plant licensing decisions.

1. INTRODUCTION

This report describes a testing project which measures the thermal mixing of HPI water in a model of the cold leg, downcomer and lower plenum of a pressurized water reactor. The data will be useful to assess the applicability of existing thermal mixing and heat transfer models and to develop additional models if needed. The test program is being carried out by Creare Incorporated with joint sponsorship by the Electric Power Research Institute (EPRI), and the U.S. Nuclear Regulatory Commission (NRC).

In this section, we present the background of the problem under investigation and the objectives of the testing project. Section 2 describes the test facility design including a discussion of the basis for the selection of the test geometry (cold legs, downcomer and lower plenum) and describes the capabilities of the support test facility. Section 3 provides a detailed discussion of the test measurements and facility instrumentation. The plans and procedures for conducting the tests are presented in Section 4, including possible test matrices, procedures for establishing and controlling steady-state conditions, and data acquisition procedures. Finally, Section 5 describes the data reduction procedures including conversion of raw data to engineering units, data display methods and plans for presenting test data in quick look reports.

1.1 BACKGROUND

During certain loss-of-coolant accidents or cooling transients in pressurized water reactors, cold water is injected at high pressure into the primary coolant system. Theoretical models and data are being developed to determine the potential for thermal shock and fracture of the reactor vessel under the combination of the following adverse conditions:

1. a reactor vessel material with a very large degree of radiation embrittlement,

2. a crack in the embrittled material of sufficient size to propagate,

3. the presence of extremely cold water cascading by the belt line region of the vessel,

4. sufficient heat transfer to produce high induced thermal stresses, and

5. repressurization of the primary system following the thermal shock.

EPRI has carried out an extensive program underway (1) to address the pressurized thermal shock issues. Creare has performed 5 earlier experimental studies (2 - 8) of fluid thermal mixing in the cold leg and downcomer of transparent models of pressurized water reactors at 1/5 of reactor scale. Those tests investigated the effects of

facility geometry (loop seal and cold leg geometry, injector type and location, presence of annulus thermal shield, and lower plenum geometry) and operating conditions (vent valve flow, loop and HPI flow rates, and fluid density differences) on the location and degree of fluid mixing. Temperature measurements in the cold leg and downcomer and flow visualization showed substantial mixing of the HPI flow with the loop flow or with the stagnant loop water.

The USNRC is currently sponsoring a comprehensive program to evaluate the likelihood, consequences and risk of various PTS events for three nuclear power plants. A detailed method of performing such plant specific analyses is being developed in order to provide appropriate quidance to the nuclear industry. This work is the coordinated analysis effort of four national laboratories (ORNL, INEL, LANL, and BNL). The program also includes fracture mechanics and thermal hydraulic experimentation at ORNL, Purdue University and Creare Incorporated. The Creare 1/2-scale experiments described in this report have provided valuable heat transfer data for the assessment of predictive models being developed and applied in NRC's PTS evaluation programs (9-13).

The present experimental project provides large-scale data to support further analysis of the thermal mixing phenomena in the cold leg and downcomer and heat transfer from the vessel and core walls to the fluid in the downcomer. The tests are conducted at larger scale (1/2 of prototypical vessel and cold leg dimensions) and at greater loop to HPI flow temperature differences (up to about 2/3 of the temperature difference at reactor conditions of significance to pressurized thermal shock) than in the earlier studies. The facility also includes the effects of heated walls and is extensively instrumented.

1.2 PROJECT OBJECTIVES

The principal objectives of this testing project are to:

1. Provide experimental steady-state and transient data on thermal mixing in cold leg and downcomer geometries due to safety injection for

   - phenomenological understanding of thermal mixing
   - development of heat transfer correlations and thermal mixing models
   - computer code assessment

2. Provide scaling rationale to apply data to reactor conditions

3. In conjunction with EPRI, NRC and their contractors develop, assess and improve turbulent mixing models in computer codes.

As a major part of the effort to accomplish these objectives, a testing project has been undertaken. That test project is the only subject of this report.

Based on a scaling analysis, a test facility has been designed and fabricated to model prototypical features of several cold leg geometries, locations and types of injectors, downcomer geometry and internals (thermal shield, baffles, vent valves) and lower plenum geometry. Tests can be conducted over a range of loop, HPI and vent valve flow rates and loop to HPI fluid density differences to permit extrapolation of test data to the full-scale safety injection transients. A measurement system is available to record temperatures and fluid velocities in the cold leg, loop seal, downcomer and lower plenum, and wall-to-fluid heat transfer rates in the downcomer.

1.3 EXPECTED RESULTS

The results of this testing project will be data on the temperatures and velocities in the 1/2-scale model cold legs and downcomer, and wall-to-fluid heat transfer in the downcomer, for a range of steady-state and transient test conditions. It is expected that these test data will cover a range of conditions and be reported in such a way as to be useful to verify the applicability of existing models and correlations of thermal mixing and heat transfer during safety injection transients, or to develop new models if necessary.

The facility includes capabilities for:

1. tests to establish baseline data for prototypical conditions

2. tests to display the major parameter sensitivity and assist in the development of heat transfer correlations

3. transient tests simulating various cooldown scenarios.

The output from the tests will be displayed as plots of temperature, velocity, heat flux and wall-to-fluid differential temperature as functions of time and position. Test conditions such as flow rates, loop and vent flow temperatures and HPI temperature, will be displayed in tables.

2. TEST FACILITY DESIGN

A major task in this program was the design and construction of a facility, including 1/2-scale models of prototypical loop seals, pumps, cold legs and downcomer geometries, for conducting the steady-state and transient tests. In this section we review the design basis for the test facility and describe the design and capabilities of the test geometries and support facility.

2.1 FACILITY DESIGN BASIS

The basic design specifications for the test facility were defined (14) and updated following the Design Review meeting in September 1982.

1. Test geometries which are 1/2-scale representations of prototypical pressurized water reactor components:
   a) cold legs of Combustion Engineering, Babcock & Wilcox and Westinghouse designs, including loop seals and pump simulators,
   b) high pressure injection ports for the above cold legs,
   c) a 90° planar sector of a reactor vessel downcomer, including one cold leg from a plant having 4 cold legs, and
   d) a lower plenum having a correctly scaled volume and internal flow baffles

2. Test vessel pressure limit of 1.38 MPa (200 psia)

3. Thermally thick walls to study heat transfer rates

4. Replication of all geometric features that bear significantly on thermal mixing or heat transfer for all pressurized water reactors

5. Capability to add a thermal shield in the downcomer

6. Two different cold leg configurations (horizontal and inclined)

7. Multiple injection locations for each cold leg

8. Steady-state and transient testing capability

9. Extensive instrumentation summarized below:
   a) 90 thermocouples in the cold leg and loop seal (at least 10 with fast response)
   b) 71 thermocouples in the downcomer centerline
   c) 40 thermocouples in the downcomer, near the walls
   d) 40 thermocouples on the downcomer wall surfaces
   e) 40 heat flux sensors in the downcomer
   f) 20 locations for velocity probes in the cold leg to measure radial velocity distributions at several axial locations

g) 20 locations for velocity probes in the downcomer to measure velocities on the centerline and near the walls
h) 15 thermocouples in the downcomer below the cold leg nozzle center-line to measure gapwise temperature distribution
i) 5 thermocouples in the lower plenum

10. Additional process instruments to monitor loop pressure, loop, HPI and vent valve flows and temperatures installed throughout the loop as required in order to establish and control steady-state and transient test conditions.

A scaling analysis (15) was conducted of the mixing of HPI water in the cold leg and downcomer of a pressurized water reactor under conditions of importance to the issues of pressurized thermal shock. The scaling analysis, which considers analytical and empirical evaluations of the heat transfer and fluid dynamic aspects of the problem, was used to aid in the design of the test geometries and test matrix and to define the requirements for the support facility. An abbreviated summary of the scaling approach is given below:

1. Geometric similarity
   a) all ratios of flow path physical dimensions and all angles will be preserved
   b) the model size scale will be 1/2

2. Kinematic similarity -- all ratios of boundary velocities will be preserved

3. Dynamic similarity
   a) Froude scaling will be emphasized
   b) Froude number will be preserved
   c) Reynolds number will also be preserved in special tests
   d) Froude and Reynolds numbers cannot be simultaneously preserved

4. Thermal similarity
   a) temperature difference ($T_L - T_H$) will be varied over a factor of three range extending up to about 60% of prototype
   b) density ratio will be varied over a factor of four range extending up to about 50% of prototype
   c) vessel wall thickness of at least 50.8 mm (2 in.) will provide applicable data for heat transfer coefficient h and fluid temperature T for three periods
      - o h, T for early transient, t<100 s
      - o h, T for conduction-limited transient, 100s<t<400s
      - o T for steady adiabatic period, t>400s

2.2 TEST GEOMETRY DESIGN

Typical reactor dimensional information was supplied by Babcock & Wilcox (B&W), Westinghouse (W) and Combustion Engineering (CE). That data was used to develop a composite geometry for the downcomer with

accommodations for vent valves and a horseshoe baffle (to be used only in tests of B&W designs), three cold leg geometries including loop seals and pump simulators, and a thermal shield for use with the W/CE designs.

Because the geometry data is proprietary to the vendors, it is not displayed here. However, the information supplied to us has been verified with the vendors and has been checked by the Program Management Group (PMG). Also, the logic used to develop the composite and the model from that composite has been discussed with the PMG.

The basic criteria used to develop the composite geometry and the model are as follows:

1. The cold legs are approximately 1/2-scale representations of typical designs from W and CE (horizontal configuration) and from B&W (inclined) with accommodations for various injectors and injector locations.

2. The cold leg nozzles are approximately 1/2-scale for each of the cold leg designs.

3. For the model, the cold leg diameter is based on available commercial pipe and fittings which most nearly match the prototype diameters at 1/2-scale and which meet the needs for the pressure boundary design. The diameter ratio between the model pipe and the prototype is a main scale factor for each prototype.

4. All cold leg and nozzle angles are preserved.

5. The downcomer width represents the unwrapped length at 1/2-scale of a 90° sector of a typical reactor at the mid-gap radius, and includes one cold leg nozzle. The intent is to represent one typical sector of a plant having four cold legs.

6. Within the sector, the cold leg is located in a typical manner consistent with the so-called "60°- 120°" layout of plants with four cold legs.

7. Major geometries within the sector are modeled; for example, the downcomer includes the blockage of 1/2 of a hot leg.

8. The downcomer is designed to include certain special features such as the vent valves and baffle of a B&W plant, and a typical thermal shield, all at about 1/2-scale. These are inserted or removed as needed for specific geometries.

9. The vent lines are sized at approximately 1/2-scale using available steel pipe or tubing.

10. The downcomer is approximately 1/2-scale of a typical reactor gap and the walls are smooth without steps as in some plants.

In the following subsections, we discuss some of the features of these components of the facility design.

2.2.1 Downcomer and Lower Plenum

Several views of the basic downcomer geometry are shown in Figure 2-1. The width W is based on the mid-gap length of a 90° sector from a prototypical reactor at a scale factor of about 1/2. The height of the downcomer above the cold leg nozzle centerline Z_1 provides a properly scaled upper downcomer to accommodate the vent flow when the vent valves are used for a B&W-representative test series.

Dimensions for the downcomer gap S and the length from the centerline of the nozzle location to the bottom of the downcomer Z_2 are also based on prototype geometry at a scale factor of 1/2; the length being modeled is to the bottom of the reactor core barrel. The thermal shield thickness t_s and length L_s are based on the same prototype reactor data at a scale factor of 1/2, and the width matches the full internal width of the downcomer.

The location of the top of the thermal shield below the nozzle centerline Z_s is selected as the higher of two prototype thermal shield elevations. This maximizes the effect of the thermal shield for comparison with tests not having the shield in place, and the dimensionless location Z_s/D_{CL} is close to that in earlier 1/5-scale tests (5).

The hot leg blockage, the size and locations of the vent valve nozzles, and the size and location of the horseshoe baffle are based on the B&W data, at the same scale factor used for the downcomer width.

Table 2-1 lists the characteristic dimensions of the downcomer geometry shown in Figure 2-1. The dimensions are normalized by gap thickness S and cold leg diameter D_{CL} and they are compared with the equivalent dimensions from the 1/5-scale models also tested at Creare (2, 3, 5).

Access to the interior of the downcomer is provided in order to install the horseshoe baffle for the B&W tests, and to install and remove the thermal shield.

The downcomer vessel and core barrel walls are fabricated from carbon steel plate (SA 516-70) having a nominal thickness of 70 mm (2.75 in.). A vessel with at least 50.8 mm (2 in.) inch thick walls will:

1. Accurately simulate the convection limited period.

2. Simulate and respond to the surface conditions during the conduction limited period (i.e., provide data for wall temperature, T and wall to fluid heat transfer coefficient, h).

3. Cool fast enough to provide an adiabatic period in tests of acceptable duration.

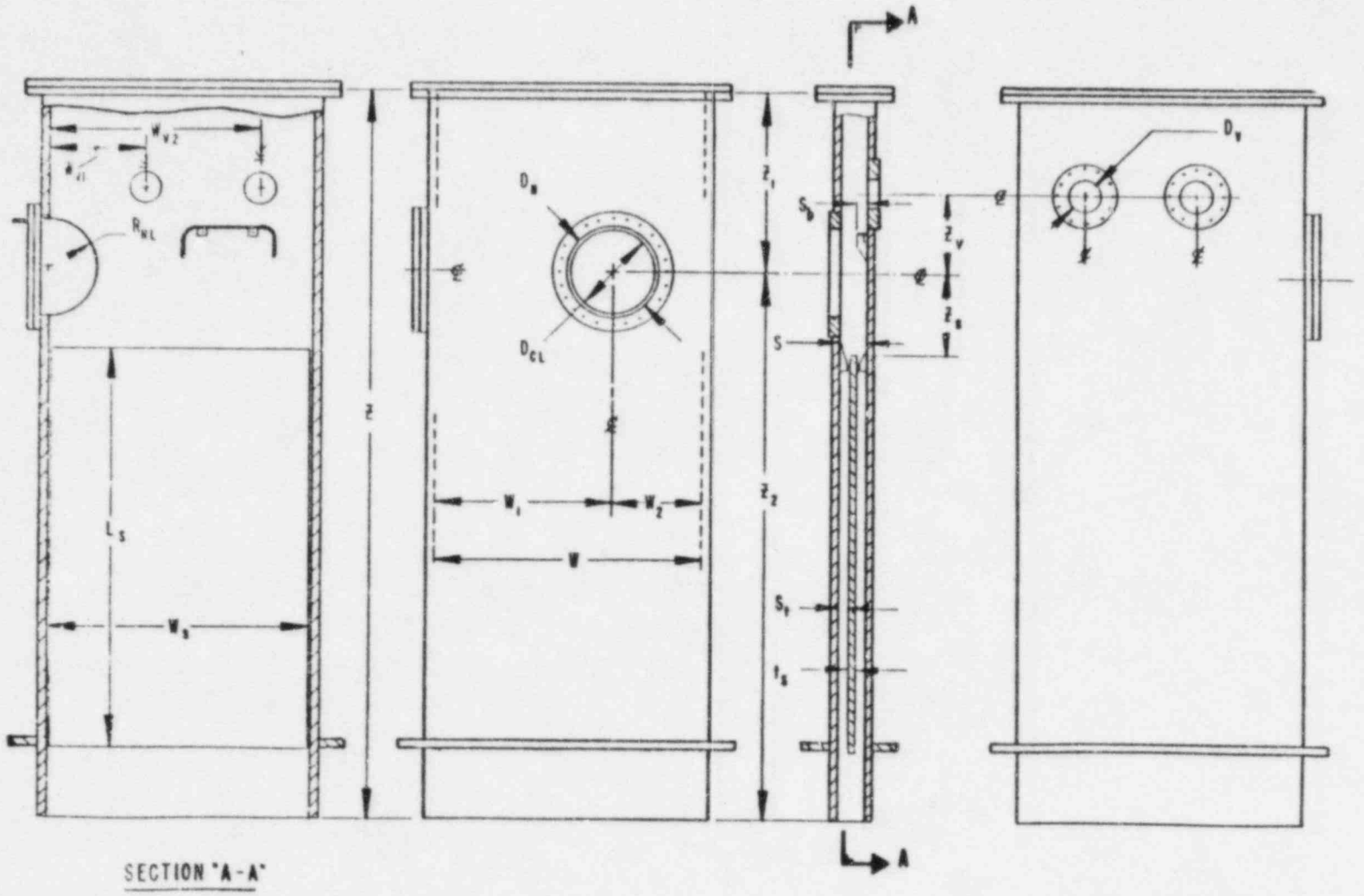

Figure 2-1. Downcomer Model Major Dimensions

Table 2-1 DOWNCOMER CHARACTERISTIC DIMENSIONS

Parameter	Name	1/2-Scale	1/5-Scale (No Thermal Shield) (Ref. 1.2,1.3)	1/5-Scale (Thermal Shield) (Ref. 1.5)
D_{CL}	Cold Leg Diameter	363.5 mm (14.31 in.)	142.9 mm (5.625 in.)	142.9 mm (5.625 in.)
S	Gap	137.2 mm (5.4 in.)	50.8 mm (2.0 in.)	46.2 mm (1.82 in.)
D_N/D_{CL}	Ratio of Cold Leg Nozzle Diameter to Cold Leg Diameter			
	a) Horizontal	1.26	1.33	1.33
	b) Inclined	1.31	1.31	-
D_V/D_{CL}	Ratio of Vent Valve Diameter to Cold Leg Diameter	0.49	0.51	-
L_S/D_{CL}	Ratio of Thermal Shield Length to to Cold Leg Diameter	6.70	-	5.91
R_{HL}/D_{CL}	Ratio of Hot Leg Radius to Cold Leg Diameter	0.76	1.03	1.03
S_b/S	Ratio of Horseshoe Baffle Thickness to Gap	0.53	-	-
S_t/S	Ratio of Thermal Shield Spacing to Gap	0.43	-	0.43
t_s/S	Ratio of Thermal Shield Thickness to Gap	0.28	-	0.27
W/D_{CL}	Ratio of 90° Planar Sector Width to Cold Leg Diameter	4.45	4.44	4.36
W_1/D_{CL}	Dimensionless Cold Leg Nozzle Location	2.97	2.95	2.90
W_2/D_{CL}	Dimensionless Cold Leg Nozzle Location	1.48	1.50	1.45
W_S/D_{CL}	Ratio of Thermal Shield Width to Cold Leg Diameter	4.45	-	4.31
W_{V1}/D_{CL}	Dimensionless Vent Valve Location	1.63	1.63	-
W_{V2}/D_{CL}	Dimensionless Vent Valve Location	2.81	3.48	-
Z/D_{CL}	Ratio of Downcomer Length to Cold Leg Diameter	12.21	10.40	10.31
Z_1/D_{CL}	Ratio of Downcomer Length Above Cold Leg Centerline to Cold Leg Diameter	3.00	2.55	2.51
Z_2/D_{CL}	Ratio of Downcomer Length Below Cold Leg Centerline to Cold Leg Diameter	9.20	7.85	7.80
Z_S/D_{CL}	Normalized elevation of top of thermal shield	1.25	-	1.24
Z_V/D_{CL}	Normalized elevation of vent valve centerlines	1.35	1.42	-

The rationale for the selection of a minimum wall thickness is discussed in greater detail in the scaling analysis report (15).

The downcomer is terminated with the lower plenum shown in Figure 2-2. This design is similar to the lower plenum used in tests at 1/5-scale (6). On theoretical grounds the lower plenum might be expected to affect the mixing response because it provides a large volume of hot fluid that can communicate with the downcomer (16). Therefore, a lower plenum is included to provide data for comparisons with 1/5-scale tests and to provide a realistic simulation of the volumes and volume distribution in a prototypical reactor.

The basic criteria used to design the lower plenum were:

1. A volume of about 60 to 70% of the downcomer volume, typical of the lower range of lower plenum volume in full-scale reactor geometries.

2. The radius of curvature and depth of the lower plenum approximately 1/2-scale of prototype geometries.

3. A flow boundary at the exit of the lower plenum to produce nominally uniform, vertical upflow, simulating the flow into the core region of reactors.

The lower plenum geometry that satisfies these design requirements consists of a pie-shaped sector of a semi-cylinder situated inside a pressure vessel that also supports the downcomer. The circular arc surface of the lower plenum provides a reasonable simulation of the curvature of a reactor lower head, while the side and end walls limit the active volume of the lower plenum. The volume contained in the lower plenum is approximately 60% of the total downcomer fluid volume and 70% of the downcomer fluid volume when the thermal shield is in place.

Flow enters the lower plenum from the downcomer and is discharged from the lower plenum upward through a horizontal perforated plate which serves as a flow distributor. From there the flow exits through a 102 mm (4 in.) diameter pipe connection at the top of the pressure vessel. A second connection on the bottom of the pressure vessel is used to circulate water through the "hot well" volume surrounding the lower plenum simulator both during the pre-test heatup period and during the cooldown transients. This circulated water provides a nearly adiabatic boundary for the lower plenum thereby minimizing energy loss from the lower plenum during a test.

A perforated plate is also provided at the inlet to the lower plenum, directly below the bottom of the "core wall", to simulate the "flow skirt" typical of one vendor's design. The hole size (35 mm) and percent open area (50%) are based on the full scale design to provide a similar pressure drop characteristic. The perforated plate can be removed for those tests where this flow skirt is not appropriate.

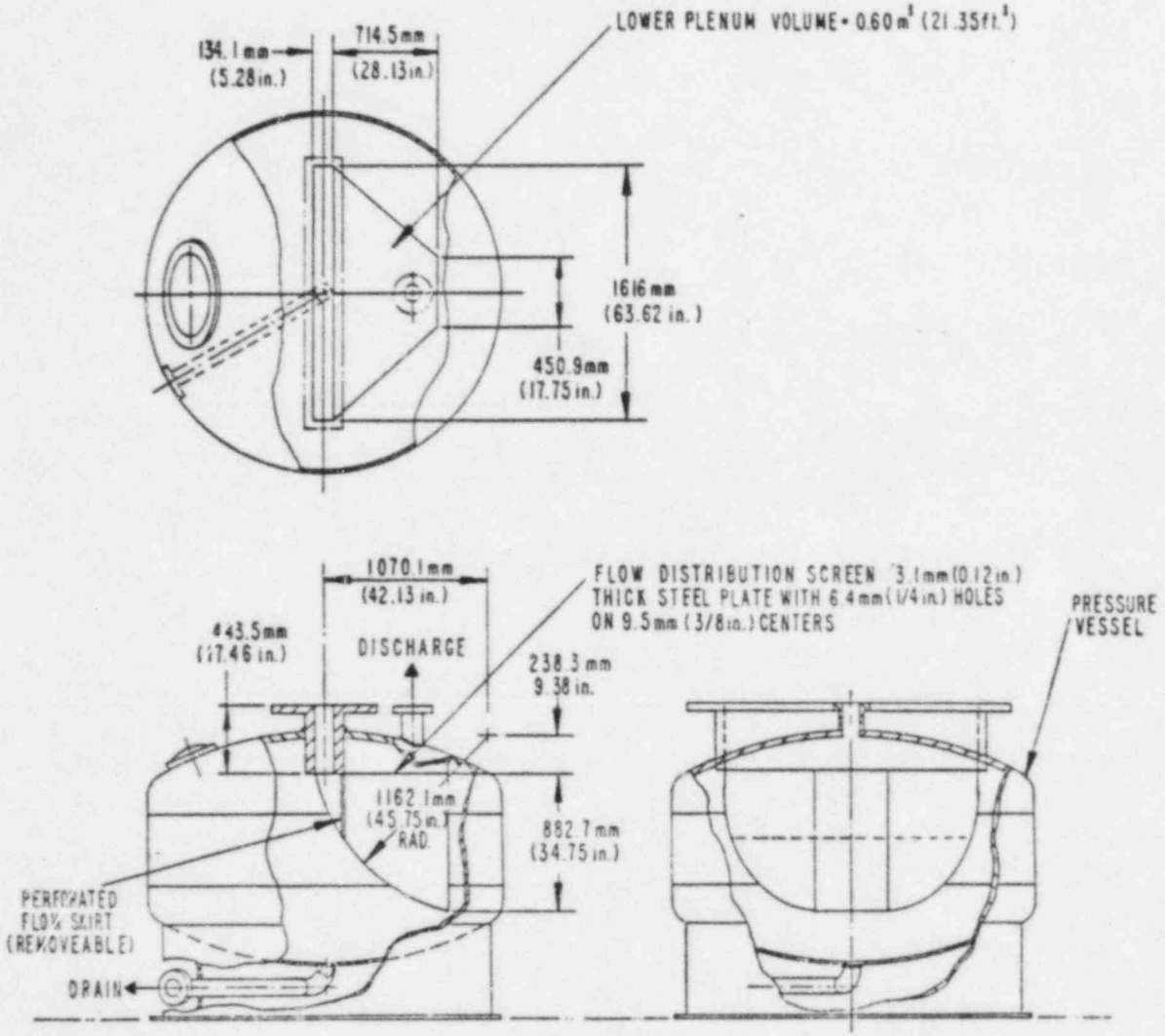

Figure 2-2. Lower Plenum Simulator

2.2.2 Cold Leg Assemblies

Three complete cold leg assemblies were designed for the test facility. Each assembly consists of the following components:

1. loop seal piping at the pump inlet,
2. reactor coolant pump (RCP) simulator,
3. cold leg piping with injector nozzles,
4. cold leg reactor vessel nozzle

Schematics of the assemblies are shown in Figures 2-3, 2-4 and 2-5, representing designs at approximately 1/2-scale for each of the pressurized water reactor vendors.

Two types of cold legs are available for this test facility. One simulates a cold leg which lies wholly in a horizontal plane between the reactor coolant pump (RCP) discharge and the nozzle, typical of W and CE geometries. The other cold leg simulates a typical lowered-loop B&W design, having an inclined section (sloping down toward the reactor) between the RCP and nozzle. The horizontal cold leg is installed to have nominally zero slope between the pump and nozzle.

Both cold leg designs employ commercial steel pipe and fittings having a nominal inside diameter of 363.5 mm (14.31 in). This is about 1/2-scale for the prototype W/CE and B&W cold legs. The cold leg lengths are based on the diameter scale factors.

The safety injection locations are shown on the cold leg assembly drawings. Five different injectors are provided (noted as B through F), covering sizes, orientations and locations which are typical of plant conditions. Several of the injectors shown are similar to those used in earlier thermal mixing tests (2 and 3) and will provide data for comparison between two scales. The HPI nozzle diameters (indicated on the cold leg assembly figures) are based on the scale factor for each cold leg and the vendor-specific HPI line sizes, and selecting the closest available commercial steel pipe or mechanical tubing. Each injector has a minimum of 10 pipe diameters of straight length (10 L/D) between the isolation valve and its penetration in the cold leg.

The cold leg nozzle geometries are shown in Figure 2-6. Note that there are two nozzle configurations to match the characteristics of the W/CE and B&W designs. The length of the nozzle expansion section and the expansion angles are different, and the B&W nozzle has a circular arc lip at the discharge into the downcomer whereas the W/CE design has a straight discharge. Each nozzle attaches directly to the downcomer vessel wall through a bolting arrangement.

Earlier testing at 1/5-scale has shown the importance of the added volume of the loop seal and pump to decreasing the rate of cooling in the downcomer (6). In the 1/2-scale test facility, loop seals and pump simulators are part of the cold leg assemblies.

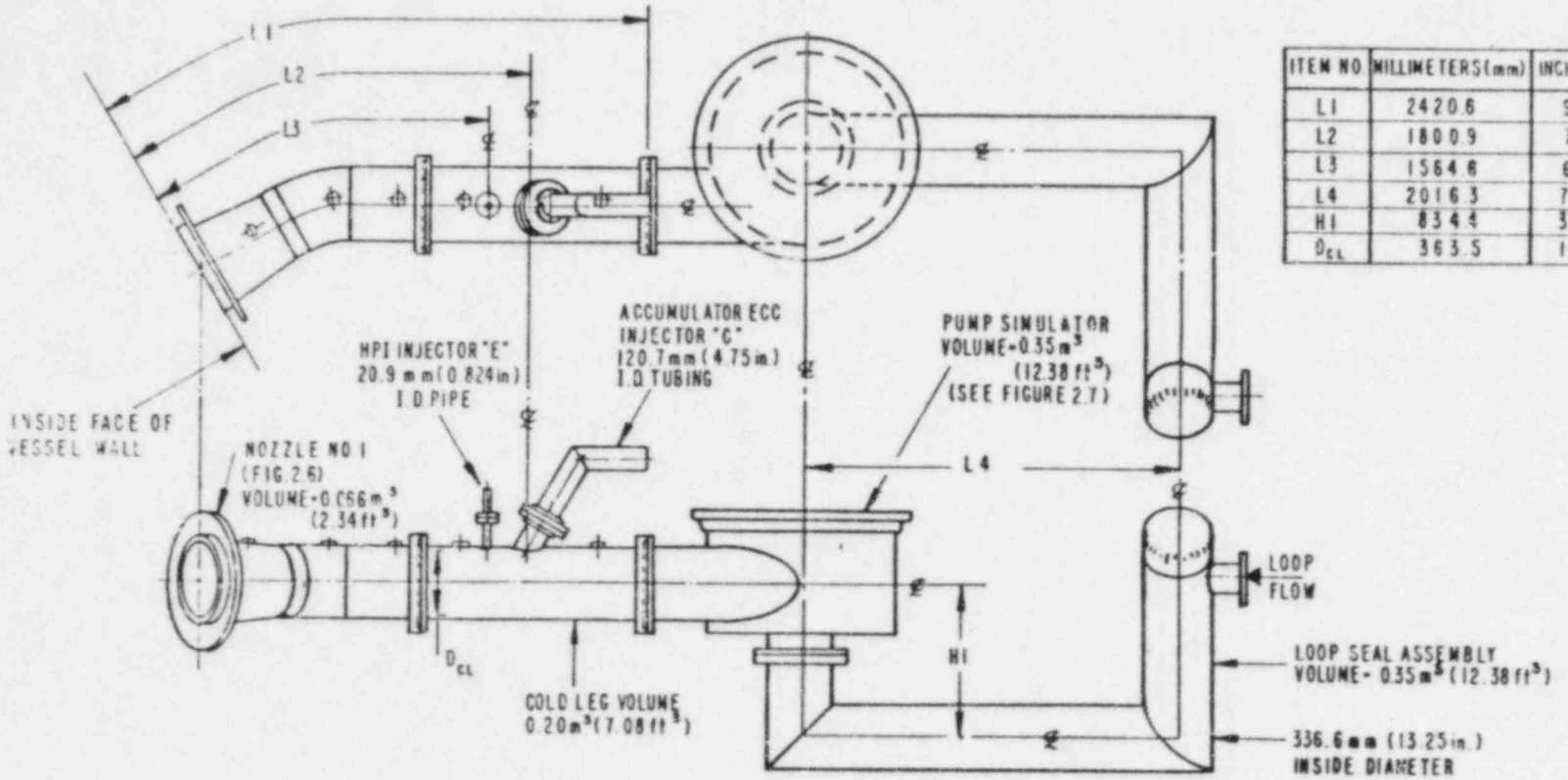

ITEM NO	MILLIMETERS (mm)	INCHES (in)
L1	2420.6	95.3
L2	1800.9	70.9
L3	1564.6	61.6
L4	2016.3	79.38
H1	834.4	32.85
D_{CL}	363.5	14.31

Figure 2-3. Horizontal Cold Leg Assembly Number 1

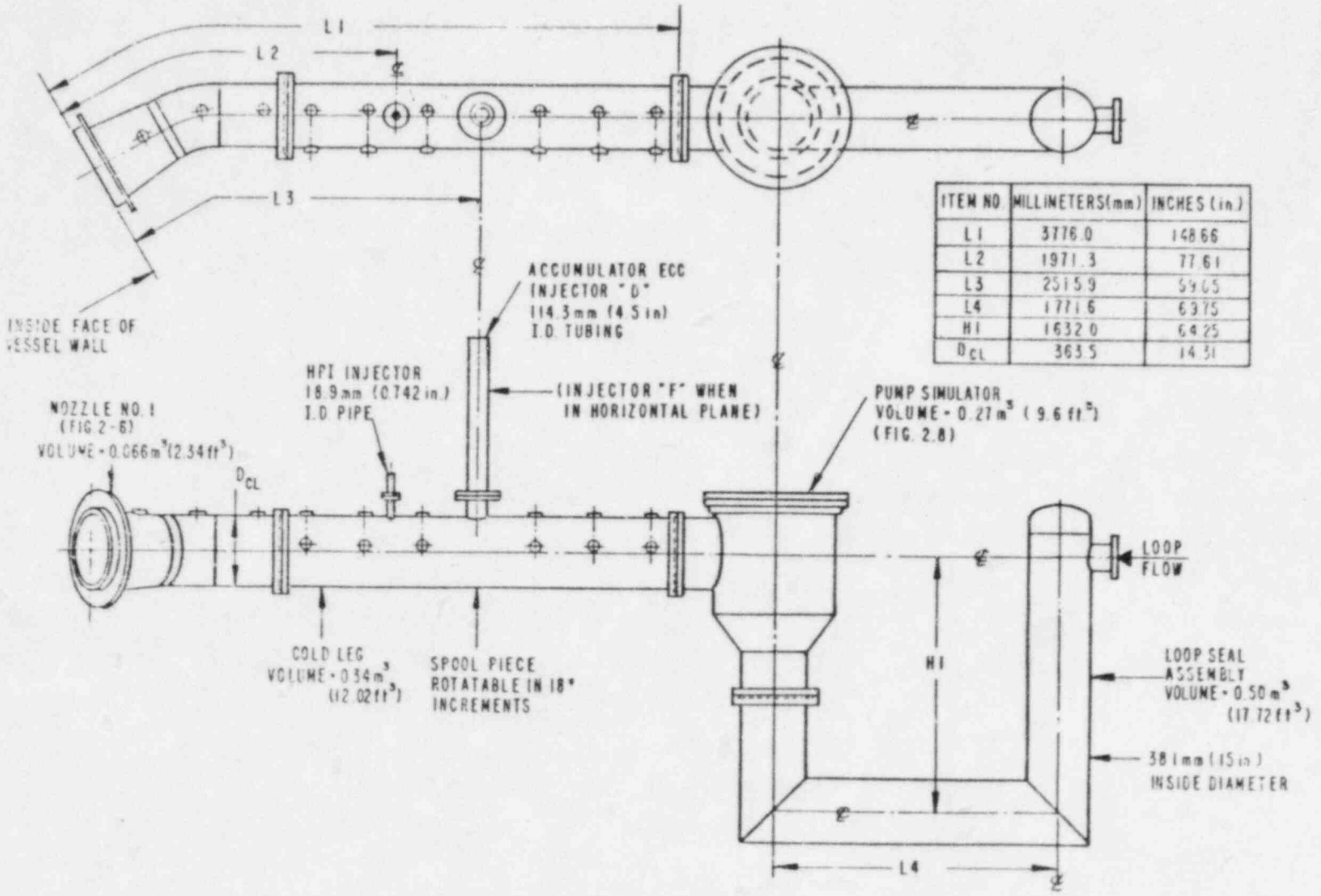

ITEM NO	MILLIMETERS(mm)	INCHES (in.)
L1	3776.0	148.66
L2	1971.3	77.61
L3	2515.9	99.05
L4	1771.6	69.75
H1	1632.0	64.25
D_{CL}	363.5	14.31

Figure 2-4. Horizontal Cold Leg Assembly Number 2

ITEM NO.	MILLIMETERS (mm)	INCHES (in.)
L1	3692.1	145.36
L2	2914.1	114.73
L3	2016.1	79.375
L4	838.2	33.0
H1	542.9	21.375
D_{CL}	363.5	14.31

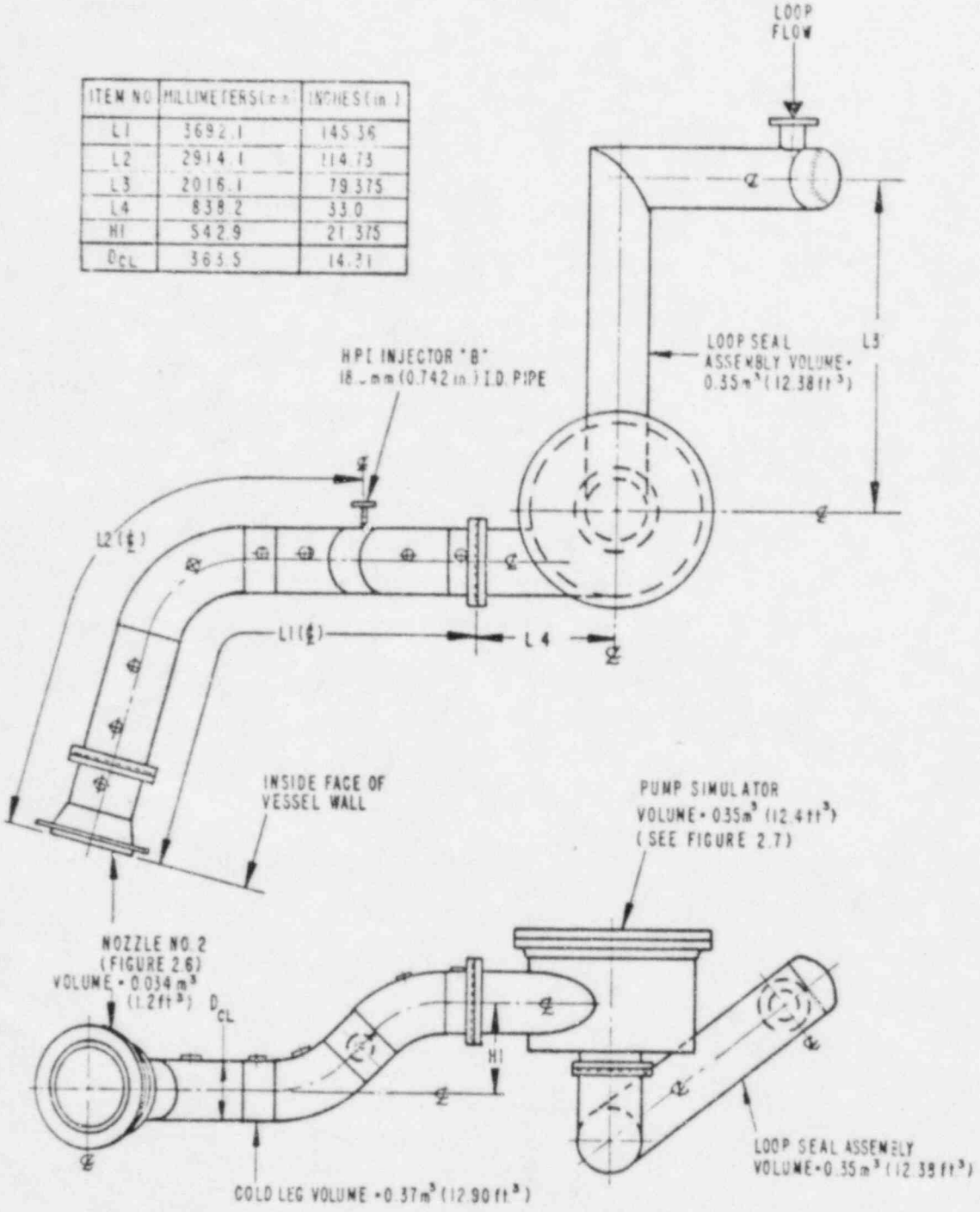

Figure 2-5. Inclined Cold Leg Assembly

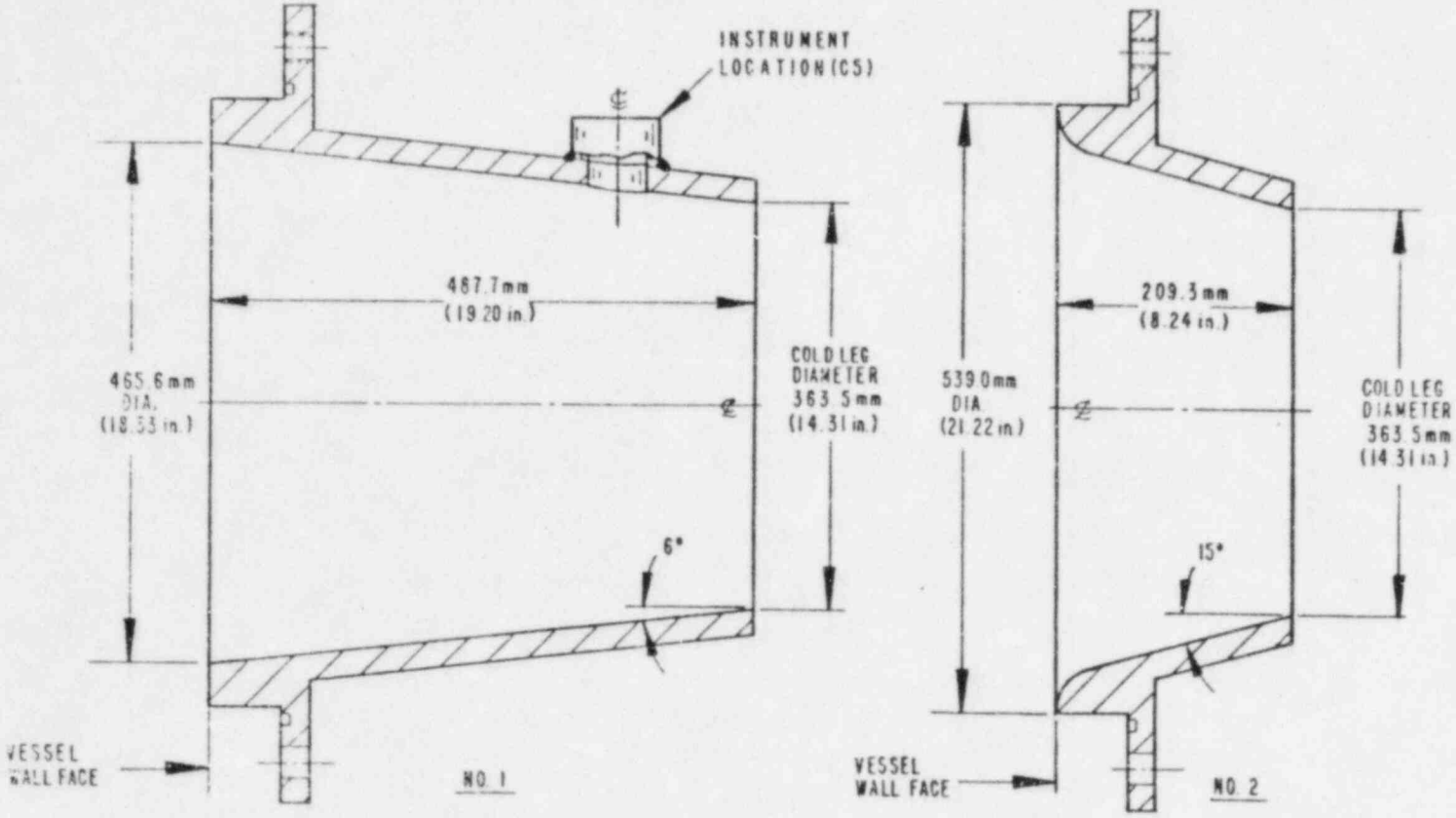

Figure 2-6. Cold Leg Nozzles

The loop seal designs shown in Figures 2-3, 2-4 and 2-5 are based on prototypes for two of the reactor vendors, and represent a minor compromise for the third vendor's cold leg design. Elevation changes in the loop seal have been scaled by the cold leg diameter ratio, while loop seal volumes are in proportion to the cold leg volumes for the two horizontal cold leg assemblies. The loop seal volume and elevations are not modeled for the inclined cold leg assembly (Figure 2-5).

The reactor coolant pump simulators (Figures 2-7 and 2-8) correspond to the designs used with the cold leg loop seals being modeled and are based on geometry data supplied by the vendors. Pump internal volume and general flow path orientation (vertical upflow at the pump inlet, with tangential or radial discharge in the horizontal plane) dictate the overall design of the models. Some internal details of the pumps are also modeled, such as minimum flow area, numbers and angles of impeller blades, total internal volume distribution above and below elevation barriers and elevations of barriers with respect to cold leg elevation, with the impeller in the "locked-rotor" condition.

2.3 SUPPORT FACILITY DESIGN

A test facility was built to support the thermal mixing experimental project. The facility uses existing Creare equipment such as a 9100 kg/hr (20,000 lbm/hr), 1.48 MPa (215 psia) steam generator, two 76 m^3 (20,000 gallon) water storage tanks, a cooling tower with a capacity of 2.64×10^5 W (9×10^5 Btu/hr), coolant circulation pumps, piping and control valves and a data acquisition system and computer. Some new equipment was added to the existing facility to meet special needs for this program. Figure 2-9 shows a schematic of the test facility, and below are described the capabilities of the facility for conducting steady-state and transient thermal mixing tests.

The general capabilities of the test facility are:

1. Design pressure limit of 1.48 MPa (215 psia) corresponding to a saturation temperature of about 198°C (388°F).

2. Loop and vent valve flow rate (singly or combined), to 2.2 m^3/min (575 gpm) at 194°C (382°F).

3. Loop and vent valve fluid storage of 18.9 m^3 (5,000 gallons) at 194°C (382°F).

4. Safety injection (HPI) flow to about 0.38 m^3/min (100 gpm) at 27°C (80°F).

5. HPI fluid storage of greater than 18.9 m^3 (5,000 gallons).

6. Controls for conducting transient tests with either variable loop flow rate or variable loop flow temperature.

7. Instrumentation for establishing and controlling the test conditions of flow rates, pressure, temperatures and test duration.

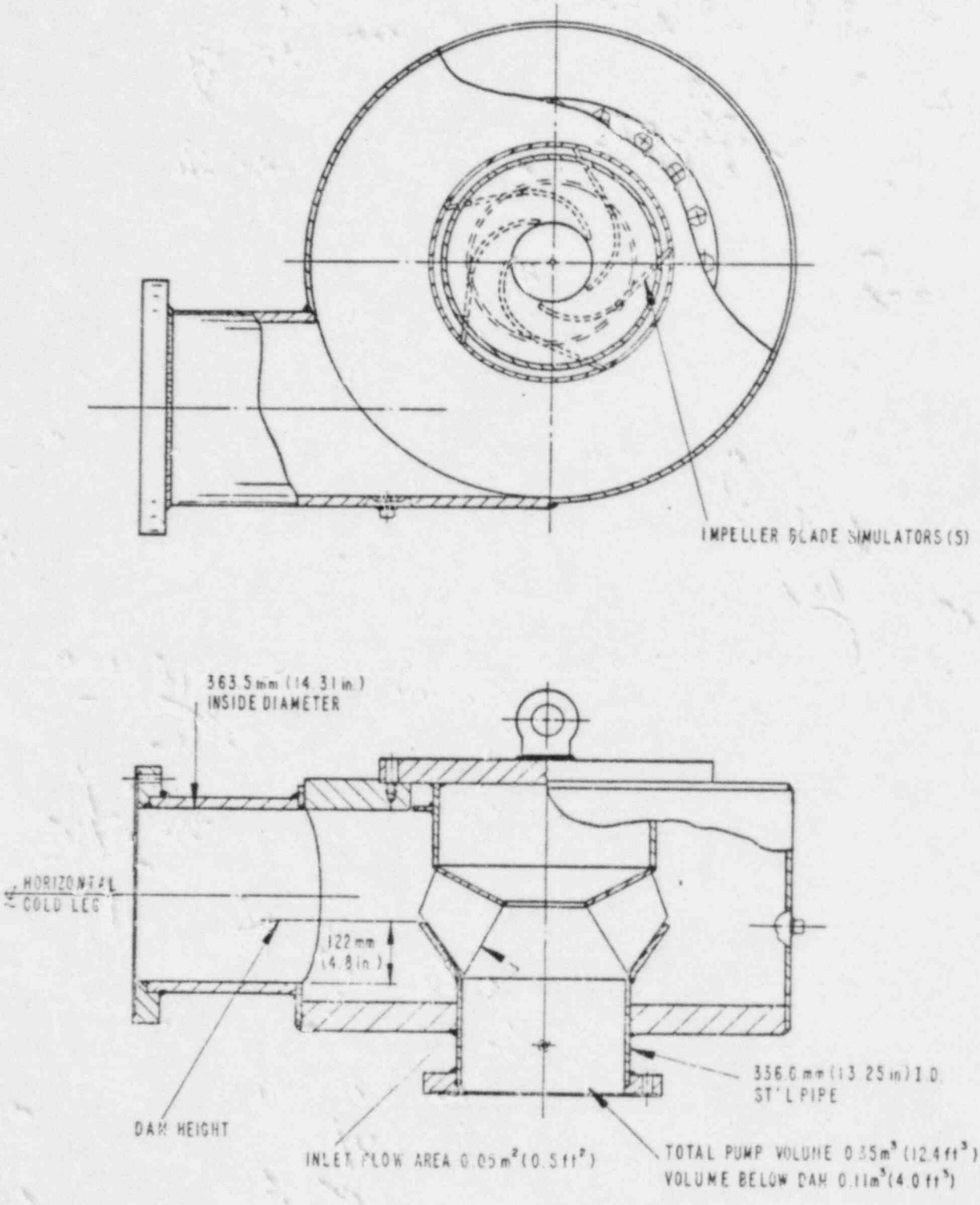

Figure 2-7. Pump Simulator - Horizontal Cold Leg Assembly Number 1

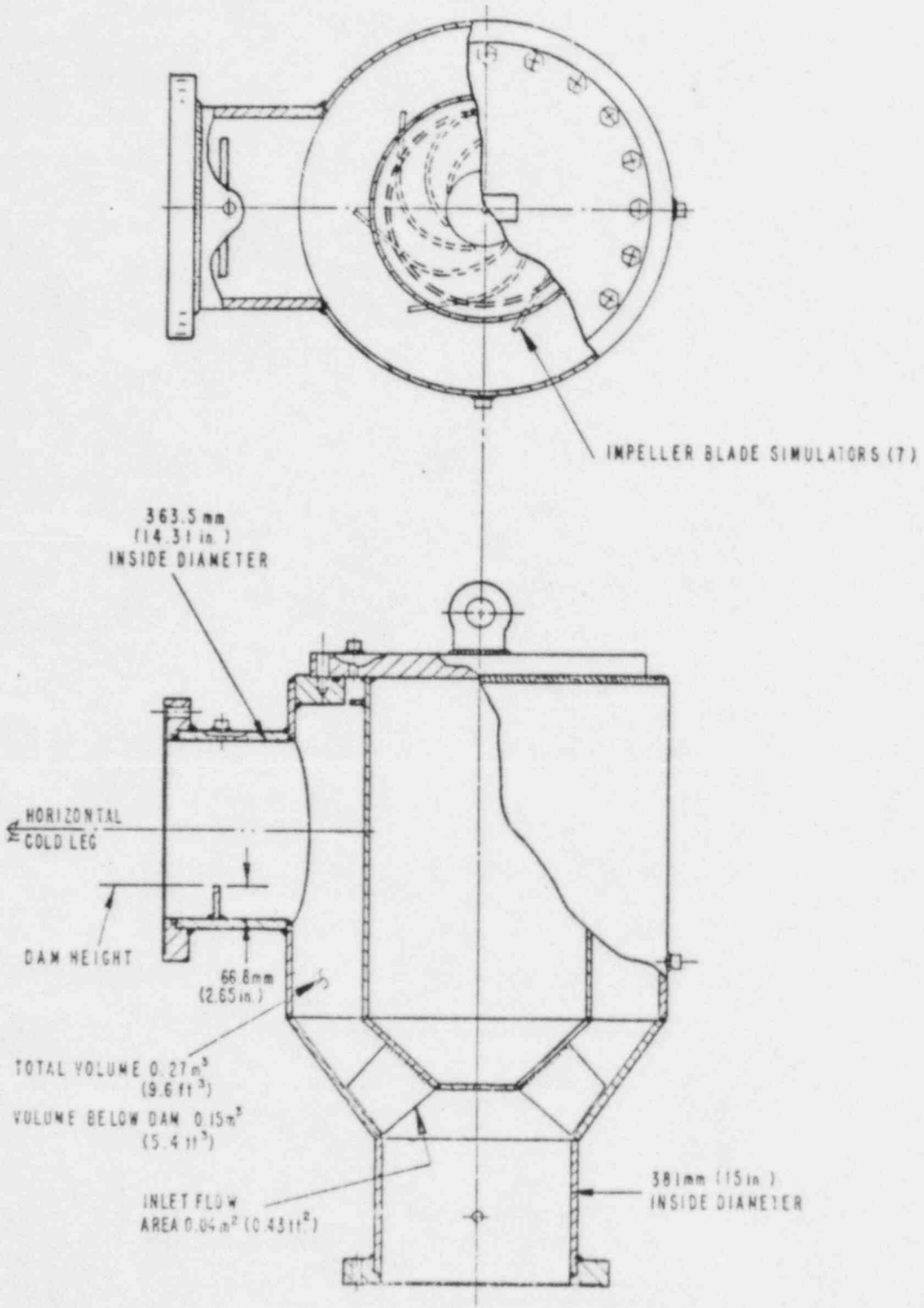

Figure 2-8. Pump Simulator - Horizontal Cold Leg Number 2

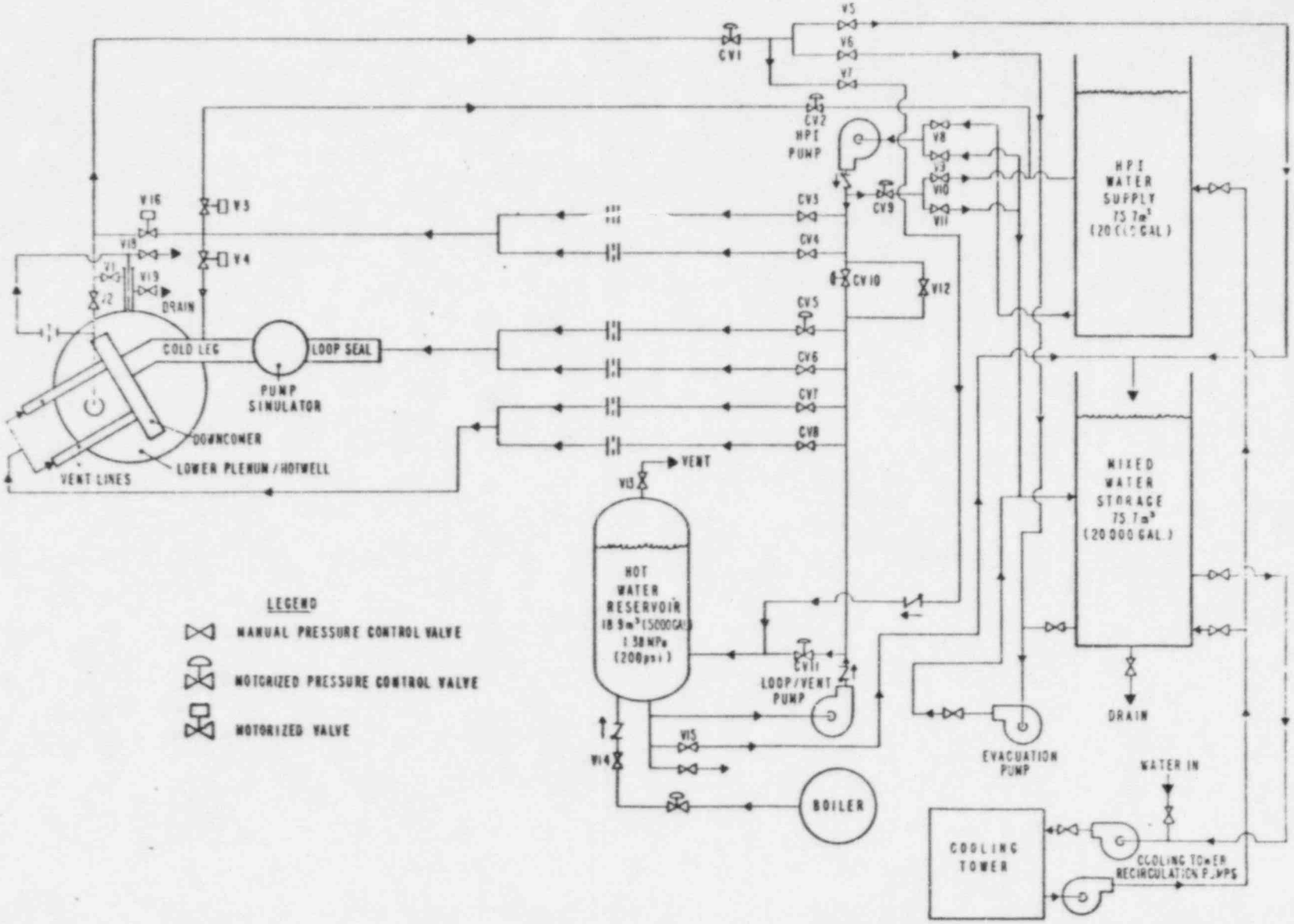

Figure 2-9. Test Facility Schematic

The loop and/or vent flow is from a 18.9 m^3 (5,000 gallon) "primary" storage tank with a pressure rating of 1.48 MPa (215 psia) at 204°C (400°F). A submerged steam heater installed in the tank is used to heat the water to the desired operating temperature using steam from the Creare steam generator. During the tests, tank pressure is maintained by leaving open the steam supply valve connecting the heater to the steam generator. The water in the feed tank is slightly subcooled (3°C to 5°C) relative to the operating pressure at the top of the downcomer.

Loop and vent flow water is drawn from the primary tank using a centrifugal pump having a characteristic curve approximately as shown in Figure 2-10. Following the pump, the flow stream can be divided to supply both the loop flow and the vent valve flow when tests with vent flow are required. Each of those flow lines has a parallel set of orifice flow meters, designed and installed in accordance with ASME procedures (17). The flow meters are sized to provide a continuous turndown ratio of about 25 from the maximum for each flow line and with a flow measurement uncertainty of less than 5% at all flow rates.

Flow control valves for the loop and vent flows are located upstream from the flow meters. The loop flow enters the test section through the reactor coolant pump simulator section. When provided, vent flow splits downstream of the flow meter and control valve to enter the two vent valve lines. These lines will be orificed to produce an equal flow split between the two vents.

Safety injection (HPI) flow is supplied from one of the two 76 m^3 (20,000 gallon) storage tanks. The Creare cooling tower is used to cool the water to as low a temperature as possible, set by ambient temperature and relative humidity conditions. Experience has shown that water can be provided at or less than 27°C (80°F), even in the summer months.

The HPI pump draws water from the storage tank and supplies it through an orifice flow meter and control valve to the injector(s) located on the cold leg. The HPI pump installed in the test facility has the capability shown in Figure 2-11.

Additional details of the fluid exit boundary from the test facility are shown in Figure 2-12. As described earlier, the cooled water from the lower plenum exits through a standpipe at the top of the pressure vessel. That flow is circulated through an orifice meter and then into the hot well where it is distributed adjacent to the lower plenum side walls and mixes with the water in the hot well. The water

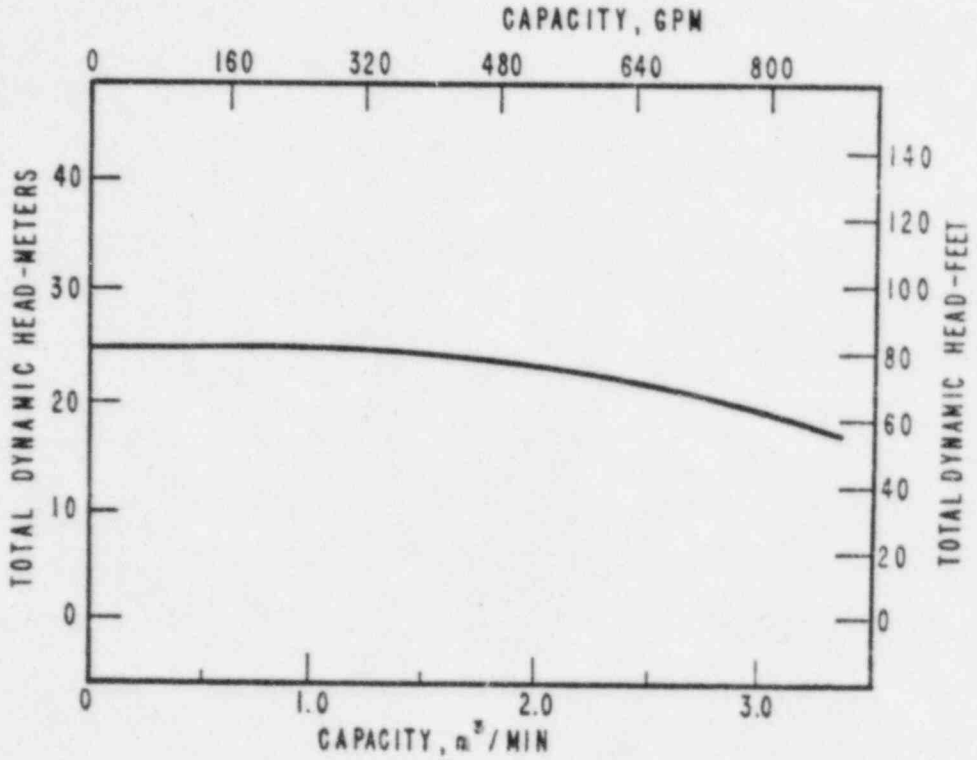

Figure 2-10. Loop Pump Curve

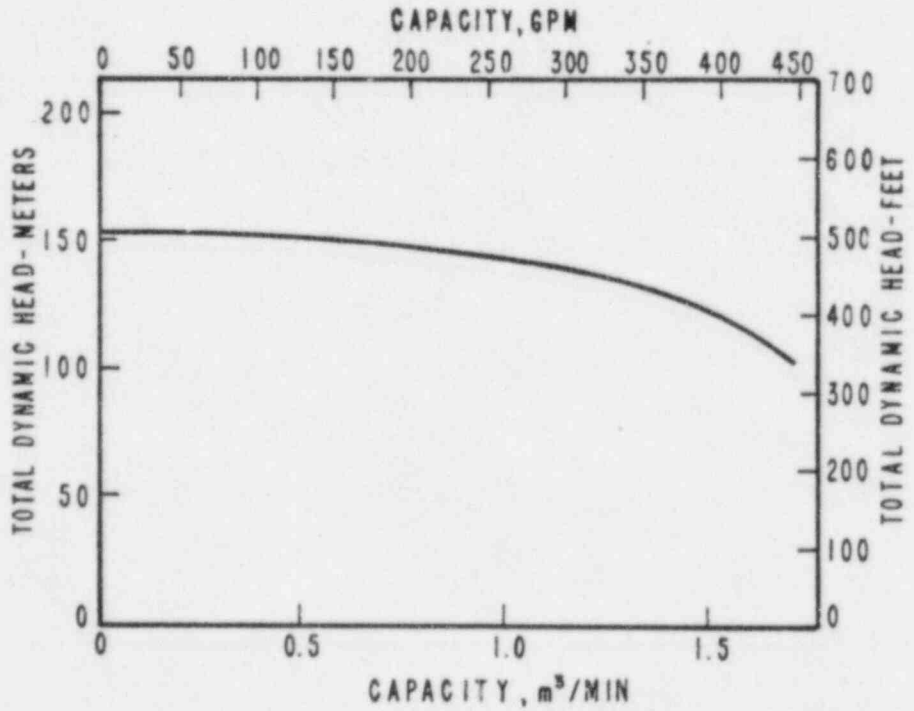

Figure 2-11. HPI Pump Curve

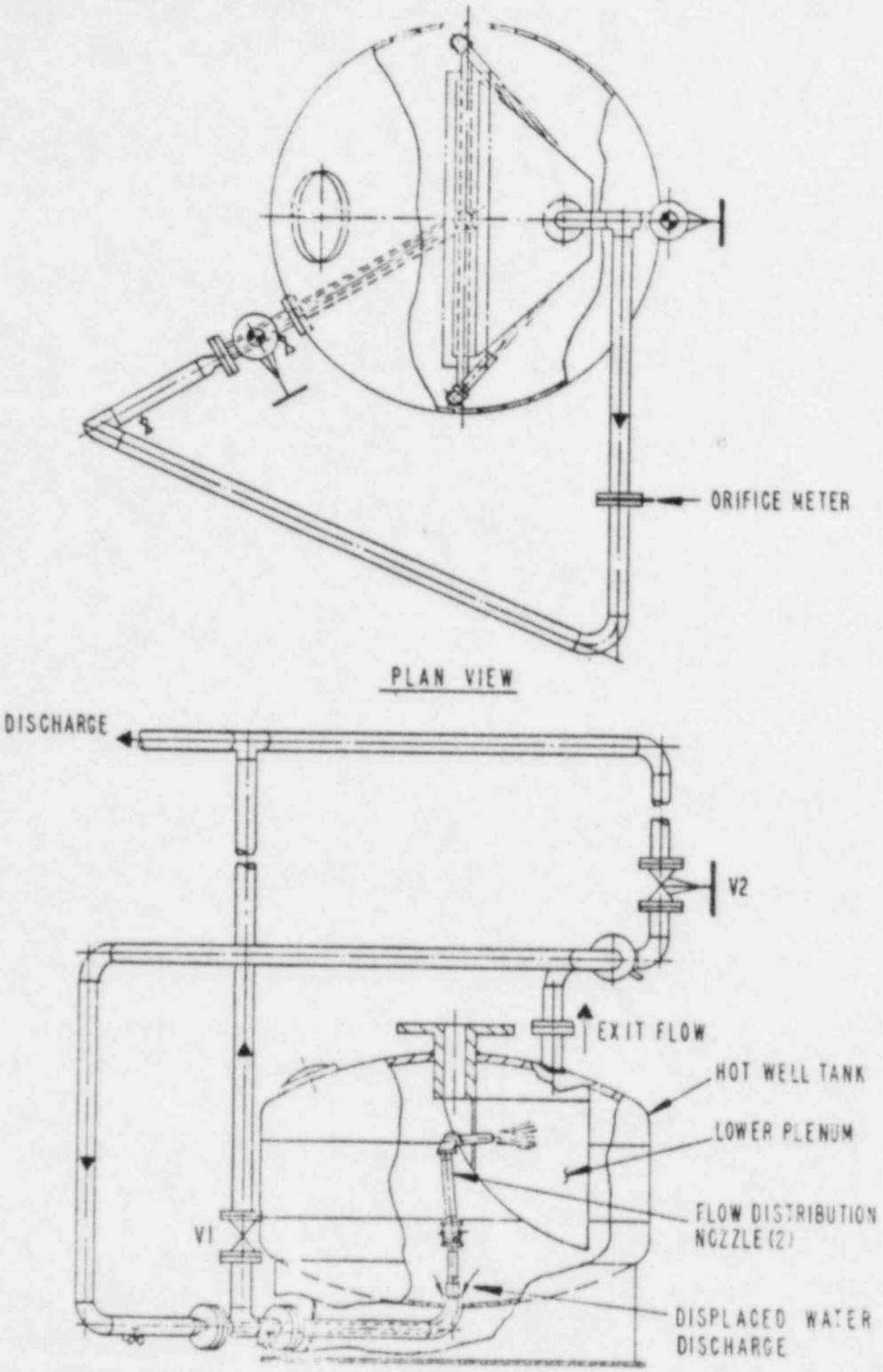

Figure 2-12. Piping Arrangement Details at Lower Plenum and Hot Well

displaced from the hot well leaves through the annular connection at the bottom of the hot well and then is finally discharged from the test facility through valve V1 and is returned to one of the 76 m^3 (20,000 gallon) storage tanks. This arrangement of external lines also serves to nearly equalize the pressure inside and outside the lower plenum volume, ensuring that any leakage flow would be both very small and, most importantly, would not affect the temperature and temperature distribution inside the lower plenum.

Although the details of the types of transient boundary conditions tests have not been established, the facility has been designed to permit either loop flow rate transients (at constant loop temperature and constant HPI flow rate and temperature) or loop flow temperature transients (at fixed loop flow rate and fixed HPI flow and temperature). Through the use of a valve controller and pneumatic or motorized operators, the rate of loop flow valve closure can be set to provide the desired flow rate vs. time transient.

For the loop flow temperature transients, cold fluid can be mixed with the loop flow at a predetermined rate with a corresponding reduction in the loop flow rate to provide a constant total flow at reduced temperature. These flow rates could be controlled using valves with known characteristics as in the case of the variable loop flow transients.

The maximum duration of steady-state and transient tests is set by the loop plus vent valve flow rates and the stored volume of hot water. For the transient tests, the duration depends on the rate of change of the transient as well as the initial loop flow rate. More will be said about test durations in Section 4.

All piping, pumps, valves, instrumentation, etc. have been designed and selected for service at the operating pressures and temperatures specified for this test program. The maximum pressure in the test loop is expected to be about 1.55 MPa (225 psig), while the maximum fluid temperature will be about 193°C (380°F).

The hot water supply tank and lines are fully insulated, primarily for personnel safety consideration. The model cold legs and downcomer are also insulated to minimize the ambiguity in vessel wall or near-wall fluid temperature measurements which result from heat conduction through the boundaries. Standard commercial fiberglass insulation is used to reduce the heat loss to ambient to less than 158 W/m^2 (50 $Btu/hr-ft^2$) at the maximum operating temperature in the cold leg and downcomer.

3. MEASURE SYSTEM DESIGN

This section describes the measurements to be made during the course of the thermal mixing experiments and gives some details of the designs for the instruments and data acquisition system and provides some estimates of measurement accuracy.

3.1 MEASUREMENT OBJECTIVES

The measurements to be made during the tests fall into two categories:

1. System measurements
2. Principal measurements.

The system measurements provide data for the operator, such as pressures, pressure drops, temperatures and flow rates, to assist in establishing and controlling the desired test conditions and test duration. These data are also used in the post-test data reduction to correlate test results as a function of flow rates, density, temperatures and non-dimensional groupings such as Froude and Reynolds numbers.

The principal measurements are those which provide detailed data on temperature and velocity profiles in the cold leg and downcomer and wall to fluid heat transfer. It is these data which may be used to assess and develop appropriate thermal mixing and heat transfer correlations and models.

Each of these categories of measurements is discussed in detail in following sections.

3.2 SYSTEM MEASUREMENTS

Figures 3-1a and 3-1b show the locations and types of measurements which are made in the support facility---external to the model cold legs, downcomer and lower plenum. These measurements include the pressures and temperatures in the loop and HPI flow lines and supply tanks, flow rates for loop, vent and HPI flows and supply tank level. Vent flow rate and temperature can be measured for tests which require vent valve flow. Additional detailed temperatures and lower plenum discharge flowrate are measured in order to carryout test facility energy balance. Pressure drops in the cold leg and downcomer can be measured during special tests (at uniform temperature and at different flow rates) to calibrate the pressure drop characteristics of the cold legs and downcomer. These measurements are listed in Table 3-1 with cross-reference to the nomenclature used in Figure 3-1. That list includes some specific information regarding the instrument type, the estimated instrument accuracy (based on anticipated calibration data from the instrument vendors and re-calibration capability), and the expected overall measurement accuracy which includes the instrument accuracy and an estimated uncertainty contribution from instrument installation effects and from the data acquisition system.

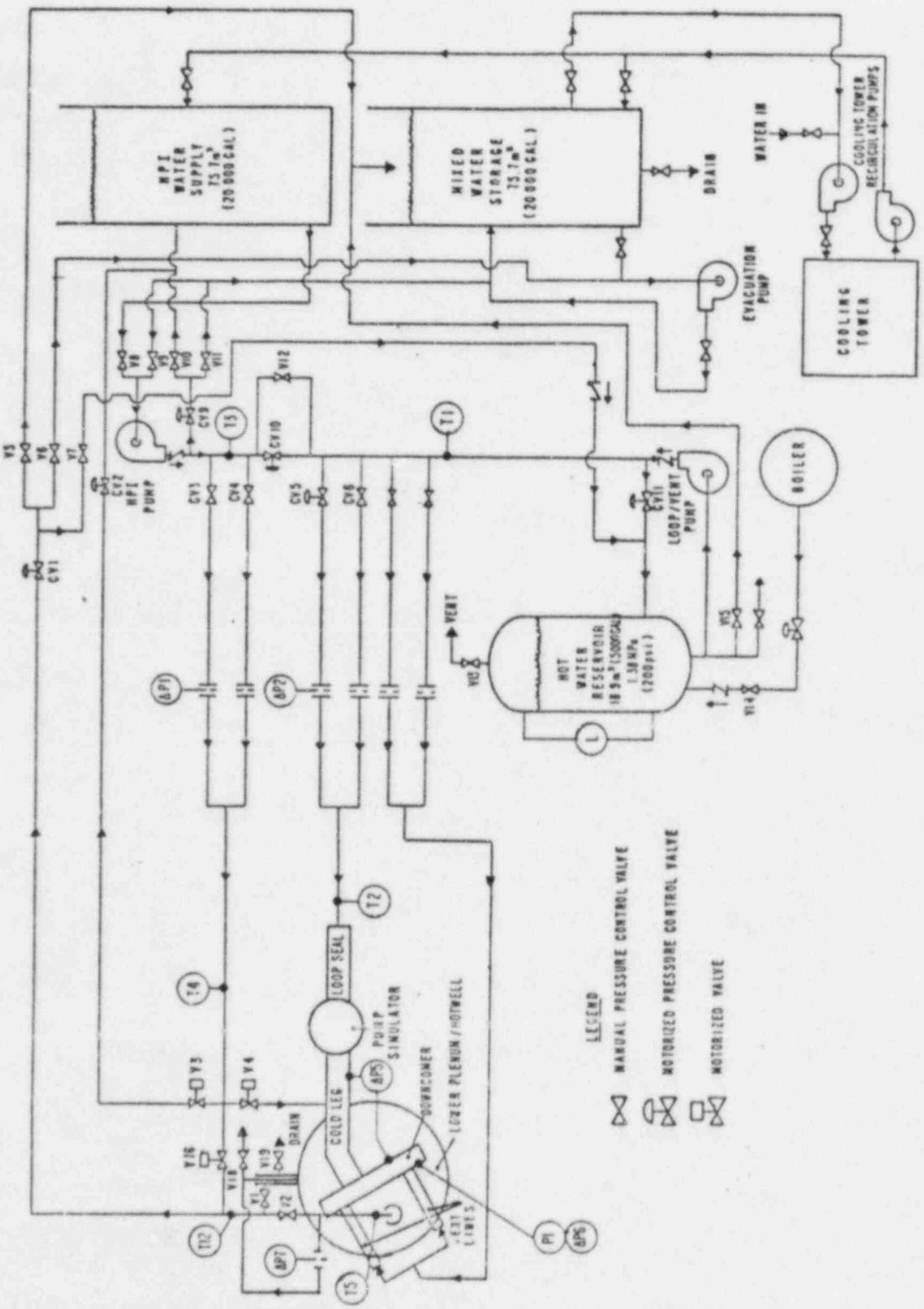

Figure 3-1a. Test Facility System Measurements

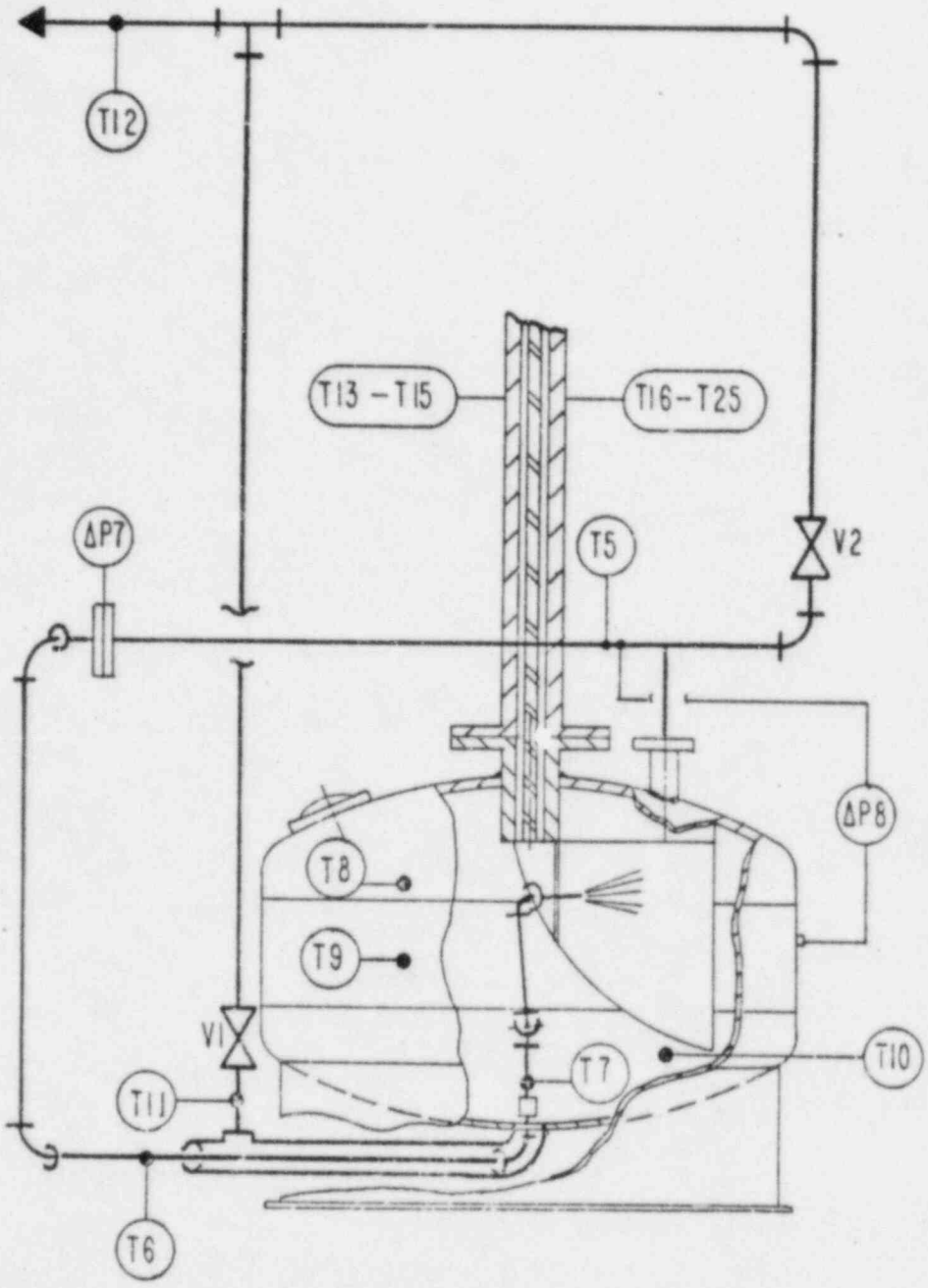

Figure 3-1b. System Measurements at Facility Boundary

Table 3-1 SUPPORT FACILITY INSTRUMENTATION

INSTRUMENT[1] LABEL	CODE[2]	MEASURED VARIABLE	INSTRUMENT TYPE	INSTRUMENT CALIBRATION UNCERTAINTY	TOTAL EXPECTED MEASUREMENT UNCERTAINTY	INSTRUMENT RISE TIME
T1	LOOPT	Loop supply temperature	Type E Thermocouple	1°C (1.8°F)	1.5°C (2.8°F)	<1 sec.
T2	LOOPT2	Loop seal inlet temperature	Type E Thermocouple	1°C (1.8°F)	1.5°C (2.8°F)	<1 sec.
T3	HPISUPT1	HPI supply temperature	Type E Thermocouple	1°C (1.8°F)	1.5°C (2.8°F)	<1 sec.
T4	HPISUPT2	HPI temperature at injector inlet	Type E Thermocouple	1°C (1.8°F)	1.5°C (2.8°F)	<1 sec.
T5	SPWT	Standpipe water temperature	Type E Thermocouple	1°C (1.8°F)	1.5°C (2.8°F)	<1 sec.
T6	SPWTC2	Recirculated standpipe water temperature	Type E Thermocouple	1°C (1.8°F)	1.5°C (2.8°F)	<1 sec.
T7	SPWTC3	Recirculated standpipe water temperature	Type E Thermocouple	1°C (1.8°F)	1.5°C (2.8°F)	<1 sec.
T8	HWUTC	Upper hotwell temperature	Type E Thermocouple	1°C (1.8°F)	1.5°C (2.8°F)	<1 sec.
T9	HWBTC	Bulk hotwell temperature	Type E Thermocouple	1°C (1.8°F)	1.5°C (2.8°F)	<1 sec.
T10	HWLTC	Lower hotwell temperature	Type E Thermocouple	1°C (1.8°F)	1.5°C (2.8°F)	<1 sec.
T11	HWETC	Hotwell exit temperature	Type E Thermocouple	1°C (1.8°F)	1.5°C (2.8°F)	<1 sec.
T12	CVITC	Facility exit temperature	Type E Thermocouple	1°C (1.8°F)	1.5°C (2.8°F)	<1 sec.
T13-T15	C**VWTC[3]	Core outside wall temperature	Type E Thermocouple	1.7°C (3°F)	2.8°C (5°F)	<1 sec.
T16-T17	V**VWTC	Vessel outside wall temperature	Type E Thermocouple	1.7°C (3°F)	2.8°C (5°F)	N.A.[4]
T18-T25	V**PWTC	Probe outside wall temperature	Type E Thermocouple	1.7°C (3°F)	2.8°C (5°F)	N.A.
P1	TVP	Test vessel pressure	Pressure Transducer	6.8kPa (1psi)	13.8kPa (2 psi)	<1 sec.
ΔP1	HPIFLOW	HPI flow rate	Orifice Meter	1%	5%	N.A.
ΔP2	LOOPFLOW	Loop flow rate	Orifice Meter	1%	5%	N.A.
ΔP5	CLDP5	Cold leg pressure drop	Pressure Transducer	1Pa	2.5Pa	<1 sec.
ΔP6	DDP6	Downcomer pressure drop	Pressure Transducer	1Pa	2.5Pa	<1 sec.
ΔP7	SPHWFLO	Standpipe to hotwell flow rate	Orifice Meter	1%	5%	N.A.
ΔP8	HWRDP	Hotwell to standpipe pressure drop	Pressure Transducer	0.3kPa	0.5kPa	<1 sec.

[1] The Instrument Label corresponds to symbols used in Figures 3-1a and 3-1b.
[2] The CODE designation in this column refers to the nomenclature used to label the data in the computer-generated plots and tables. (see Reference 4.1)
[3] The asterisks (**) refer to the row and column on the downcomer (Fig. 3-6) where the instruments are located
[4] N.A. means that the rise time is not applicable because the measurement of interest is essentially steady state.

All of the instruments used for system measurements are conventional and were selected for reliability and performance. Further, there are redundant panel gauges and meters installed on the test facility for use by the operator to assist in setting test conditions, and to verify the operation of the instruments connected to the data acquisition system.

3.3 PRINCIPAL MEASUREMENTS

The measurements of principal interest in the testing project are the temperature and velocity distributions in the cold leg and downcomer and the wall to fluid heat transfer in the downcomer as a function of input loop, vent and HPI flow rates, fluid densities and geometric parameters. Table 3-2 gives an overview of the number and types of instruments and measurements which can be made in the scaled test facility.

3.3.1 Instrument Locations

A systematic approach was taken in the selection of the number and locations for the instruments to provide for grouping of certain instrument types. These groupings are necessary in some instances to facilitate data reduction while in other cases the pairings will enhance the quality of the data. For example, fluid temperatures will be measured adjacent to each velocity probe location in order to convert the velocity probe differential pressure reading to a fluid velocity using the correct fluid density. Another grouping concept is the measurement of fluid velocity near the vessel wall heat flux probes, to provide data to assist the analyst in understanding the influence of fluid velocity on wall heat transfer.

COLD LEG INSTRUMENTATION

Instrumentation ports are provided in the cold legs to measure the fluid temperature and velocity profiles at several specific axial locations:

1. Upstream of the principal HPI injector location for each cold leg, to characterize the inlet loop flow.
2. Several locations downstream from the injector, to characterize the fluid velocity and temperature in the mixing zone.
3. Just upstream of the cold leg nozzle penetration through the vessel wall, to characterize the fluid conditions entering the downcomer.

In addition to these specific locations, 15 thermocouples are distributed along the length of the cold leg pipe on the upper and lower walls, 10 fluid thermocouples are distributed through the loop seal and pump simulator and there is a velocity rake which can be installed at various points along the cold leg. In total there are 90 fluid temperature measurements and up to 20 fluid velocity measurements distributed throughout the cold leg. The number and locations of

Table 3-2 INSTRUMENTS FOR PRINCIPAL MEASUREMENTS IN COLD LEG AND DOWNCOMER

Thermocouples	261
Velocity (Pitot) Probes	40
Heat Flux Sensors	40

Instrument Type	Number	Measurement/Location
Thermocouple	90	Cold leg, loop seal and pump simulator fluid temperature, radial and axial distribution (10 with rapid response)
Thermocouple	15	Downcomer fluid temperature, above thermal shield, gap-wise temperature distributions
Thermocouple	71	Downcomer fluid temperature centerline of gap on both sides of thermal shield
Thermocouple	40	Downcomer fluid temperature near wall, for use with heat flux measurements to obtain heat transfer coefficients
Thermocouple	40	Downcomer wall surface temperature, for use with heat flux measurement to obtain heat transfer coefficients
Thermocouple	5	Lower plenum fluid temperature distribution
Heat Flux Sensor	40	Downcomer wall heat flow rate, 12 on core wall, 28 on vessel wall
Velocity Probe Optional Locations	20	Cold leg radial velocity distribution, several axial locations
Velocity Probe Optional Locations	20	Downcomer fluid velocity, centerline of gap on each side of thermal shield, located with wall heat flux probe

these instruments are intended to be sufficient to determine the extent of the mixing which occurs in the cold leg and also to provide a detailed map of the fluid entering and exiting from the cold leg.

Figures 3-2, 3-3 and 3-4 show possible arrangements for these instrument locations in the three 1/2-scale cold leg assemblies. There are five measuring stations (C-1, C-2, C-3, C-4, C-5) which each have ten temperature probes situated on a single rake in a vertical array along the nominal centerline of the cold leg. At the nozzle station (C-5), an additional 10 temperature probes are distributed between two more rakes which, along with the main centerline rake, define a measuring plane to characterize the flow at the inlet to the downcomer. Up to 5 velocity probes can be installed on some of these rakes, each having an integral fluid temperature thermocouple along with 5 separate temperature probes. A sixth instrument rake is available having five velocity probes and five integral temperature probes, and which can be placed at any of the unassigned measuring locations in the cold legs that have more than 5 instrumentation ports. Figure 3-5 shows details of the probe spacings at the measuring locations on the cold legs. Because all of the instrumentation ports are identical, other arrangements of velocity and temperature rakes are possible.

Three of the centerline temperature rakes have miniature thermocouple probes which can provide rapid response temperature measurements. A total of 10 of these miniature thermocouples are available, distributed as follows:

1. two at measuring plane C-1, upstream of the injector
2. five at measuring plane C-5, at the entrance to the downcomer
3. three at measuring plane C-2, downstream of the injector.

The miniature thermocouple junctions have a measured time constant of about 35 milliseconds and therefore can follow fluctuations up to about 5Hz.

Ten thermocouples are installed in the loop seal and pump simulator region of the cold leg assemblies (see Figures 3-2, 3-3, 3-4). These thermocouples will provide data on the extent of thermal mixing and stratification in the pump and loop seal, particularly for low and zero loop flow situations.

DOWNCOMER AND LOWER PLENUM INSTRUMENTATION

The downcomer is instrumented to measure fluid and wall temperature profiles, fluid velocity profiles, and wall heat transfer coefficients. There are 40 heat flux probes, 40 vessel wall and core wall temperature probes, 126 downcomer fluid temperature probes, 20 fluid velocity probe locations in the downcomer and 5 fluid temperature probes in the lower plenum.

Previous small scale thermal mixing experiments have demonstrated that the mixing process in the downcomer is not instantaneous and that the relatively cooler fluid emerging from the nozzle spreads as a two-dimensional plume, gradually mixing with the fluid in the annulus and

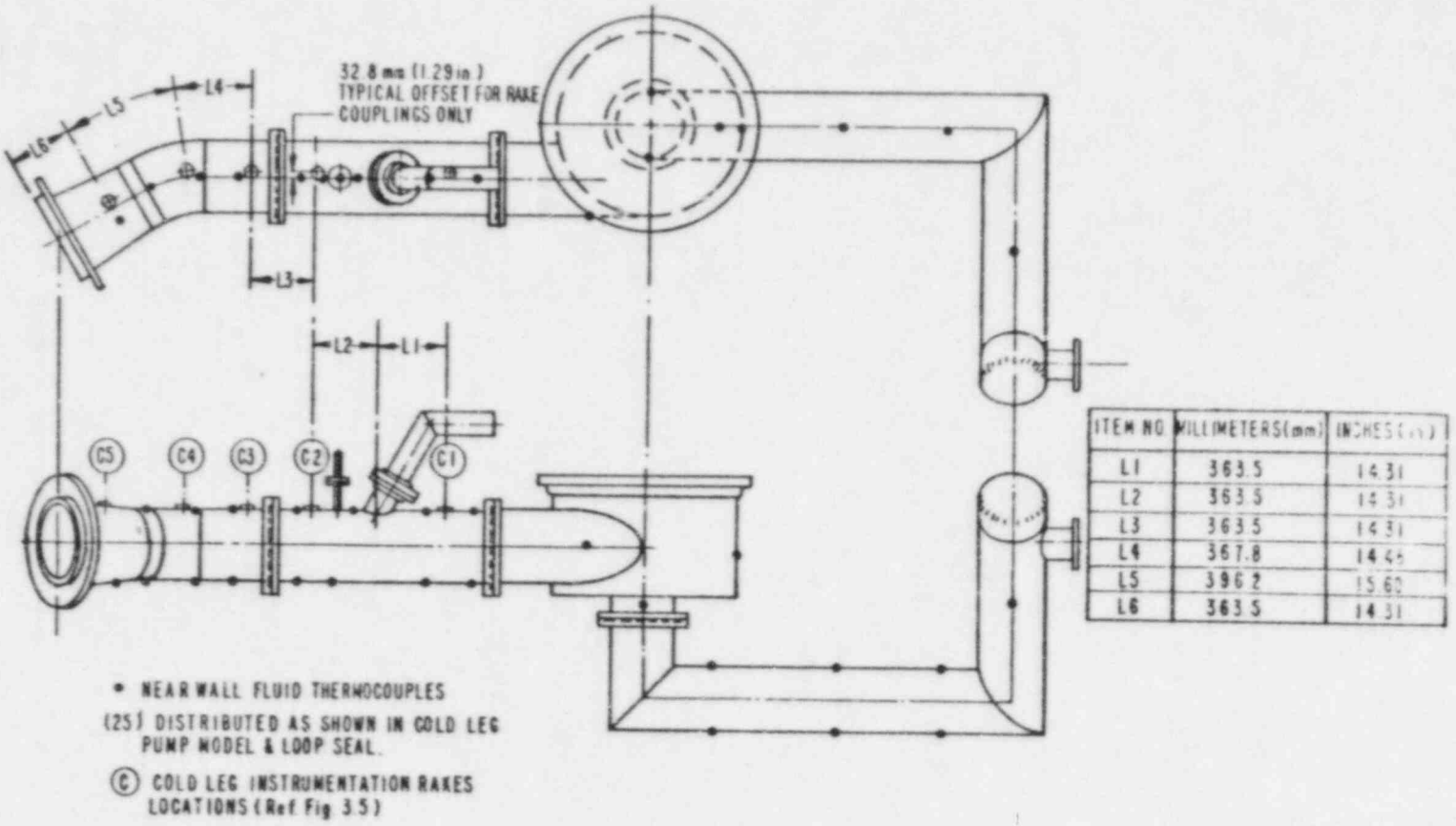

ITEM NO	MILLIMETERS(mm)	INCHES(in)
L1	363.5	14.31
L2	363.5	14.31
L3	363.5	14.31
L4	367.8	14.48
L5	396.2	15.60
L6	363.5	14.31

Figure 3-2. Instrument Locations in Horizontal Cold Leg Number 1

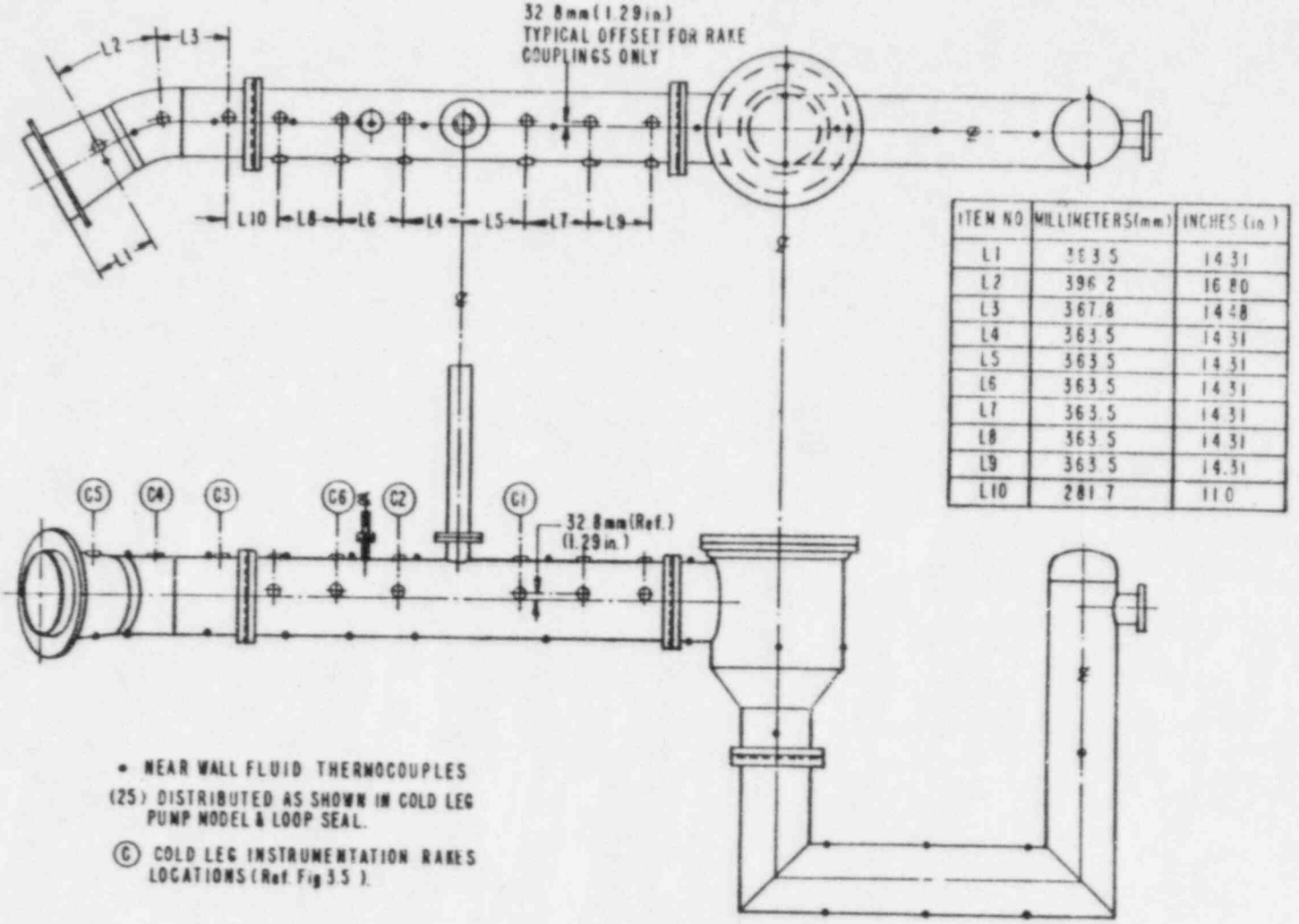

ITEM NO	MILLIMETERS(mm)	INCHES (in.)
L1	363.5	14.31
L2	396.2	16.80
L3	367.8	14.48
L4	363.5	14.31
L5	363.5	14.31
L6	363.5	14.31
L7	363.5	14.31
L8	363.5	14.31
L9	363.5	14.31
L10	281.7	11.0

Figure 3-3. Instrument Locations in Horizontal Cold Leg Number 2

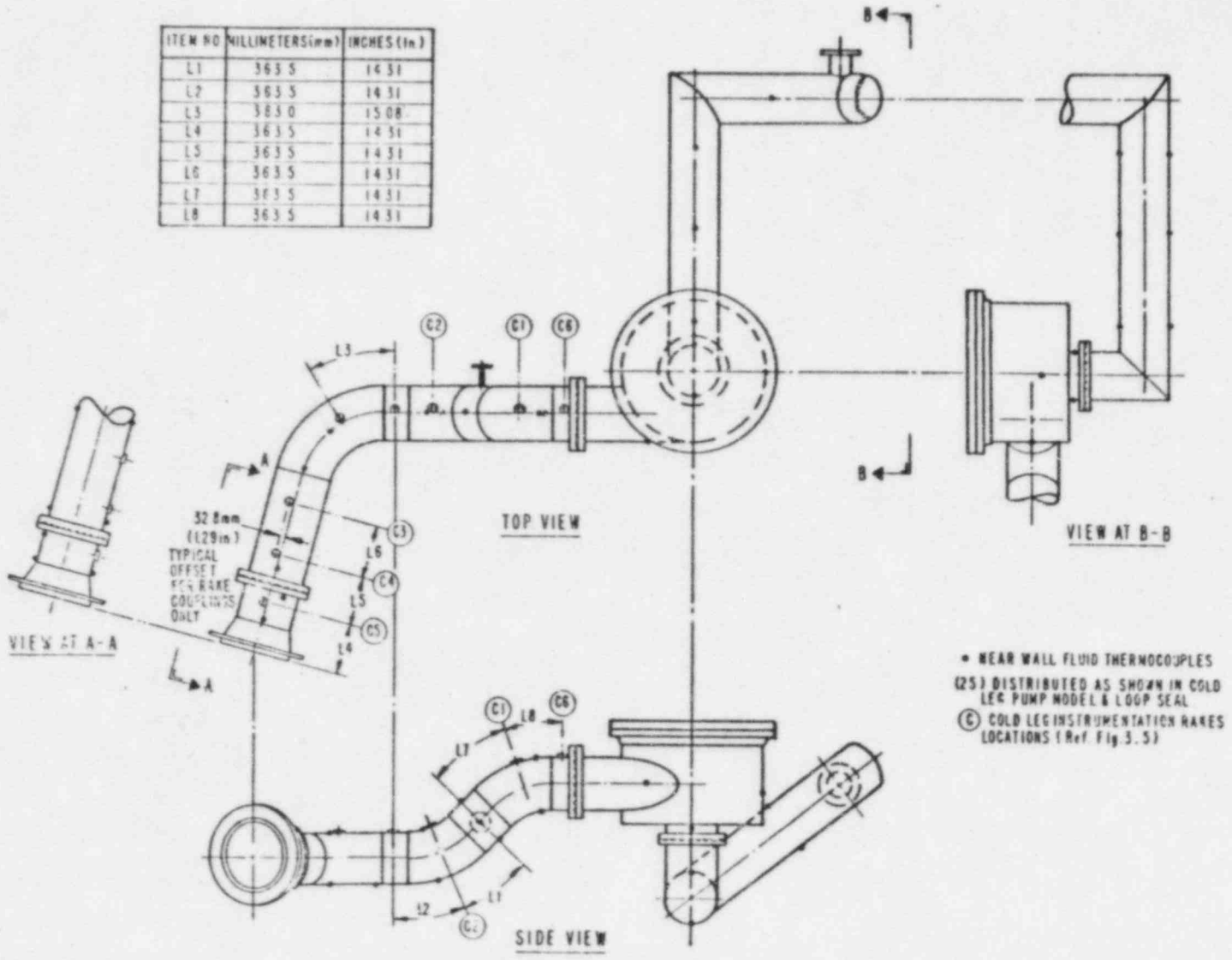

Figure 3-4. Instrument Locations in Inclined Cold Leg

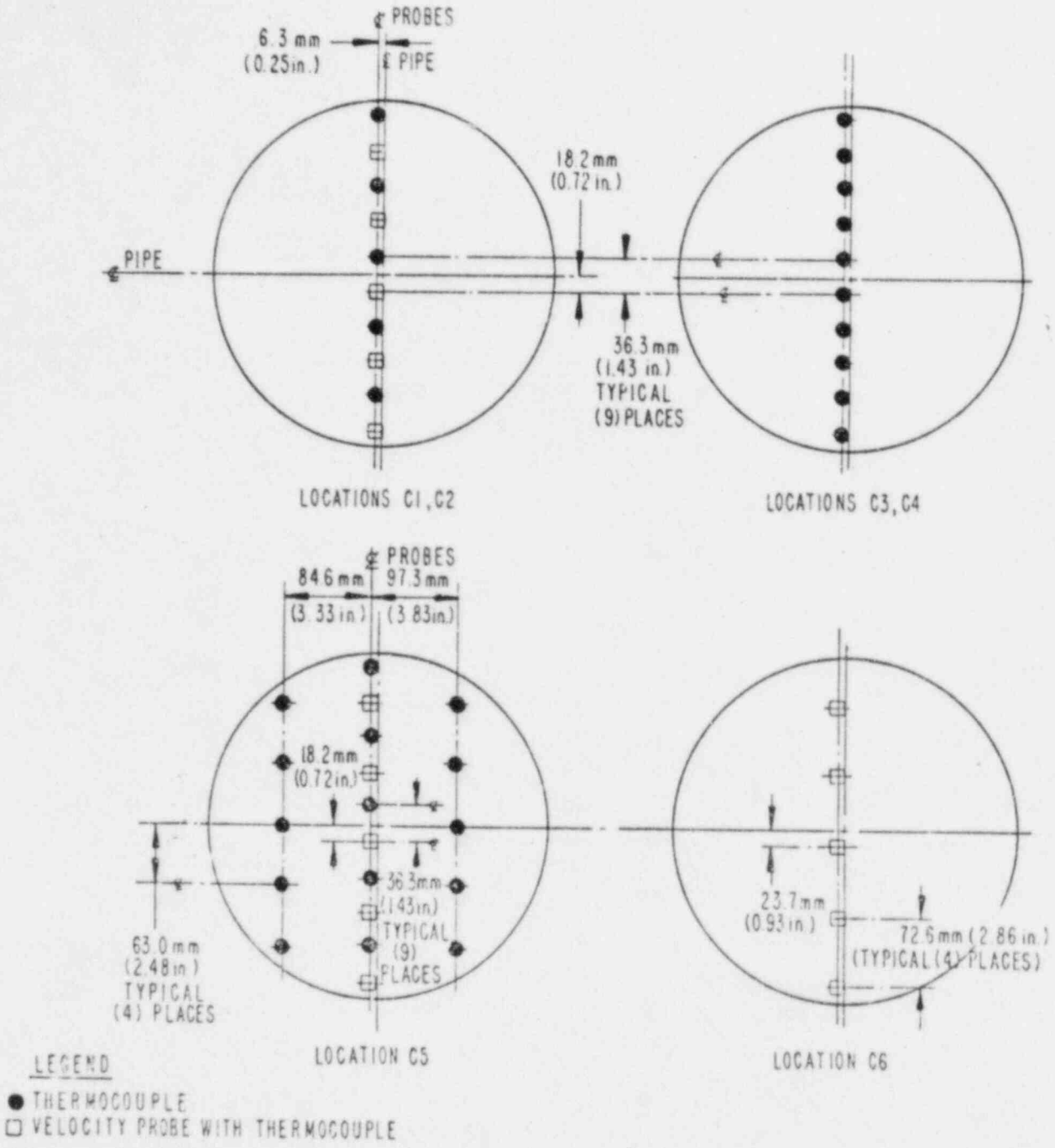

Figure 3-5. Detailed Cold Leg Probe Radial Locations

lower plenum. Thus, the instruments in the downcomer are arranged to measure the horizontal and vertical temperature and velocity profiles in the fluid below the cold leg (and below the vent valves when those are used). Wall heat transfer measurements will be made in the downcomer to provide data for correlation with heat transfer models.

Approximately 140 instrumentation ports are provided in the downcomer walls, equally split between the vessel and core sides. Figure 3-6 shows one possible arrangement of the downcomer instruments for a test geometry without vent valve flow, with the thermal shield in place. There are corresponding instrument locations on each wall, however the majority of instruments are on the vessel wall side of the thermal shield. A systematic approach has been followed in grouping the instrument types which is discussed in more detail below.

There are a total of 40 wall heat flux probes in the downcomer distributed between the vessel and core sides. Associated with each heat flux probe is a wall surface temperature probe, a near-wall fluid temperature probe and a center-of-gap fluid thermocouple probe located as shown in Figure 3-7. The heat flux probes are installed with their face flush to the inside wall surface and they are removable.

The center-of-gap and fluid "film" temperature probes are situated to the side of and below the heat flux sensor so as not to affect the heat flux measurement by locally disturbing the fluid film.

Twenty of the center-of-gap thermocouples are integral with downcomer fluid velocity probes which can be mounted from the heat flux probe bodies, and the other 20 center-of-gap measurements are made with single element probes containing a grounded thermocouple junction. Both of these configurations are shown in the section view in Figure 3-7.

There are 31 additional center-of-gap fluid temperature probes in the downcomer besides those associated with the heat flux probes. Twenty-three of these probes are distributed in the downcomer to provide detailed "mapping" of the thermal mixing process in regions immediately below the cold leg nozzle and 8 are situated at the bottom of the downcomer where the flow enters the lower plenum.

Fluid temperature profiles across the downcomer gap are measured with thermocouple rakes at three locations between the nozzle centerline elevation and the top of the thermal shield as shown in Figure 3-8. Each rake contains 5 thermocouple junctions uniformly spaced across the gap (S = 137.2 mm) and located below the nozzle centerline as follows:

1. approximately $D_{CL}/3$ above the bottom elevation of the cold leg (73 mm below nozzle centerline)

2. approximately at the bottom elevation of the cold leg (203 mm below nozzle centerline)

3. approximately $D_{CL}/3$ below the bottom elevation of the cold leg (305 mm below nozzle centerline)

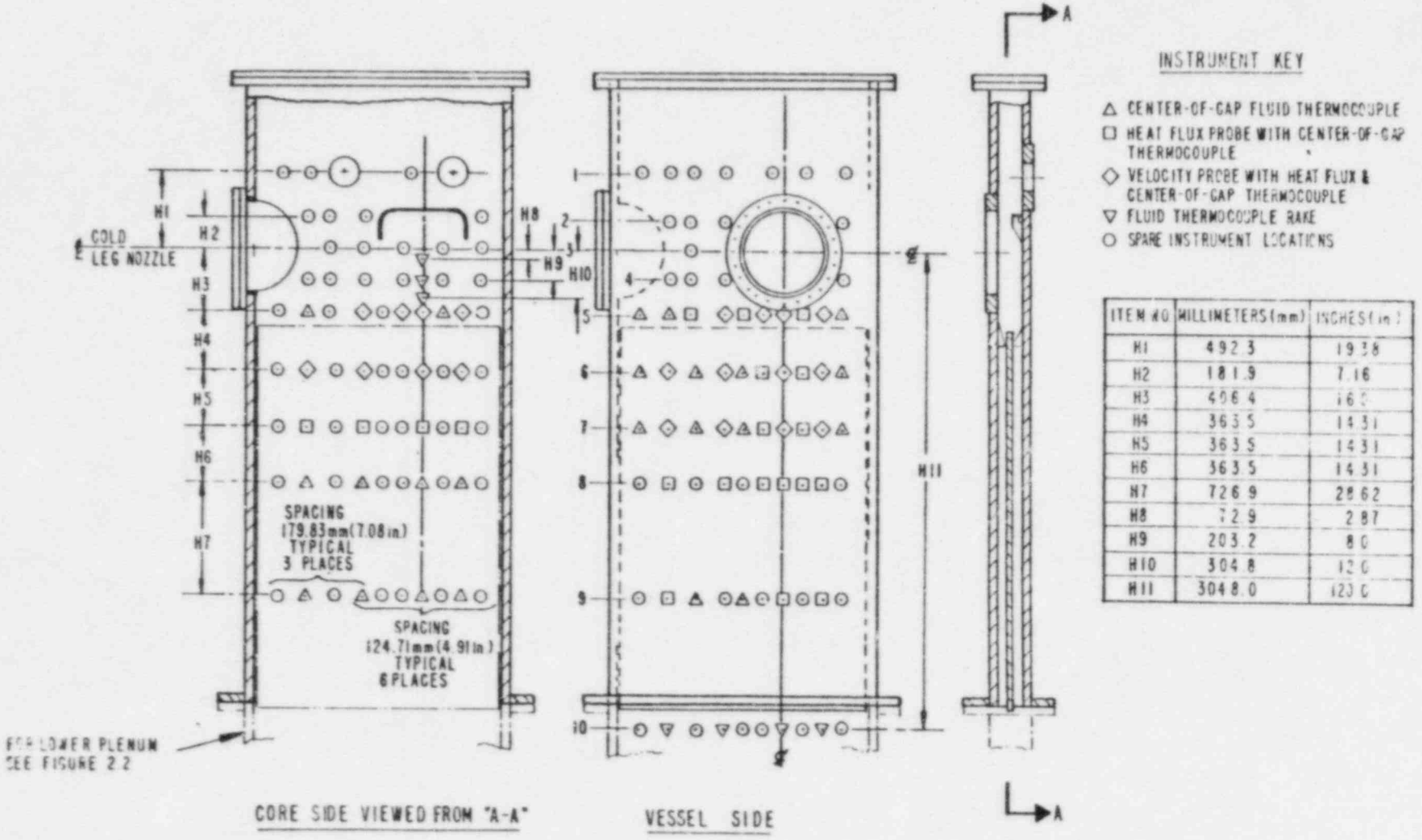

Figure 3-6. Downcomer Instrumentation

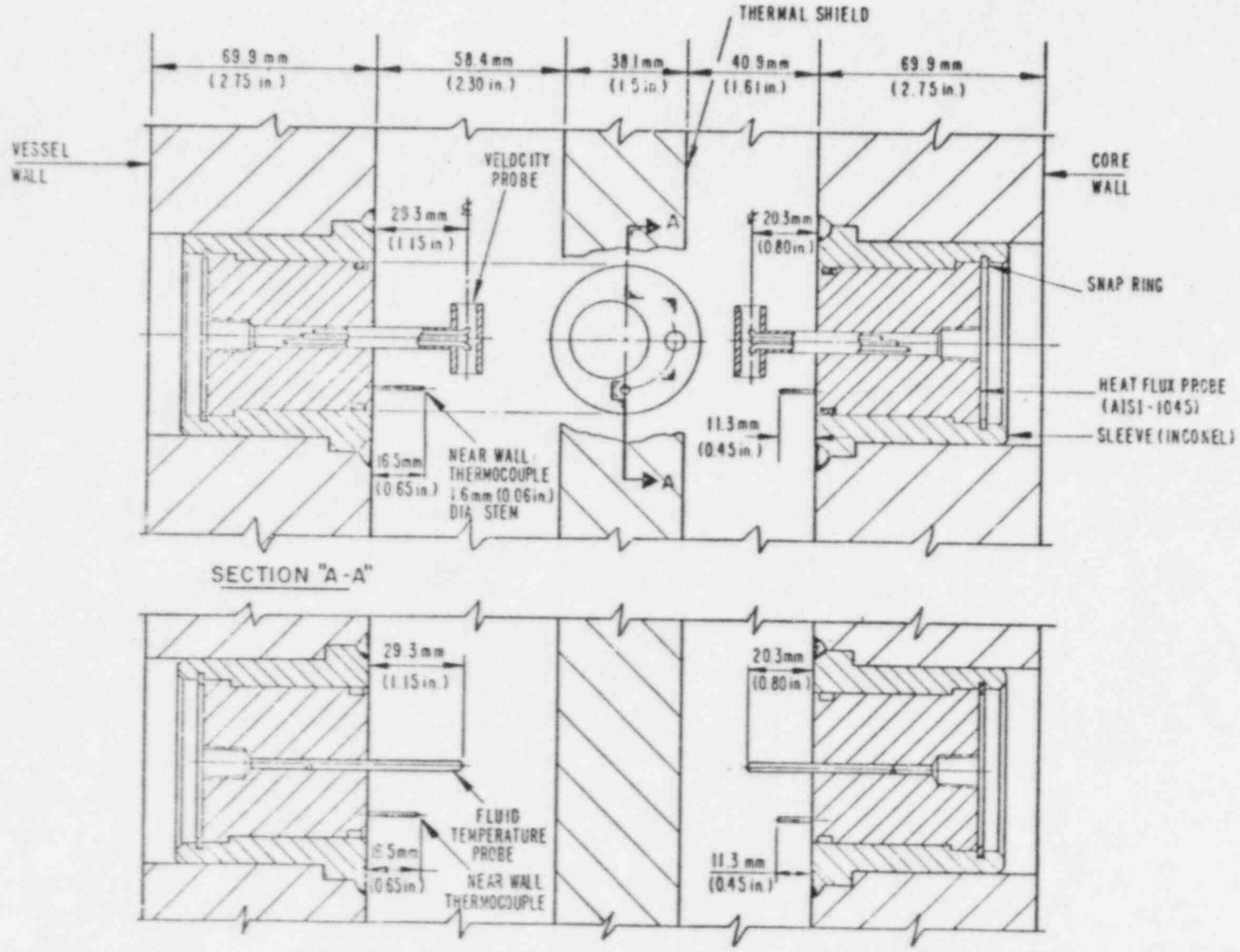

Figure 3-7. Test Vessel Wall Instrumentation Details

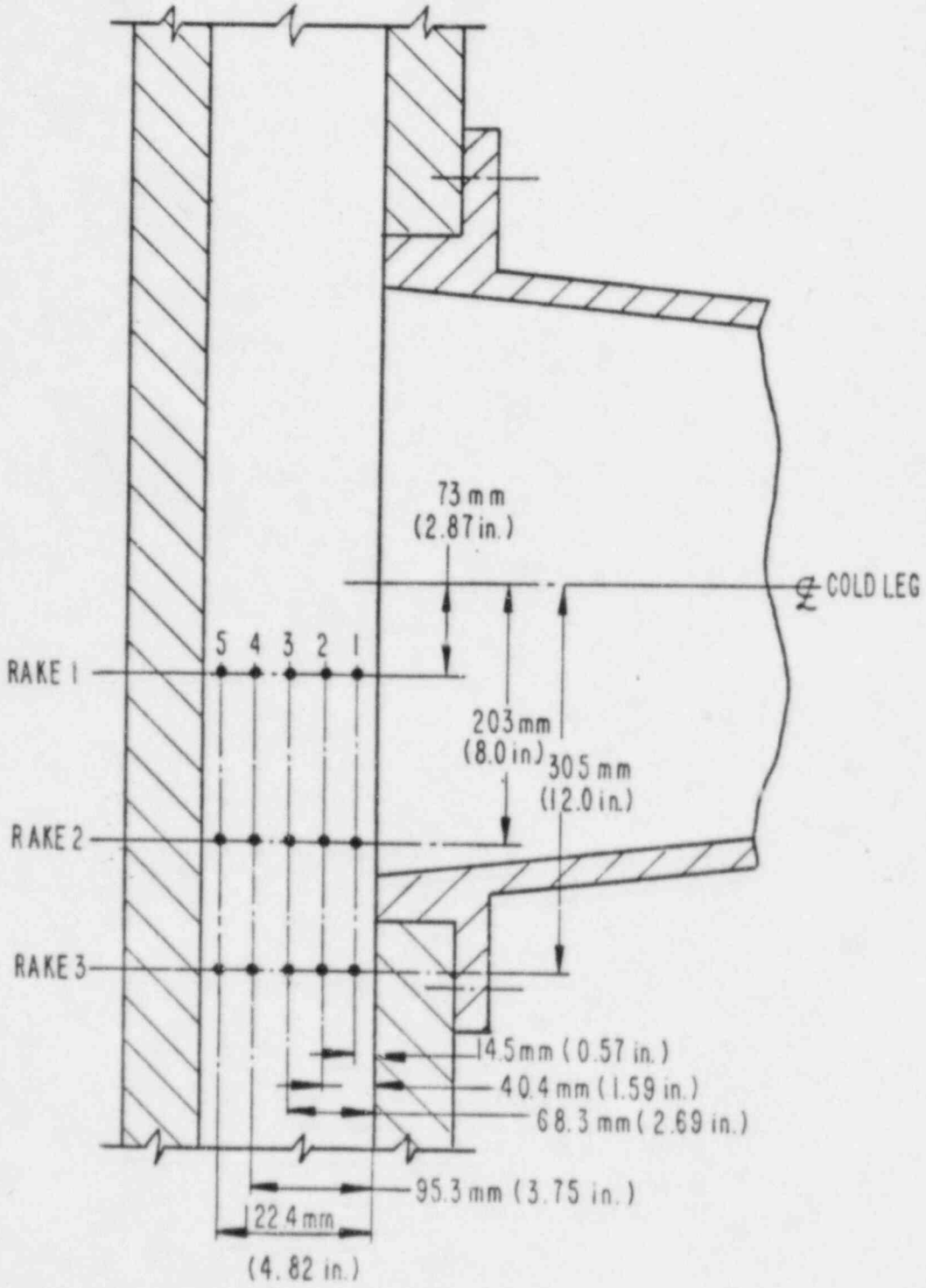

Figure 3-8. Downcomer Gap Temperature Rakes Near Nozzle Elevation

Finally, 5 fluid temperature probes are installed in the lower plenum to measure the vertical and span-wise temperature distributions before the fluid is discharged to the standpipe (see Figure 3-9).

The preceding discussion of instrument locations has concentrated on the layouts for tests with combinations of HPI and loop flow and with the thermal shield in place, which will constitute the majority of the anticipated tests. Thermocouples, velocity probes and wall heat flux probes can also be installed near the vent valves to study the thermal mixing and heat transfer in the region between the cold leg nozzle and the vent valves in those tests with vent valve flows. Figure 3-6 shows a number of spare instrumentation ports, including locations near the vent valves, and additional locations below the nozzle to facilitate instrument changes and additions if they are required later. Removal of the thermal shield will not require adjustment and relocation of instruments, but that can be done if indicated by test needs.

3.3.2 Instrument Design

As discussed earlier, the principal data from the testing are the temperatures and velocities of the fluid in the cold leg and downcomer models, and the rate of heat transfer between the walls of the downcomer and the fluid in the annulus. Following are descriptions of the instruments that are used to make these measurements and a discussion of the instrument measurement uncertainty.

VELOCITY PROBE

Several different fluid velocity measuring systems were considered for this testing project, including hot wire/film sensors, laser velocimetry, propeller and turbine probes and head probes. Hot wire/film velocity measurements are very difficult to achieve in the face of significant fluid temperature fluctuations and water impurities. Laser velocimetry is not easily applied and is quite expensive for multiple measurement locations in a high pressure test facility. Prior experience with insertable turbine probes showed that the bearings are a frequent cause of probe failure, particularly when low velocities must be measured. The major causes for bearing failure are accelerated wear due to contaminants in the fluid entering the bearings and overspeeding due to uncontrolled process variables. Of the candidate methods considered, only the head-type probe meets the requirement for being rugged and reliable and having a high probability of success in achieving the desired velocity measurements.

A head probe functions by measuring the total fluid pressure p_T and the fluid static pressure p_s in a flowing stream. The equation relating these pressures for an incompressible fluid is:

$$p_T = p_s + K \frac{\rho V^2}{2g_c} \qquad (3.1)$$

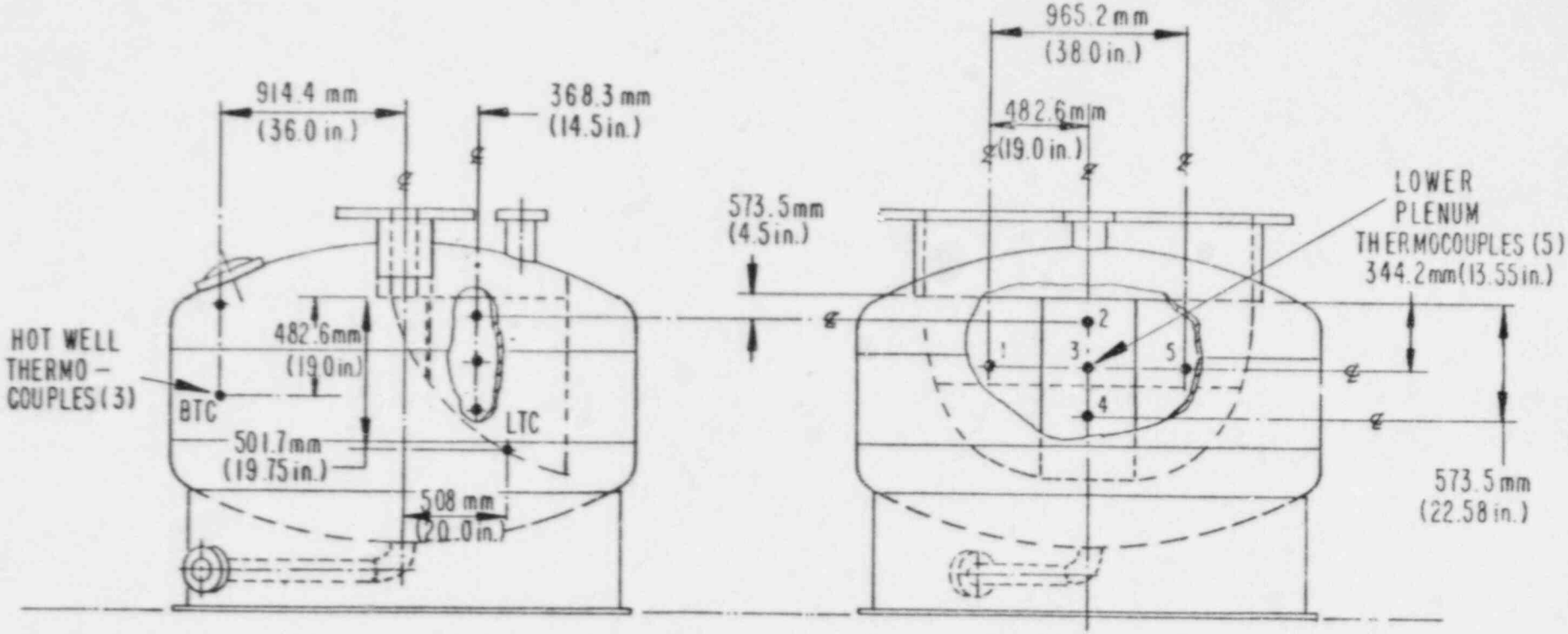

Figure 3-9. Lower Plenum Thermocouple Location

where

V = fluid velocity at the probe

P_T, P_s = total pressure and static pressure

ρ = fluid density at the probe

K = the probe pressure coefficient

g_c = dimensional proportionality constant (g_c = 1 in SI units, g_c = 32.174 lbm-ft/lb_f-s^2 in conventional English units)

In the common application the total to static pressure difference is measured directly using a differential pressure sensor, e.g. manometer or transducer, and when that difference is divided by the fluid density the velocity "head" H is obtained.

$$H = \left(\frac{P_T - P_s}{\rho} \right) \frac{g_c}{g} \tag{3.2}$$

Then the velocity of the fluid stream can be written as:

$$V = \left(\frac{2gH}{K} \right)^{\frac{1}{2}} \tag{3.3}$$

For conventional pitot-static probes, the pressure coefficient K is close to unity, whereas for the Kiel-static probe (Figure 3-10) being used in this program a pressure coefficient greater than unity has been measured. The pressure coefficient "gain" results from using the backfacing tap for measuring the static pressure where it is expected that the static pressure in the wake of the probe is less than the stream pressure.

Figure 3-11 displays the correlation obtained from calibration of a Kiel-static probe over the range of probe Reynolds numbers expected in the 1/2-scale test program. The pressure coefficient is seen to vary from K=2.0 at low Reynolds number to about K=1.7 at high Reynolds number. The uncertainty in the K-factor calibration is shown by the dashed lines on the graph. At low Reynolds number the uncertainty in K is about 30% ($\Delta K/K \approx 0.3$), and at higher Reynolds number (corresponding to a velocity greater than 0.1 m/s for water at 193°C) the uncertainty is decreased to about 10%.

Because of its symmetrical design, the Kiel-static probe can be used to measure fluid velocity in a bi-directional flow field, i.e. it can measure "reverse" flow. The pressure transducers that are used to measure the differential head are also bi-directional in order to measure velocity in both directions.

The shroud used on the Kiel-static probe reduces the sensitivity of the probe to flow angle deviations. We have found through our test work that the pressure coefficient remains essentially constant for flow angle deviations up to about 40° off-axis.

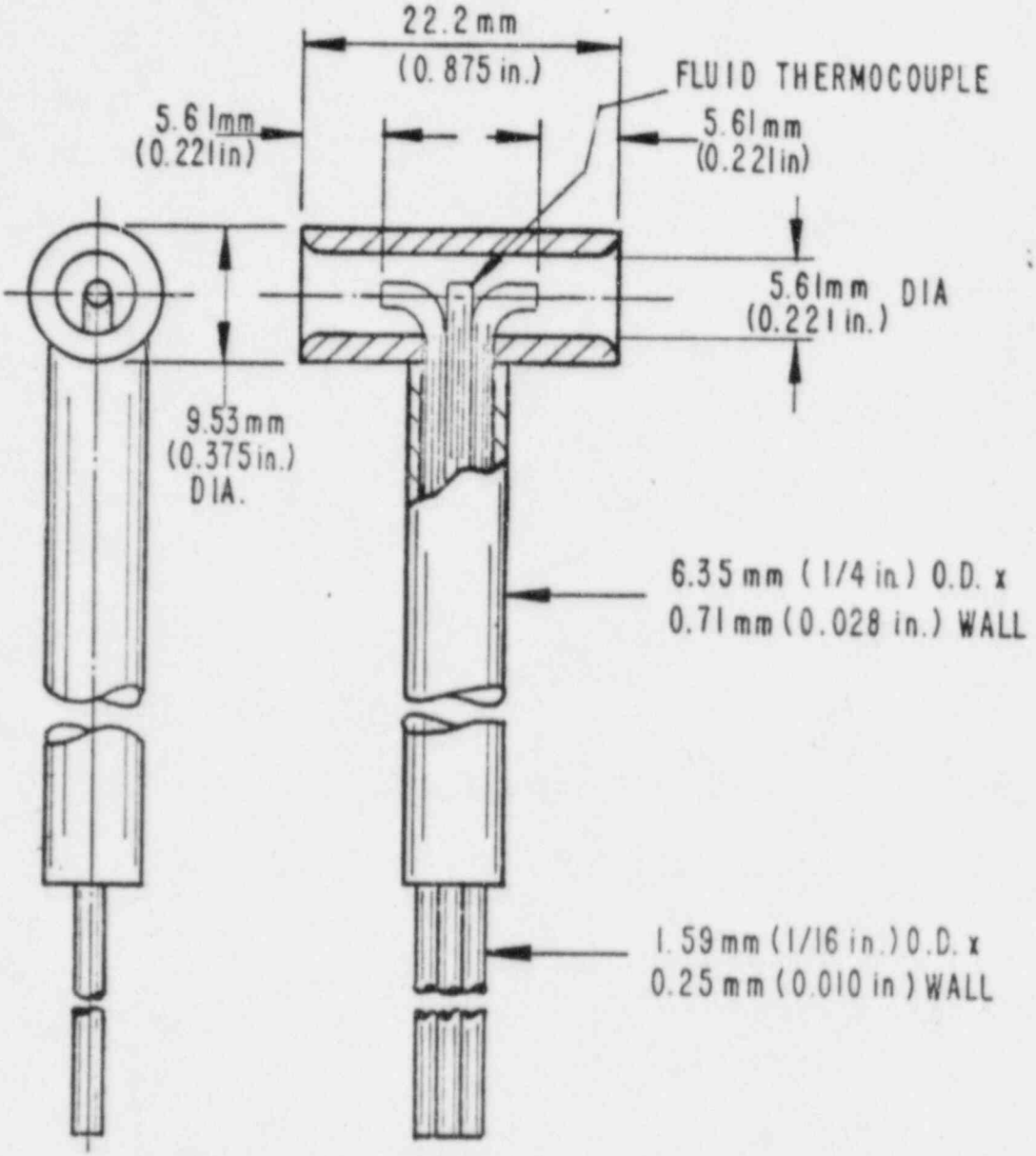

Figure 3-10. Kiel Static Velocity Probe

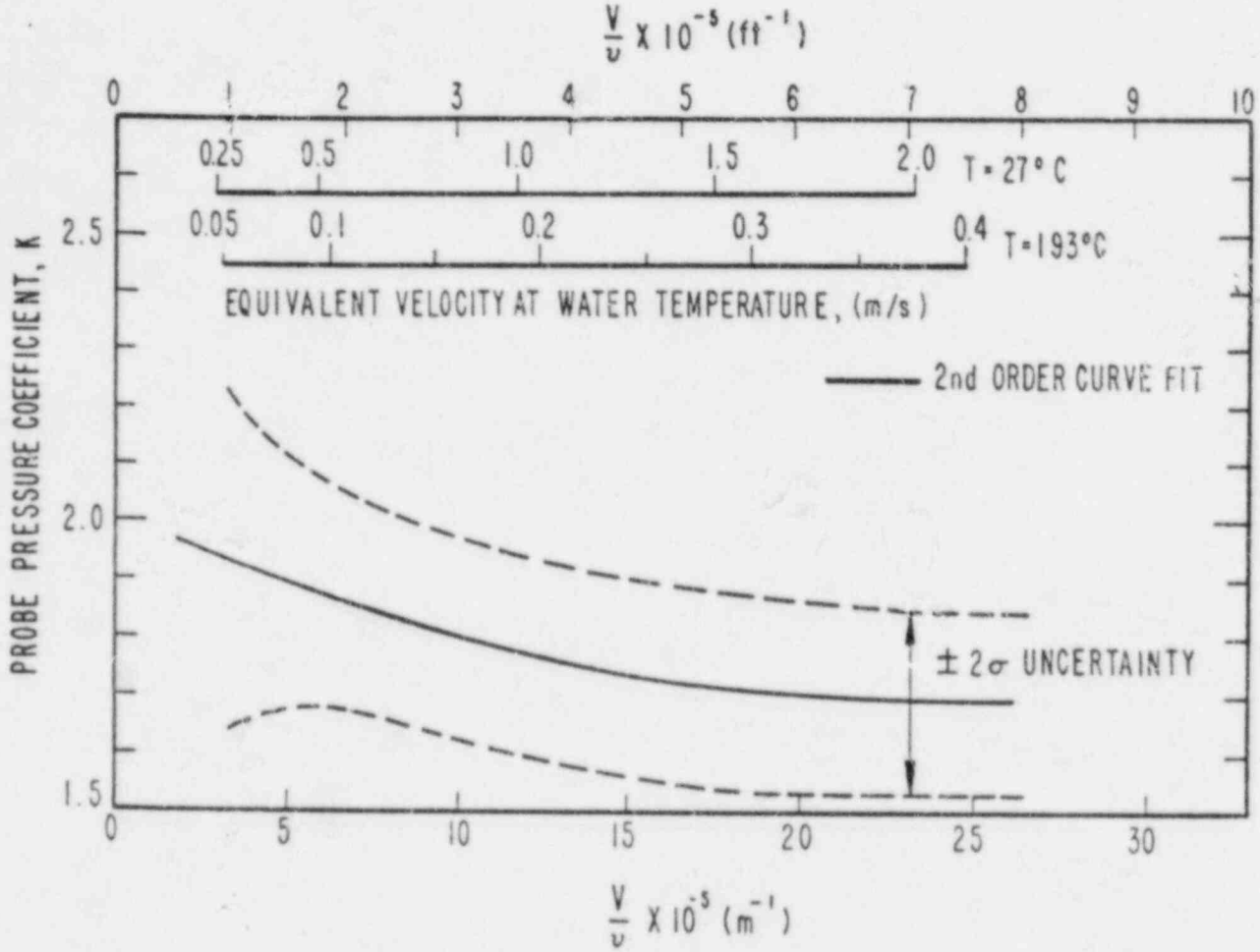

Figure 3-11. Velocity Probe Pressure Coefficient Calibration

The uncertainty in measured velocity can be calculated using the standard definition of uncertainty for a process in which the measurement errors are random and independent (18):

$$\left(\frac{\Delta V}{V}\right)^2 = \left(\frac{H}{V}\frac{\partial V}{\partial H}\frac{\Delta H}{H}\right)^2 + \left(\frac{K}{V}\frac{\partial V}{\partial K}\frac{\Delta K}{K}\right)^2 \qquad (3.4)$$

Performing the indicated differentiations and simplifying:

$$\left(\frac{\Delta V}{V}\right)^2 = \left(\frac{1}{2}\frac{\Delta H}{H}\right)^2 + \left(\frac{1}{2}\frac{\Delta K}{K}\right)^2 \qquad (3.5)$$

where $\frac{\Delta V}{V}$ = uncertainty in the velocity V calculated from Eq. 3.3

$\frac{\Delta H}{H}$ = uncertainty in the measured velocity head H

$\frac{\Delta K}{K}$ = uncertainty in the probe pressure coefficient K.

The probe pressure coefficient calibration uncertainty was described earlier and is shown in Figure 3-11. The uncertainty in the measured differential head $\Delta H/H$ is comprised of several components:

1. pressure transducer accuracy, including linearity, hysteresis and repeatability, E_p
2. transducer calibration accuracy, E_c
3. probe manometer effect, E_{pm}
4. line manometer effect, $E_{\ell m}$
5. transducer static pressure effect, E_{sp}
6. transducer ambient temperature effect, E_a
7. transducer reading error, E_r

Transducer accuracy refers to the ability of the transducer to correctly reproduce (via its voltage output) the value of the applied pressure, in this case considering errors due to non-linearity, hysteresis (up-scale vs. down-scale offsets) and repeatability. For the transducers used to measure velocities in this facility, the manufacturer quotes this error to be 0.25% of the calibrated span. Based on experience with use of these transducers a more likely error estimate is 0.15% of the calibrated span, amounting to 0.3 mm H_2O for a span of 200 mm H_2O. On the other hand, the calibration error E_c is proportional to the uncertainty in the applied pressure used to set the full-scale transducer span. This error is estimated to be less than 1.2 mm H_2O (0.05 in. H_2O) for a full scale span of 200 mm (8 in. H_2O) or about 0.6% of the indicated differential pressure.

Probe and line manometer errors (E_{pm}, $E_{\ell m}$) result from differences in the fluid density between the two pressure lines extending from the probe head to the pressure transducer. Even with the large differences in water temperature ($\Delta T=25°C$) in the lines within the velocity probe body, the probe manometer error E_{pm} will be less than 0.25% of the differential head. The potential for manometer errors caused by density differences in the lines from the probe to the transducer $E_{\ell m}$ is essentially eliminated by locating the transducers very close to the same elevation as the probes and by insulation on the lines to maintain them at uniform temperature.

Transducer static pressure effects can cause a shift in the output at zero differential pressure and an error in the calibrated span. In practice the zero shift is compensated by the testing and data reduction procedures while the span error is very small (estimated to be 0.04% of calibrated range at the nominal test pressure of 1.3 MPa).

Changes in the ambient operating temperature of the transducers can also cause an error in their reading. This error might be as large as 0.15% of the calibrated span for an ambient change of about 5°C (10°F).

The last error contributing to the uncertainty in the measured head is the accuracy with which the data acquisition system can read the transducer voltage. Regular and frequent calibrations of the data system reduce this uncertainty to less than 0.1% of the full-scale transducer output.

These error terms and magnitude estimates are summarized in Table 3-3.

The individual error contributions can be combined as the sum of squares to calculate the total uncertainty in measured head:

$$(\Delta H)^2 = E_p^2 + E_c^2 + E_{pm}^2 + E_{\ell m}^2 + E_{sp}^2 + E_a^2 + E_r^2 \qquad (3.6)$$

Notice in Table 3-3 that the calibration and probe manometer effect errors (E_c and E_{pm}) are proportional to the measured head. Because these two errors are relatively small compared with the others, Eq. (3.6) can be simplified to:

$$(\Delta H)^2 = E_p^2 + E_{sp}^2 + E_a^2 + E_r^2 \qquad (3.7)$$

Substituting the error magnitudes in Table 3-3, the estimated uncertainty in measured head $\Delta H/H$ is 0.48 mm H_2O (0.019 in. H_2O).

Figure 3-12 shows the estimated uncertainty in the measured velocity for a range of velocities of interest in the experimental project. This plot combines the effects of probe calibration uncertainty $\Delta K/K$ and head uncertainty $\Delta H/H$ as expressed by Eq. 3.5. At low velocities the uncertainties can be quite large, primarily due to the error in the head measurement. The expected situation is much more favorable since tests at 1/5-scale indicate that actual velocities in the cold leg are 3 to 10 times higher than the superficial velocity, j_{CL}. This

Table 3-3 VELOCITY HEAD UNCERTAINTY CONTRIBUTIONS

COMPONENT	ESTIMATED UNCERTAINTY	SOURCE OF ESTIMATE
E_p	0.3 mm H_2O (0.012 in. H_2O)	0.15% of calibrated span of 200 mm H_2O, based on application experience
E_c	0.6% of head	Based on estimated error of 1.2 mm H_2O at full scale of 200 mm H_2O
E_{pm}	0.25% of head	Based on 25°C temperature difference between lines, error proportional to transducer volumetric displacement
E_{lm}	0	Controlled by installation design
E_{sp}	0.08 mm H_2O (0.003 in. H_2O)	Manufacturer estimate for span error; zero offset compensated in data reduction
E_a	0.3 mm H_2O (0.012 in. H_2O)	Manufacturer estimate of ambient temperature effect for 5°C change
E_r	0.2 mm H_2O (0.008 in. H_2O)	Based on application experience with data recording system

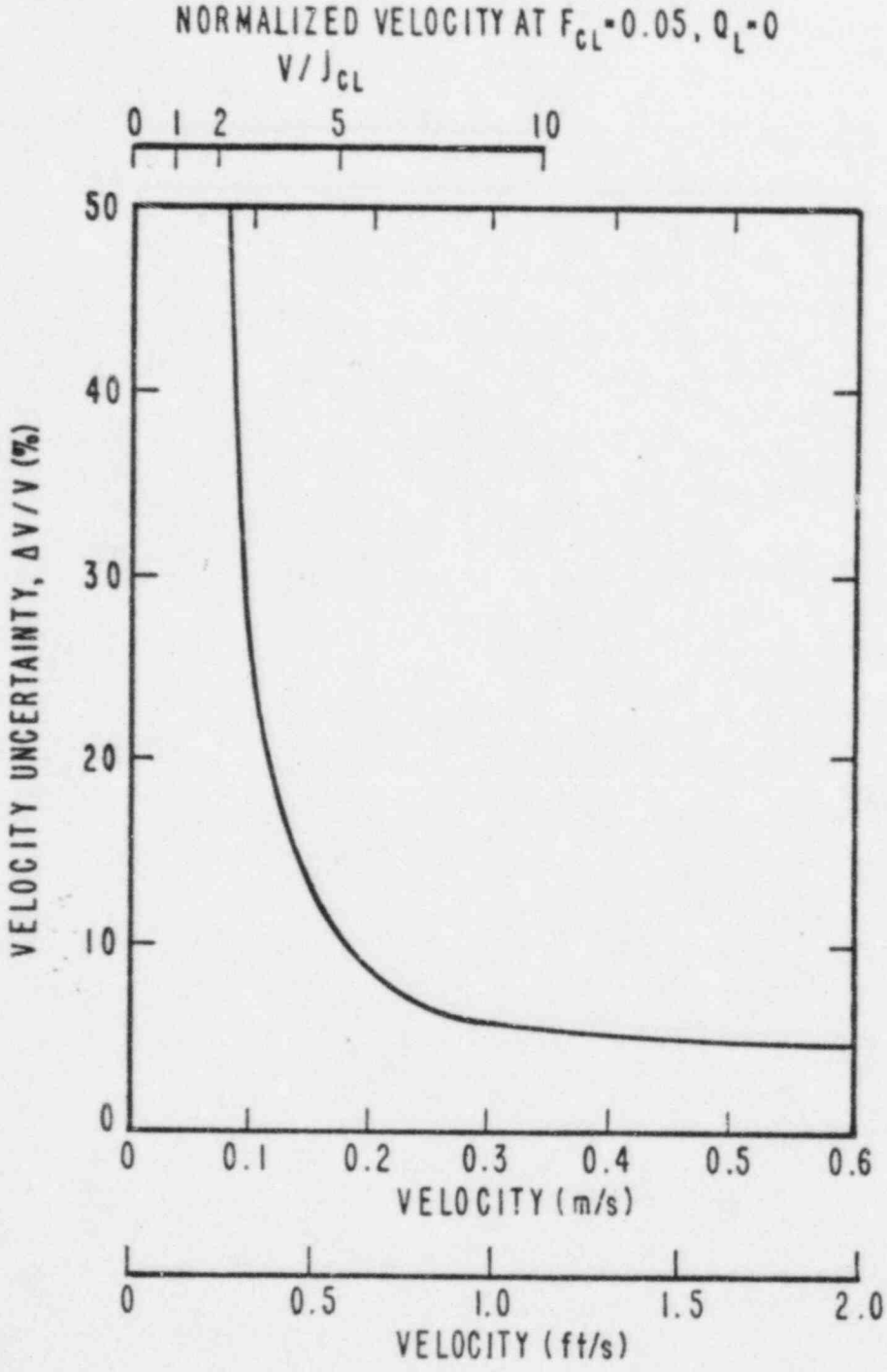

Figure 3-12. Velocity Probe Measurement Uncertainty

effect is illustrated by the upper scale in Figure 3-12 which shows the measured velocity V normalized by the HPI flow superficial velocity for a situation with zero loop flow and cold leg Froude number F_{CL} = 0.05. For V/j_{CL} >3 the uncertainty is less than about 30%.

TEMPERATURE PROBE

The test facility design includes 261 temperature probes in the cold legs, downcomer and lower plenum to measure fluid and metal surface temperatures. Ten of the temperature measurements in the cold leg will be made with probes having a "fast" response.

All temperature measurements in the facility are made using grounded junction, ANSI Type E (Chromel-Constantan) thermocouples. There are a number of different configurations of thermocouple probes, some are integral with the velocity probes, (see Figure 3-10), others are installed on multi-probe rakes in the cold legs and downcomer or as single probes inserted through the cold leg and downcomer walls to measure fluid temperatures, and the metal wall thermocouples are fabricated as part of the heat flux probes.

A typical grounded junction probe tip design is shown schematically in Figure 3-13. It is constructed from a 3.18 mm (1/8 inch) diameter stainless steel sheath with 0.51 mm (0.02 inch) diameter thermocouple wire protected with ceramic (usually MgO) insulation. The thermocouple wires extend to the end of the sheath and are welded or silver-soldered together, sealing the tip of the sheath and forming the thermoelectric junction. This probe has a thermal time constant (1/e response to rapid temperature change) of less than about 0.5 seconds.

Thermocouples installed on multi-probe rakes are similarly constructed, except that they are fabricated from 1.59 mm (1/16 inch) diameter sheath material with 0.25 mm (0.01 inch) thermocouple leads. The smaller sheath is more flexible and facilitates assembly of the rakes, and is adequately rugged to withstand the anticipated fluid forces.

The fast response thermocouple design is also shown in Figure 3-13. It is fabricated from very small thermocouple wire (0.08 mm diameter) which is formed into a twisted junction and then silver-soldered, closing off the end of the support stem. These thermocouples have a measured rise time of 33 ms to a step change in temperature.

All thermocouples in the test facility are fabricated from wire having special limits-of-error calibration equivalent to a maximum temperature error of 1°C for the Type E material. Other contributing factors in evaluating the overall temperature measurement accuracy include:

1. stem conduction effects
2. reference temperature uniformity
3. reference temperature accuracy
4. amplifier gain stability and accuracy

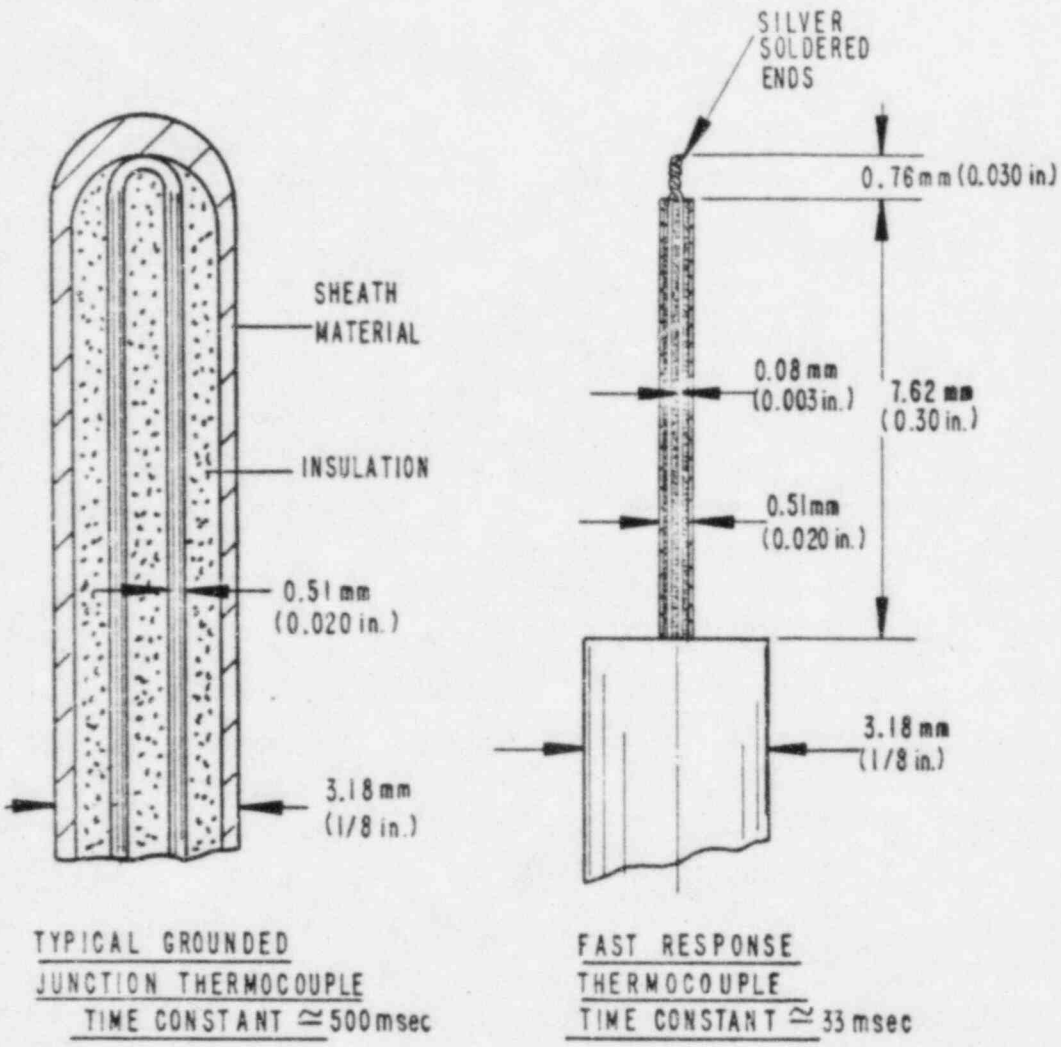

Figure 3-13. Fluid Thermocouple Designs

Stem conduction errors arise from heat conduction between the thermocouple measuring junction and a warmer or colder boundary through which the probe is inserted. This error can be approximated by using standard "fin-tube" heat transfer correlations, and these same correlations can be used to design an installation configuration which minimizes the conduction error. The maximum stem conduction error occurs with the 1.6 mm diameter probe used to measure the near-wall fluid temperature in the downcomer. That error is approximately 0.3°C for a wall to fluid temperature difference of 15°C.

The stability and accuracy of the reference temperature is described with the aid of Figure 3-14. The lead wires from all thermocouples are terminated in an isothermal "zone block" from which copper leads are used to connect the signal to the input of the instrumentation amplifiers. The zone blocks consist of thick (25 mm) plates of aluminum to which are mounted screw terminals for making the thermocouple connections. The zone blocks are insulated from the ambient to minimize the rate of drift with changes in the ambient, thereby ensuring overall temperature uniformity. The manufacturer's estimate for zone block non-uniformity is less than 0.1°C for a 10°C step change in the ambient.

The temperatures of the zone blocks (there are a total of 5 zone blocks in the facility) are measured with ANSI Type T (copper-constantant) thermocouples with reference junctions immersed in an ice-water bath at 0°C. The estimated error of this reference temperature system is about 1.0°C.

Inaccuracies due to amplifier gain stability are expected to be quite small because of the scheme used to record amplifier gain each time a temperature measurement is made. Using a worst-case assumption of stability, the maximum error (including errors in the analog to digital converter) is expected to be less than 0.6°C.

Combining all of these known error sources as the sum-of-squares, the total uncertainty in measured temperatures is expected to be less than about 1.6°C.

HEAT FLUX PROBES

The wall-to-fluid heat transfer in the downcomer is the most challenging measurement in the test program. Although the fluid temperature field has dominant importance to the analysis of thermal mixing, an adequate knowledge of heat transfer rates is also desirable to the assessment of pressurized thermal shock. Unlike the velocity field, which is supportive data, the measured heat transfer coefficients are useful directly to develop and support heat transfer models.

The instantaneous wall-to-fluid heat transfer coefficient h can be determined by:

$$h = \frac{q''}{(T_w - T_f)} \qquad (3.8)$$

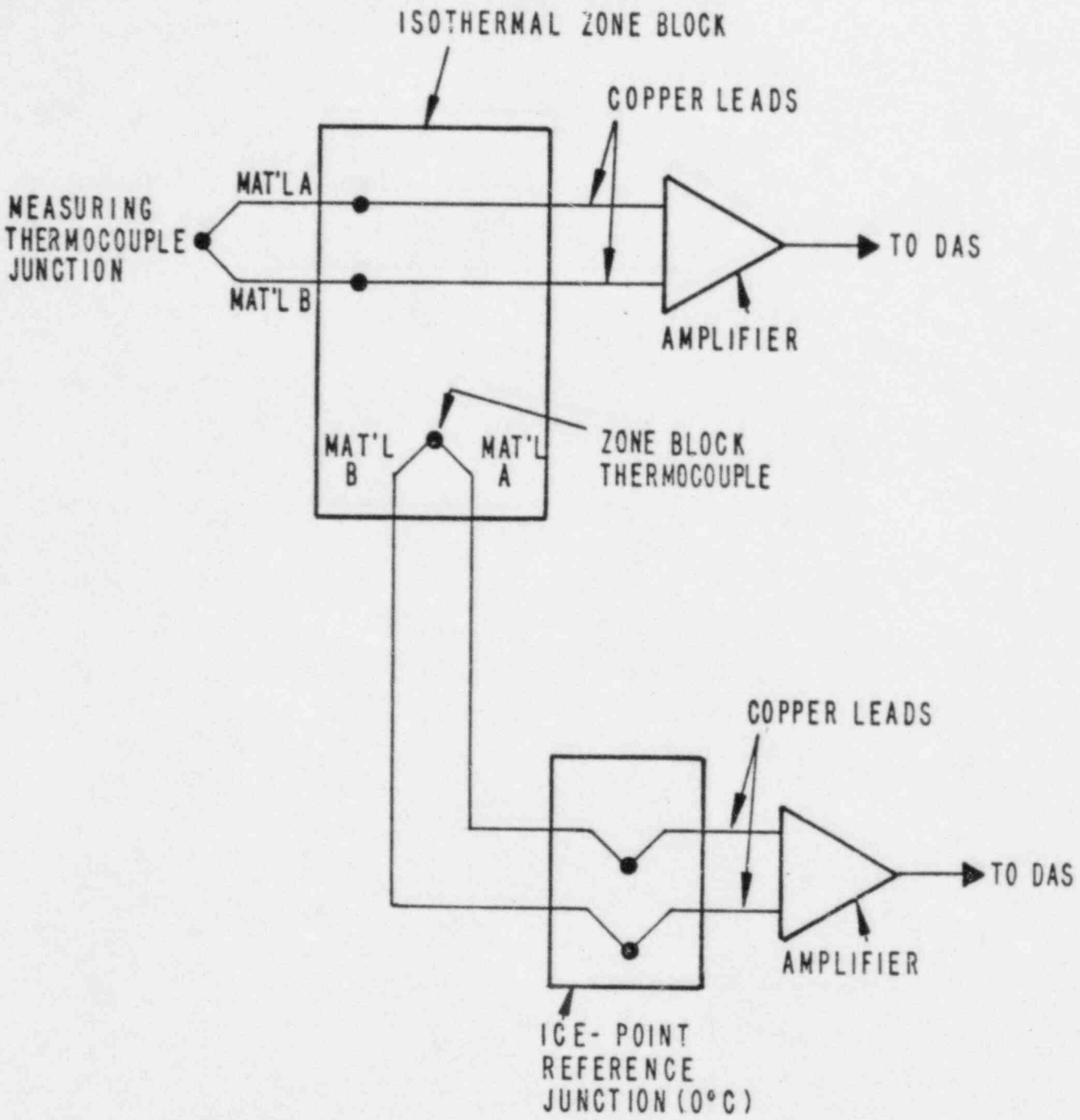

Figure 3-14. Thermocouple Reference Junction System Configuration

where q'' = wall heat flux
T_w = wall surface temperature
T_f = fluid temperature

Various means will be employed in the testing to measure each of these parameters and to determine h. These approaches are outlined here and will be specified more fully in Section 5 on Data Reduction Procedures.

The instantaneous wall temperature T_w will be determined directly from the thermocouple measurements.

The fluid temperature T_f can be determined from either the "center-of-gap" or near-wall thermocouple probes adjacent to the heat flux probe. We expect to show that the temperatures are well mixed locally so that data from either probe may be used with equal results. This approach will confirm that hypothesis generally and provide local redundancy.

The heat flux q" will be determined by two main means:

1. the instantaneous reading of the wall surface temperature probe will be inverted using the principles of one-dimensional conduction

2. heat flux probes (Figure 3-15) will measure differential temperatures very near the wall surface.

In addition to comparison of these independent and redundant approaches, the heat flux can be integrated over time and compared with the energy change of the wall.

The approach outlined above includes ample redundancy and some methods of assured performance. Following an evaluation of shakedown data, the method based on the inversion of the wall surface temperature measurement was selected. This procedure is described more completely in Section 5. In a typical test the estimated uncertainty in heat transfer coefficient ranges from 20% early in the cooldown period to about 30% later in the test. A detailed examination of heat transfer coefficient uncertainty is found in Appendix A.

3.4 DATA ACQUISITION SYSTEM

All test measurements are recorded using the computerized data acquisition system (DAS) shown schematically in Figure 3-16. The DAS is structured around the use of a Digital Equipment Corporation PDP 11/70 minicomputer with a LPA11 microcomputer, analog-to-digital (A/D) converter and multiplexer for acquiring analog data. That computer facility is configured to acquire data from 64 analog channels from the laboratory area where the thermal mixing tests are conducted.

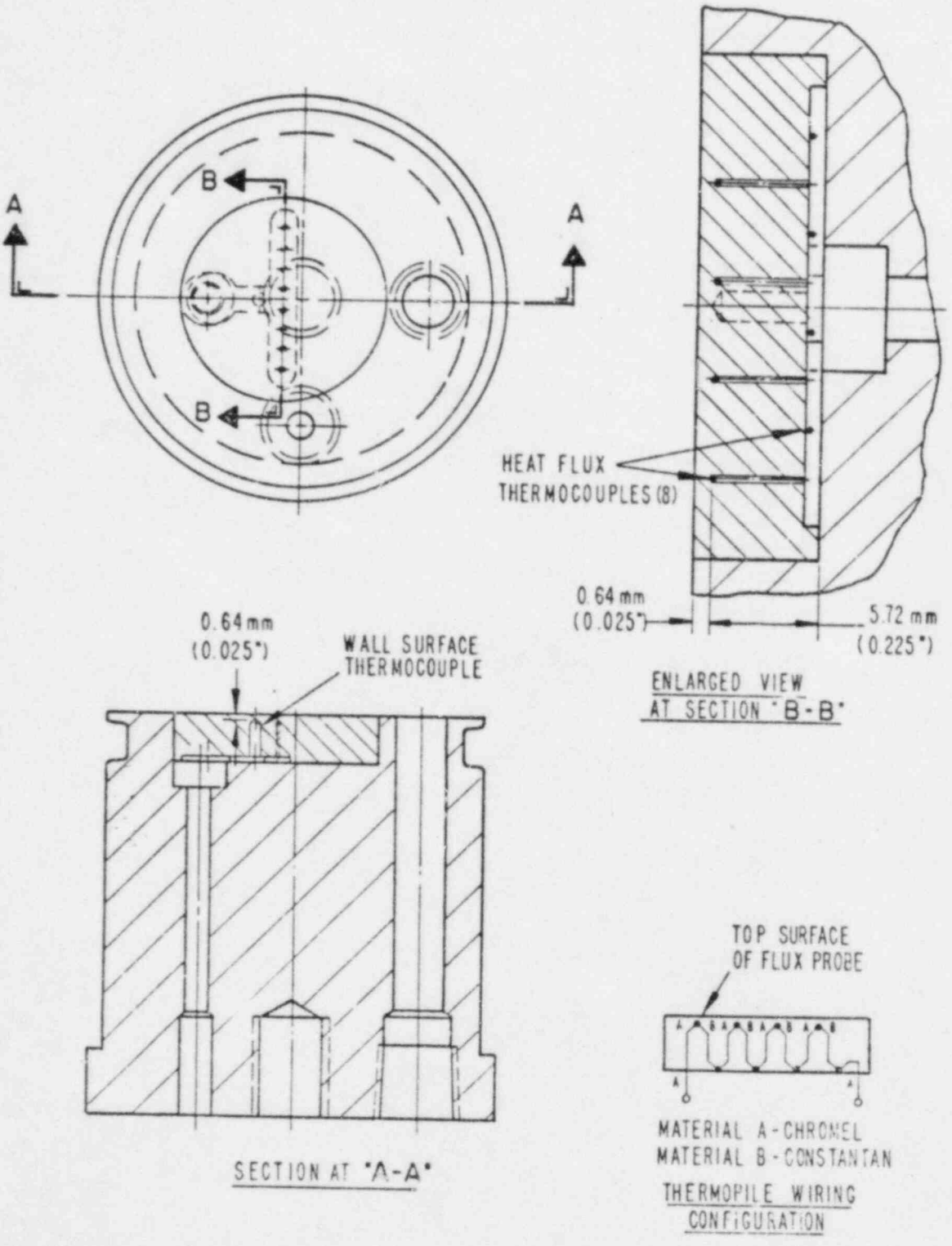

Figure 3-15. Wall Heat Flux Probe Design

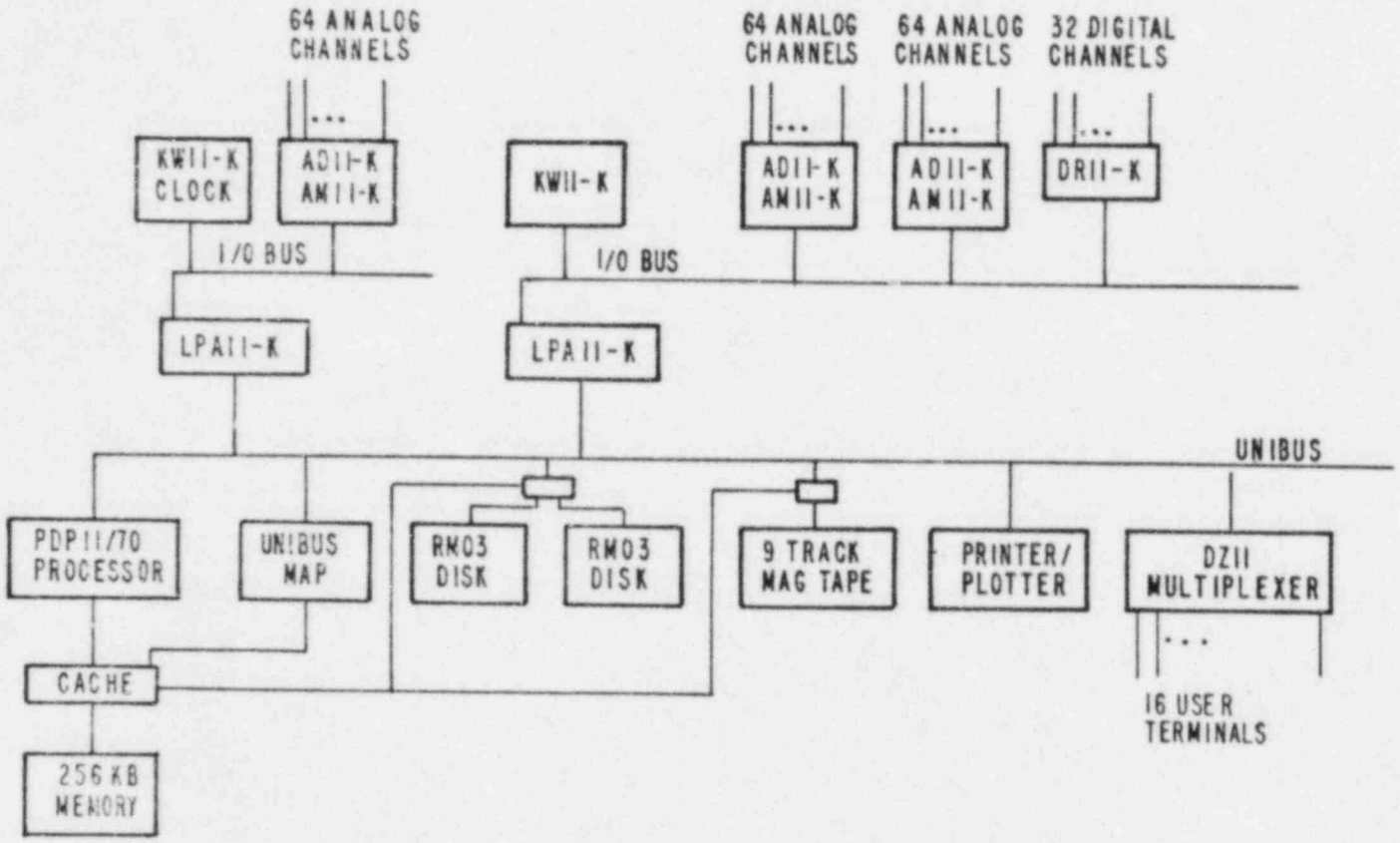

Figure 3-16. Data Acquisition and Processing Computer

Because of the increased number of measurements being recorded in this experimental project (approximately 350) a new multiplexer front-end to the A/D converter was built. Figure 3-17 is a schematic of the multiplexer concept including the control method and the input to the A/D converter of the computer. Outputs from the measurement transducers are connected to 16 channel, differential input multiplexers, each having a fixed gain instrumentation amplifier on its output. There are 28 multiplexer blocks in the system set up to handle the different types of instruments with various signal levels and conditioning requirements. The output from each block is connected through a switching system to the input of the A/D converter in the LPA.

External clocks controlled from a single oscillator are used to control the rate and sequence of switching among the instrument multiplexers and the inputs to the A/D converter, and also to enable the microcomputer to sample the input signal at the appropriate time. The rate of input channel switching is 448 Hz, providing one reading per second from each input channel (28 blocks x 16 channels/block = 448). Readings of one time per second are sufficient because basic instrument responses are not much greater than that, except for the few fast response thermocouples. Those data can be processed at higher rates by independent means, if required.

The first two inputs of each multiplexer block are used to provide calibration voltages for measuring the offset voltage and voltage gain factors of each amplifier. These inputs are sampled in sequence with the transducer outputs so that amplifier offsets and gains are available for each cycle through the 28 blocks. The use of two channels for calibration voltages reduces the useful capacity of each multiplexer to 14 signal inputs or a total of 28 x 14 = 392 signals. This is more than adequate for the present facility instrument design and provides room for future growth in the number of instruments if that is found to be desirable or necessary.

The data acquisition computer is used to acquire, store and reduce the test data and to prepare graphical and tabular data displays for quick look reports. In addition, during the pre-test period of setting test conditions and during the actual test sequence, some critical test parameters such as loop and HPI flow rates and temperatures, lower plenum exit temperature and others are monitored and displayed to the test operators to assist the setup and to alert the operators to out-of-tolerance conditions.

3.5 INSTRUMENT CALIBRATIONS

Measuring instruments are calibrated either prior to installation in the test facility or while in-place during the pre-test heatup period. The basic procedures for calibrating specific instrument types and calibration uncertainties are reviewed here.

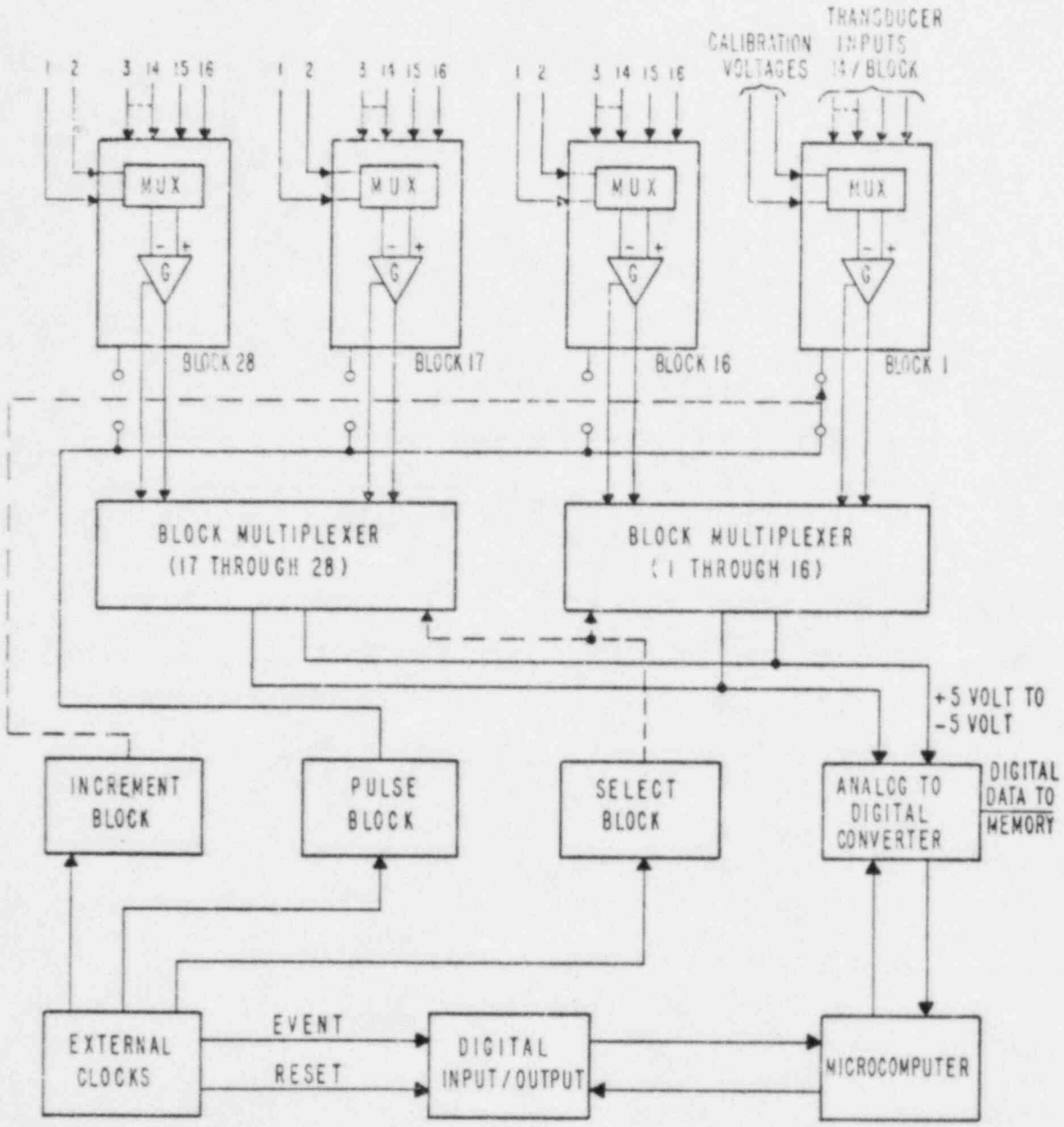

Figure 3-17. Signal Multiplexers for Data Acquisition System

3.5.1 Pressure Transducers

Pressure transducers are calibrated over their full range of expected operation, using water and mercury manometers and precision pressure gauges maintained by Creare's instrumentation laboratory. The output voltage from the transducers is measured with a precision digital voltmeter (DVM) which is also maintained by Creare's instrumentation laboratory. The voltages and applied pressures are fitted to a first-order polynomial using a least-squares regression method. The resulting coefficients are used directly in data reduction programs to convert measured transducer outputs to pressures or differential pressures.

3.5.2 Velocity Probes

Calibration of the velocity probes involved determining the pressure coefficient K over the range of Reynolds number expected to be encountered in the experimental project. This was accomplished by measuring the differential pressure between the forward-facing and reward-facing ports on a velocity probe with the probe inserted in a flow tunnel at a known total flowrate. By measuring the fluid properties (pressure and temperature) to determine density and with a known flow area the velocity at the probe was calculated.

Calibrations were performed using both air and water in order to provide viscosity variations which covered the full range of Reynolds number (Vd/ν). Also, several probes were calibrated and some of the probes were reversed in the flow tunnel to check for sensitivity of flow direction on the computed K-factor. Flowrates were measured using orifice meters and rotameters having a maximum uncertainty of 5% of the indicated flow. Differential pressures were recorded from water manometers and pressure transducers. The uncertainty in measured head ranged from 12% at the lowest calibration velocity to less than 1% at the highest velocities used. The calibration data were used to calculate a pressure coefficient as defined by Eq. 3.1, producing the calibration curve shown in Figure 3-11.

3.5.3 Heat Flux Probes

Wall heat flux probes (Figure 3-15) were calibrated in a special facility constructed for this project. In that facility the probes were subjected to a steady heat flux (two levels were used, approximately 25 kW/m^2 and 50 kW/m^2) from an electrical heater mounted on the exterior face of the probe body. The face of the probe was in contact with a copper rod that was immersed in a circulating water bath that served as a heat sink. To ensure one-dimensional heat flow and to minimize heat losses, the heater, flux probe and water bath were thoroughly insulated.

After thermal equilibrium was achieved, the electrical power input to the heater, flux probe output voltage, flux probe surface temperature, heat sink water flow rate and inlet and outlet water temperatures were recorded. These data were then used to compute a heat flux probe sensitivity factor defined as the ratio of measured thermoelectric

voltage from the differential thermocouples in the flux probe to the measured input heat flux. The sensitivity factors at the two calibration fluxes compared within about 1% for any given flux probe, demonstrating the linear behavior of the probe design. Also, the data were used to compare the energy increase in the heat sink water to the input power of the electric heater. This energy balance always compared within 5% of the power input providing a good check on the insulation effectiveness and the overall quality of the procedure.

Based on an evaluation of the calibration facility and procedures, the uncertainty in calculating the flux probe sensitivity factor is less than 10%. However, during shakedown testing it was determined that the probe output was as much as 50% higher than that corresponding to the heat flux determined from an overall energy balance on the downcomer walls. It is believed that this discrepancy is due to the transient response of the probes. While the probe calibration was conducted under steady-state conditions, the actual measurement conditions have rapid heat flux and temperature transients resulting from the plume meandering in the downcomer gap. Because the transient fluctuations vary from location to location in the downcomer, it is not possible to obtain a meaningful transient calibration of the probes. Hence it was decided to reduce the data using the more laborious, but still accurate, method of inverting the wall surface temperature measurement. As described in Section 5, the estimated uncertainty in the heat flux measurement is in the range from 10% early in the test to 25% after three characteristic mixing times.

3.5.4 Thermocouple Probes

Because of the large number of temperature probes used in the test facility and due to the bulky configuration of some of the multiprobe rakes, individual thermocouples were not calibrated for this project. Instead, the thermocouple output voltage is assumed to match that in the standard thermocouple tables, within the uncertainty (1°C) of the special grade wire used in the fabrication of the thermocouple. The validity of this assumption is substantiated by the observed uniformity of the measured temperatures in the fluid and in the wall surface during the pre-test period prior to injection of HPI.

3.6 INSTRUMENT BLOCKAGE

The test facility design includes large numbers of fluid temperature and velocity measurements in the cold leg and downcomer, and concentration of these measurements at specific locations to provide detailed temperature and velocity profiles to aid in the modeling of fluid mixing during HPI injection. Individual instruments have been designed to be as small as reasonably practical, but the presence of probes and rakes (groups of probes arrayed on a single support) in the fluid passages will cause some perturbations in local velocity producing mixing which might not otherwise occur.

The extent to which spurious mixing does occur is expected to be small because the blocked flow areas are small. For example, the maximum blocked area in the cold leg is only about 8% of the total area in the

horizontal cold leg configurations (Figures 3-2 and 3-3) and about 9% in the inclined cold leg design (Figure 3-4). The maximim blockage occurs at the C5 location near the exit of the cold leg. At other cold leg measurement locations the blockage is only 5%. In the downcomer, the maximum area blocked by probes at any horizontal measurement plane is only 1% of the flow area between the thermal shield and downcomer walls.

4. TEST PLAN AND PROCEDURES

This section describes an overall plan for the thermal mixing tests, including selection of the test conditions and a possible full matrix of tests. The procedures for conducting steady-state and transient tests are also outlined.

The actual number and conditions of tests to be performed will depend on such factors as strategic and technical needs for these data, and the results of the initial tests. To provide a larger context for evaluation of initial results we have outlined a possible multigeometry project of 75 tests based on information presently available. The reader should expect many changes to this matrix as comments on this test plan continue to be provided and as data are obtained.

The testing is carried out in accordance with Creare Quality Assurance procedures that meet the requirements of ANSI N45.2. Details of the procedures specific to this project and documentation for the as-built facility and instrumentation are incorporated in the project Design Record File (DRF).

4.1 TEST CONDITIONS

Mixing of HPI in the cold leg and downcomer is buoyancy driven and the results of the scaling analysis (15) suggest that preserving HPI Froude number will be necessary in the test program. The Froude number for the HPI flow is defined as:

$$F_{CL} = j_{CL,H}/[gD_{CL}(\rho_H-\rho_L)/\rho_H]^{\frac{1}{2}} \tag{4.1}$$

where

$$j_{CL,H} = \frac{Q_H}{A_{CL}} \tag{4.2}$$

ρ_H and ρ_L = densities of the HPI and loop flow at their inlet conditions, respectively.
D_{CL} = diameter of the model cold leg.
Q_H = volume flow rate of safety injection water.
A_{CL} = area of the cold leg.
g = gravity constant.
$j_{CL,H}$ = superficial velocity of HPI in the cold leg.

For the purposes or sizing the support facility and for selecting test conditions, the approximate ranges of hydraulic parameters and HPI characteristics of interest to the pressurized thermal shock situation are shown in Tables 4-1a and 4-1b. For comparison, the range of test conditions for the 1/2-scale program and those used in the 1/5-scale tests (2 - 8) are also given in Tables 4-1a and 4-1b. Typical water property data are shown in Tables 4-2a and 4-2b over the temperature range of interest to the prototype and testing situations.

A Froude number of 0.05 was selected as the baseline for designing a test matrix at 1/2-scale. That Froude number represents the center of the range of F_{CL} used in the 1/5-scale testing and is the Froude

Table 4-1a PROTOTYPE THERMAL AND HYDRAULIC PARAMETERS COMPARISON WITH 1/2-SCALE AND 1/5-SCALE TEST CONDITIONS (SI Units)

Parameter	Range or Value		
	Prototype	1/2-Scale	1/5-Scale
Loop pressure (MPa)	$2.07 < p < 6.89$	$0.10 < p < 1.38$	0.1
Loop temperature (°C)	$205 < T < 290$	$90 < T < 195$	65
HPI temperature (°C)	5-27	27	16
Maximum HPI Flow Rate (m^3/s) (at F_{CL} = 0.05 and maximum density ratio selected for tests)	2.83×10^{-2}	3.40×10^{-3}	3.68×10^{-4}
Cold leg diameter (mm)	711.2	363.5	142.9
Main HPI line diameters (mm) (vendor specific)	38.1 222.3 254.0	18.8 114.3 120.7	- 44.5 50.8
Other HPI line diameters (mm) (vendor specific)	42.9 34.0	20.8 17.8	6.9
Density ratios ($\Delta\rho/\rho$) selected for tests	0.215	0.034, 0.124	0.018, 0.16*
Cold leg Froude number	0.05	0.05	0.05
Loop to HPI flow ratio (Q_L/Q_H)	0 and range to 200	0 and range to 5	0 and range to 50
Vent to HPI flow ratio (Q_{VV}/Q_H)	0 and range to 10	0 and range to 5	0 and range to 20

*Density ratio $\Delta\rho/\rho$ = 0.16 achieved using salt in HPI flow

Table 4-1b PROTOTYPE THERMAL AND HYDRAULIC PARAMETERS COMPARISON WITH 1/2-SCALE AND 1/5-SCALE TEST CONDITIONS (English Units)

Parameter	Range or Value		
	Prototype	1/2-Scale	1/5-Scale
Loop pressure (psia)	$300 < p < 1000$	$15 < p < 200$	14.7
Loop temperature (°F)	$400 < T < 550$	$200 < T < 380$	150
HPI temperature (°F)	40-80	80	60
Maximum HPI Flow Rate (ft^3/s) (at F_{CL} = 0.05 and maximum density ratio selected for tests)	1	0.12	0.013
Cold leg diameter (in.)	28	14.31	5.625
Main HPI line diameters (in.) (vendor specific)	1.5 8.75 10.0	0.74 4.5 4.75	- 1.75 2.0
Other HPI line diameters (in.) (vendor specific)	1.69 1.34	0.82 0.7	0.27
Density ratios ($\Delta\rho/\rho$) selected for tests	0.215	0.034, 0.124	0.018, 0.16*
Cold leg Froude number	0.05	0.05	0.05
Loop to HPI flow ratio (Q_L/Q_H)	0 and range to 200	0 and range to 5	0 and range to 50
Vent to HPI flow ratio (Q_{VV}/Q_H)	0 and range to 10	0 and range to 5	0 and range to 20

*Density ratio $\Delta\rho/\rho$ = 0.16 achieved using salt in HPI flow

Table 4-2a PROPERTIES OF WATER AT PROTOTYPE AND MODEL CONDITIONS (SI units)

Parameter	Symbol	Temperatures (°C)				
		4.5	26.7	93.3	193	260
Saturation Pressure (kPa)	p	0.83	3.45	82.7	1351	4695
Density (kg/m^3)	ρ	1000	996	963	873	785
Absolute Viscosity (kg/m hr)	μ	5.57	3.10	1.10	0.52	0.39
$g\beta\rho^2/\mu$ ($1/m^3°C$)	-	1.46×10^8	3.56×10^9	7.06×10^{10}	4.81×10^{11}	9.73×10^{11}
Thermal Conductivity (W/m°C)	k	0.562	0.611	0.682	0.666	0.604
Heat Capacity (J/kg°C)	c_p	4187	4178	4187	4471	4982
Prandtl Number	Pr	11.6	5.89	1.88	0.964	0.87
$\rho_{4.5°C} - \rho/\rho_{4.5°C}$	$(\Delta\rho/\rho)_{4.5°C}$	-	-	-	-	0.215
$\rho_{26.7°C} - \rho/\rho_{26.7°C}$	$(\Delta\rho/\rho)_{26.7°C}$	-	-	0.034	0.124	-

Table 4-2b PROPERTIES OF WATER AT PROTOTYPE AND MODEL CONDITIONS
(English units)

Parameter	Symbol	Temperatures (°F)				
		40	80	200	380	500
Saturation Pressure (psia)	p	0.12	0.5	12	196	681
Density (lbm/ft^3)	ρ	62.4	62.2	60.1	54.5	49
Absolute Viscosity (lbm/ft hr)	μ	3.74	2.08	0.74	0.35	0.26
$g\beta\rho^2/\mu$ ($1/ft^3°F$)	-	2.3×10^6	56×10^6	1.11×10^9	7.56×10^9	15.3×10^9
Thermal Conductivity (Btu/hrft°F)	k	0.325	0.353	0.394	0.385	0.349
Heat Capacity (Btu/lbm°F)	c_p	1.00	0.998	1.00	1.068	1.19
Prandtl Number	Pr	11.6	5.89	1.88	0.964	0.87
$\rho_{40°F}-\rho/\rho_{40°F}$	$(\Delta\rho/\rho)_{40°F}$	-	-	-	-	0.215
$\rho_{80°F}-\rho/\rho_{80°F}$	$(\Delta\rho/\rho)_{80°F}$	-	-	0.034	0.124	-

number where the majority of those tests were conducted. Thus, there should be similar data at 1/2-scale for purposes of scaling comparisons.

Other F_{CL} values (higher and lower) are included in the test matrix based on specific vendor recommendations and for providing additional data for model development as well as to extend the range of HPI flows to match injector Reynolds number for some test conditions.

Although the range of prototypical loop flow ratio Q_L/Q_H in Table 4-1 is large, experience from previous studies (3 and 4) shows that little of this range is significant. At high loop flow ratio, nearly ideal mixing occurs and mixed-mean temperatures are near that of the primary fluid. Thus, the matrix emphasizes tests at $Q_L/Q_H = 0$ (stagnant loop) and in the range $0.5 < Q_L/Q_H \leq 5$, where the coldest fluid temperatures are achieved.

The maximum density ratio ($\Delta\rho/\rho$) for the test facility is about 0.124 based on a loop temperature of about 193°C (380°F) and HPI temperature of 26.7°C (80°F). That is about 60% of the density ratio (0.215) at a loop temperature of 260°C (500°F) and with 4.5°C (40°F) HPI water. Other (lower) density ratios can also be accommodated in the test facility. One other that has been selected is $\Delta\rho/\rho = 0.034$ which is achieved at a loop temperature of about 93°C (200°F) and HPI temperature of 26.7°C (80°F).

The preliminary test matrix has been designed to provide simulation of loop flow ratio Q_L/Q_H, density ratio $\Delta\rho/\rho$ and cold leg Froude number F_{CL} in the ranges of conditions discussed above. Figure 4-1 summarizes the capability of the test facility in terms of those dimensionless parameters and shows a comparison with the conditions in the primary simulation range. As seen, the facility can supply significantly higher loop and HPI flows if evaluation of early test data indicates that is required.

4.2 TEST MATRIX

The principal features of the 1/2-scale thermal mixing test outline are:

1. shakedown tests (Series A) to check out test and data reduction procedures and for directing emphasis in subsequent matrix tests

2. 75 matrix tests
   - 66 tests with steady inlet boundary conditions (Series B and C)
   - 9 tests with transient inlet boundary conditions

3. one downcomer geometry

4. three cold leg/loop seal geometries

5. multiple HPI injectors for some cold legs

6. vent flow when required by simulation

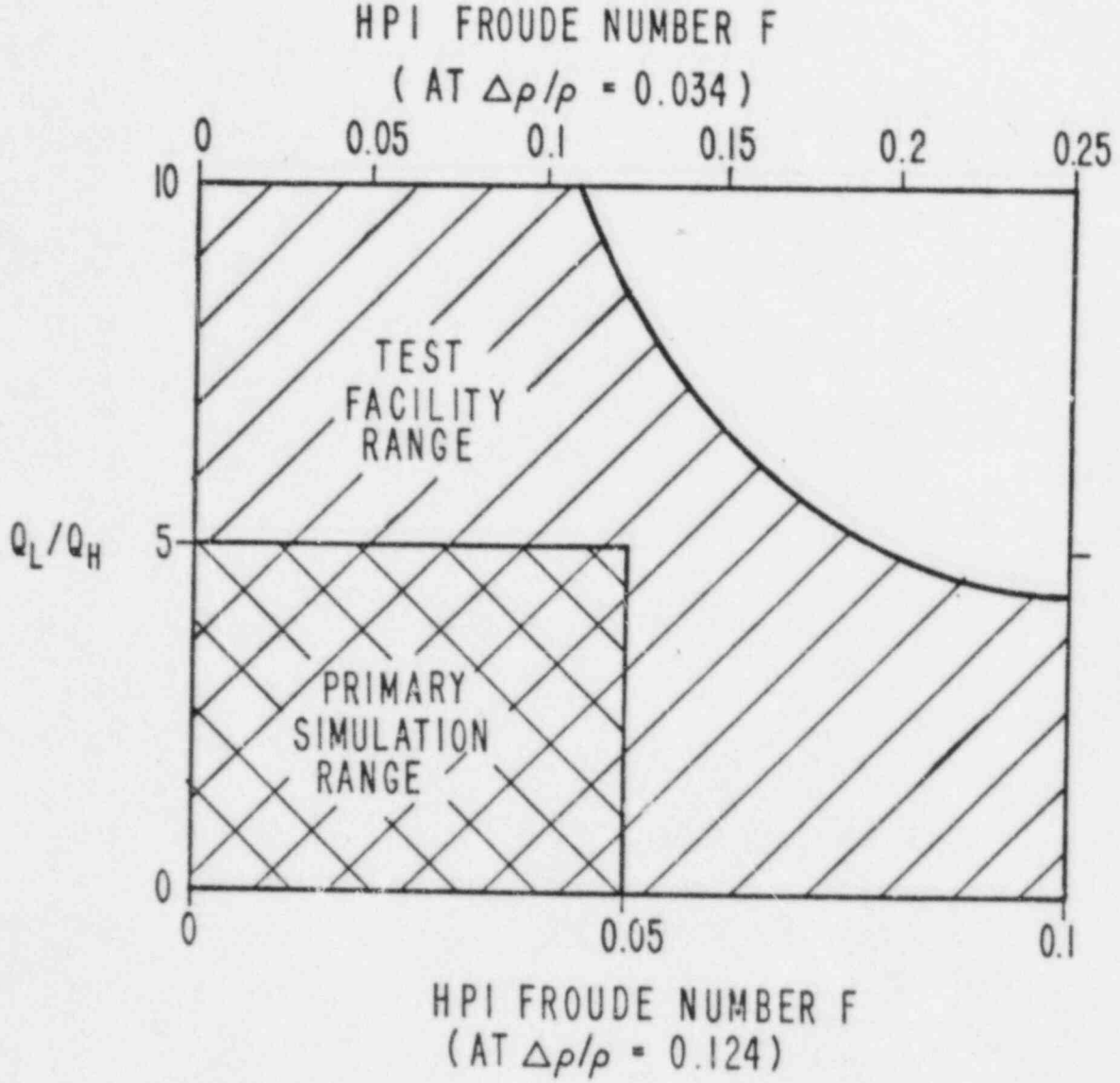

Figure 4-1. Test Facility Flow Capability

7. thermal shield when required by simulation

8. lower plenum flow skirt when required by simulation

Steady-state tests are defined as having steady input flow rates (including tests with zero loop flow) and temperatures starting from a uniform fluid and wall temperature, and proceeding until the exit water flow has reached an equilibrium temperature. Transient tests can be run by changing either the loop flow rate or temperature, again starting from a uniform loop and vessel temperature and proceeding along a prescribed transient. A sample steady-state test matrix is shown in Tables 4-3 and 4-4 for the horizontal and inclined cold legs, respectively. For the Series C tests (horizontal cold leg), the parameters in the matrix are the Froude number, density ratio, loop to HPI flow ratio, and injector type and location. There are fewer tests in the Series B matrix (inclined cold leg) with the inclusion of the vent flow rate as a test variable.

Additional test parameters, relating to the facility geometry, are the cold leg/loop seal/pump configuration, thermal shield vs. no thermal shield, and lower plenum flow skirt. For one vendor, several tests are planned with the pump/loop seal isolated from the cold leg (Q_L = 0). Table 4-5 organizes the steady state test matrix by these geometry parameters. The injector descriptors (B, C, D, E, F) are referenced on the drawings of the cold leg assemblies in Figures 2-3, 2-4 and 2-5.

The majority of the steady-state tests will be performed at the maximum density ratio possible in the test facility, $\Delta\rho/\rho = 0.124$. Tests will also be performed at a lower density ratio, approximately 0.034, so that thermal scaling can be established.

A total of 9 transient boundary conditions tests are included in this test outline, 3 for each vendor reactor type. The transient test conditions can be selected to represent cases of greatest concern relative to PTS for each vendor. The capability of the test facility in performing transient tests is described below.

The loop flow rate and temperature can be controlled to provide approximate exponential or linear ramp transients, and not to match calculated transients. We will accurately measure the actual transient conditions and will avoid erratic fluctuations in the conditions.

For tests with loop flow rate as the transient parameter, the duration of the tests is set by the initial flow rate, the time constant of the exponential decrease in flow rate and the volume of stored loop flow fluid (19 m^3, 5000 gallons). Even with high initial loop flow (F_{CL} = 0.05, $\Delta\rho/\rho = 0.124$ and $Q_L/Q_H = 5$) the transient test capability is greater than 1000 seconds. By comparison, for the same initial conditions, a steady-state flow test is expected to reach equilibrium temperature in the fluid in less than 500 seconds. In the cases where the initial loop flow is low, the test duration capability will be set by the supply of HPI. Assuming the HPI flow at F_{CL} = 0.05 is held

Table 4-3 SERIES C TESTS WITH HORIZONTAL COLD LEG

INJECTOR TYPE*	DENSITY RATIO ($\Delta\rho/\rho$)	FROUDE NUMBER (F_{CL})	LOOP TO HPI FLOW RATIO Q_L/Q_{H_2} 0	0.5	1	2	5	15	NO. OF TESTS
D	0.124	0.0125	X	-	X	-	-	-	2
		0.025	X	X	X	-	X	-	4
		0.0375	X	-	-	-	-	-	1
		0.05	X	X	X	X	X	-	5
		0.075	X	-	-	-	-	-	1
	0.034	0.0125	X	-	X	-	-	-	2
		0.025	X	-	X	-	-	-	2
		0.0375	-	-	-	-	-	-	0
		0.05	X	-	X	-	X	X	4
		0.075	-	-	-	-	-	-	0
D (Isolated Loop)	0.124	0.0125	X	-	-	-	-	-	1
		0.025	X	-	-	-	-	-	1
		0.05	X	-	-	-	-	-	1
D (Without Thermal Shield)	0.124	0.05	X	-	X	-	X	-	3
F	0.124	0.0125	X	-	-	-	-	-	1
		0.025	X	-	-	-	-	-	1
		0.05	X	-	X	-	X	-	3
C	0.0124	0.025	X	-	X	-	-	-	2
		0.0375	X	X	X	-	-	-	3
		0.05	X	X	X	X	-	-	4
	0.034	0.025	-	-	-	-	-	-	0
		0.0375	-	-	-	-	-	-	0
		0.05	X	X	X	-	-	-	3
E	0.124	0.025	X	-	-	-	-	-	1
		0.0375	X	X	X	-	-	-	3
		0.05	X	-	-	-	-	-	1
TOTAL NUMBER OF TESTS WITH HORIZONTAL COLD LEGS									49

* Injector Type refers to letter designations used on cold leg drawings, Figures 2-3 and 2-4.

Table 4-4 SERIES B TESTS WITH INCLINED COLD LEG

INJECTOR TYPE	DENSITY RATIO ($\Delta\rho/\rho$)	FROUDE NUMBER (F_{CL})	LOOP FLOW (Q_L)	VENT TO HPI FLOW RATIO (Q_V/Q_H) 0	0.5	1	2	2.5	5	7.5	15	NO. OF TESTS
A	0.124	0.025	0	-	-	-	X	-	-	-	-	1
		0.05		X	X	X	X	-	X	-	-	5
	0.034	0.025		-	-	-	X	-	-	-	-	1
		0.05		X	-	-	X	-	-	-	-	2
	0.124	0.025	$2Q_H$	-	-	-	-	-	-	-	-	0
		0.05		X	X	-	-	-	-	-	-	2
	0.034	0.025		-	-	-	-	-	-	-	-	0
		0.05		-	-	-	-	-	-	-	-	0
	0.124	0.025	Q_V	-	-	X	-	-	-	-	-	1
		0.05		-	X	X	-	X	-	-	-	3
	0.034	0.025		-	-	-	-	-	-	-	-	0
		0.05		-	-	X	-	-	-	X	-	2
TOTAL NUMBER OF TESTS WITH INCLINED COLD LEG												17

Table 4-5 THERMAL MIXING STEADY-STATE TESTS GEOMETRY VARIATIONS

GEOMETRY PARAMETERS						NUMBER OF TEST AT FLOW CONDITIONS										
						DENSITY RATIO $\Delta\rho/\rho$=0.124					DENSITY RATIO $\Delta\rho/\rho$=0.034					
TEST SERIES	COLD LEG CONFIG-URATION	INJECTOR TYPE	THERMAL SHIELD	LOWER PLENUM FLOW SKIRT	ISOLATED LOOP	FROUDE NUMBER (F_{CL}) 0.0125	0.025	0.0375	0.05	0.075	FROUDE NUMBER (F_{CL}) 0.0125	0.025	0.0375	0.05	0.075	SUBTOTAL EACH CONFIC-URATION
C	Horizontal #2	D	Yes	No	No	2	4	1	5	1	2	2	0	4	0	21
	Horizontal #2	D	Yes	No	Yes	1	1	0	1	0	0	0	0	0	0	3
	Horizontal #2	D	No	No	No	0	0	0	3	0	0	0	0	0	0	3
	Horizontal #2	F	Yes	No	No	1	1	0	3	0	0	0	0	0	0	5
	Horizontal #1	C	Yes	Yes	No	0	2	3	4	0	0	0	0	0	0	12
	Horizontal #1	E	Yes	Yes	No	0	1	3	1	0	0	0	0	0	0	5
B	Inclined	B	No	No	No	0	2	0	10	0	0	1	0	4	0	17
TOTAL NUMBER OF STEADY STATE TESTS																66

constant, the test duration could be in excess of 6 hours. These estimates of test duration are based on the use of a 19 m^3 (5,000 gallon) tank for loop flow storage and 76 m^3 (20,000 gallon) capability for HPI, and assuming use of the water on a "once-through" basis.

4.3 TEST ORDER

In the absence of any other program priorities the sequence of tests in the 1/2-scale thermal mixing program will be dictated by the logic of minimizing the number of times the hardware needs to be changed to accommodate the several test configurations. Table 4-5 shows the variations of geometry and lists the tests in their probable sequence if the present full test matrix were followed. The priority of tests within any test geometry set will probably be based on minimizing flow meter range changes, or other operational considerations. Although the tests will be carried out in a systematic way to minimize hardware modifications, any of the major geometries can be assembled at any time if required for data verification or if test priorities change.

4.4 TEST PROCEDURES

This section outlines and discusses procedures for conducting tests in the thermal mixing facility. More detailed procedures with step-by-step instructions for the operators are documented in the project DRF. These procedures were developed from experience gained during shakedown in 1983 and were used for the initial tests reported in Reference 19. Specific procedures are necessary to ensure that the desired test conditions are efficiently established and maintained throughout the test duration, and to ensure system integrity and operator safety.

The first step involves filling the test facility and loop supply tank from the large ($76m^3$) supply tanks using the HPI pump. During this process, vents located at high points in the supply piping and in the test model are opened to discharge air in order to completely fill the facility with water.

After filling is completed and adequate water is transferred to the loop supply tank, the heating process is initiated. Water is circulated through the test facility using the loop flow pump and back to the loop supply tank. At the same time, steam at controlled pressure is introduced to the heating spargers located in the supply tank, raising the water temperature there and subsequently throughout the rest of the facility. During the early part of the heatup the loop tank is open to ambient in order to discharge non-condensible gases which evolve from the water as it is heated. Later, this vent is closed so that heating above 100°C can proceed. Other high point vents are briefly cycled open during heatup to remove any additional air which might not have been purged at filling. The hotwell surrounding the lower plenum is heated by circulating water from the lower plenum, through the external pressure balance lines to the hotwell, and then back out to the discharge pipe.

Heatup continues until the desired system temperature is reached, and fluid and vessel wall thermocouple readings are uniform and steady. The heatup process can take up to about 4 hours to achieve thermal equilibrium - less time is required if the loop supply tank is already filled with hot water, for instance following a test in which little or no loop flow was used.

The desired system pressure is adjusted at the end of heatup to be slightly above the saturation pressure corresponding to the loop temperature. Usually this pressure difference amounts to an equivalent 2°C to 4°C subcooling of the water relative to the system pressure. In this way the possibility of flashing and two-phase operation are avoided. A pressure control valve on the facility discharge line automatically maintains system pressure at the desired value during the heatup and transient cooldown periods.

The warming period prior to introduction of HPI is used to check the operation of instruments in the cold leg and downcomer and to monitor numerous thermocouples throughout the facility to verify that thermal equilibrium has been achieved at the desired test temperature. Differential pressure transducers on flow meters and velocity probes are checked for zero offset which is recorded for use in the data reduction. Adjacent pairs of vessel wall and fluid thermocouples are examined as a further check on thermal equilibrium. Exterior wall thermocouples also provide data for assessing overall temperature uniformity and stability. Other instrumentation and data system checks are performed at this time, including verification and adjustment if necessary, of the clock frequency in the DAS multiplexer and the instrumentation amplifier calibration voltages.

After all pre-test checks are completed, the loop and HPI flows are adjusted to meet the specified Froude number F_{CL} and loop-to-HPI flow ratio Q_L/Q_H for the test to be performed. Both flows have parallel sets of orifice meters to cover the possible range of flow rates in the test outline discussed earlier. The operator selects the appropriate meter to be used to maximize measurement accuracy (higher differential pressure) and isolates the unused meters by closing their control valves. The HPI flow is adjusted in a bypass loop that is isolated from the model cold leg with quick-acting ball valves. A test is initiated by opening the HPI injection valve while simultaneously closing the isolation valve. For a stagnant loop test ($Q_L/Q_H = 0$) the loop flow rate is reduced to zero before HPI injection is started. A position switch on the HPI valve sends a signal to the data acquisition system marking the beginning of injection.

During the cooldown transient the test operator monitors the injection and loop flow rates on the DAS computer display and makes adjustments as needed to maintain the flow rates within an acceptable tolerance band around the nominal.

A test proceeds until temperatures have reached a steady condition and are uniform throughout the cold leg and downcomer. Experience from 1/5-scale testing and evaluation of shakedown data at 1/2-scale are instructive in this regard. It has been observed that the temperature of the water in the standpipe exiting the lower plenum provides an adequate reference measurement for assessing the approach to thermal equilibrium in the fluid. The standpipe temperature displays an essentially exponential transient for steady inlet flows and temperatures:

$$\frac{T_f - T_m}{T_L - T_m} = e^{-t/\tau_f} \tag{4.3}$$

where T_f = standpipe water temperature
T_m = mixed-mean temperature which would be achieved by perfect, adiabatic mixing of the inlet loop and HPI flows
T_L = loop flow temperature
t = time since start of HPI
τ_f = experimentally determined time constant

For tests of duration $t \geq 3\tau_f$ the fluid temperature profiles in the cold leg and downcomer are well established and near to final equilibrium condition. Based on evaluation of data at 1/5-scale the time constant τ_f can be approximated by

$$\tau_f \cong \frac{\Gamma}{Q_T} \tag{4.4}$$

where Γ = sum of system component volumes
Q_T = sum of loop (and vent) plus HPI volume flow rates

Thus, the operators can estimate the minimum expected test duration using a $3\tau_f$ criterion and Eq. 4.4 for purposes of setting up the data system and for judging whether stored water volumes will be adequate for a test. Operator awareness of a minimum expected test duration assists in scheduling tests to make most efficient use of the facility and resources. Actual test duration is under control of the operator, and a decision to extend beyond $3\tau_f$ can be made if indicated by the test measurements.

Following completion of a mixing test, the HPI flow is secured and the system is either shutdown or re-filled and reheated in preparation for a new test.

4.5 DATA ACQUISITION

The DAS is used to acquire and store data from the test facility during two periods. The first period is just prior to the introduction of the HPI flow, when the loop has reached its equilibrium state. This data is used to define test initial conditions and to check for malfunction in instrument readings. This period will have a duration

of at least 60 seconds prior to the introduction of HPI or the beginning of a temperature or flow transient. As noted earlier, the start of HPI is marked by a signal from a position indicator on the injection valve.

The second period of data acquisition encompasses the full duration of the test itself. That duration will be set by one of several criteria:

1. Supply of loop and vent flow is exhausted.

2. Temperatures in the cold leg and downcomer have reached a steady condition.

3. Test duration has achieved minimum specified value, e.g. approximately 3 time constants, where the time constant is determined from the test facility volumes and the loop and vent plus HPI flow.

The worst case situation for limiting test duration is exhaustion of the loop flow supply. Based on estimates using the present facility design and test matrix, the minimum test duration will be at least about 8 times the facility mixing time τ_f for tests with steady inlet boundary conditions (flow rates and temperatures). Recall that times of $3\tau_f$ are expected to produce an equilibrium condition in the facility. Thus, the supply of loop flow (19 m^3, 5000 gallons) will be adequate for all test conditions in the present matrix. Priority tests at zero or low loop flow rate can be run almost indefinitely (many hours).

Data acquisition rates were discussed previously. Data from all instruments will be recorded once per second during each of the test periods. If required, the fast thermocouples can be recorded by parallel, independent means at rates up to 10 times per second.

In addition to the computer data records, the test operators record readings from panel gauges and meters and valve position settings prior to the introduction of HPI flow. These manual records serve only as backup, they do not contain any information that is not also available from the data acquisition system. During the tests, the operators note and describe any unusual events and any other actions taken to adjust or correct flow rates, pressures, etc.

4.6 TEST ACCEPTANCE CRITERIA

This section describes several criteria for assessing the acceptability of tests from the 1/2-scale thermal mixing experimental project. The basic purpose for specifying any acceptance criteria is to ensure that data from the tests will permit adequate analysis of the results for comparison with other tests and for phenomenological understanding of the mixing behavior, and for developing and validating mixing models and code calculations.

Criteria presented below specify tolerances on measured inlet boundary conditions, initial equilibrium conditions, test duration limits and types and numbers of functioning instruments. Insofar as possible, all criteria will be satisfied for each test, although some deviations may be permissible in the interest of testing efficiency and schedule. On the other hand, certain criteria, e.g. tolerances on inlet flow rates and temperatures, must be satisfied to provide even a minimum data set for a test and those will be specified as basic requirements for all tests.

The criteria described here are aimed at the initial steady-state tests in the facility. Similar criteria will be established for other tests in the outlined project (Section 4.2) with configuration (e.g. vent flow, isolated loop) or procedures (e.g. transient loop flow) significantly different than the present arrangement.

4.6.1 Test Conditions Tolerances

The test matrix describes the steady state boundary conditions in terms of the HPI Froude number F_{CL}, the loop to HPI volumetric flow rate Q_L/Q_H, and the loop to HPI density difference $\Delta\rho/\rho$. Each of these test parameters is a derived quantity, i.e. not directly measured. Therefore, any tolerance on setting the test parameters will be subject to the estimated uncertainties in the measured quantities used to calculate the parameters. While it is possible to "fine-tune" the flow rates and temperatures such that the calculated parameters are precisely at the target test condition, in fact the actual values of the parameters will not be known to an uncertainty less than the measurement uncertainties. Therefore, acceptance criteria on inlet conditions are derived from the single-sample experimental uncertainty in the calculated parameters, based on the expected errors in the measurements. For tests with small flow rates, additional criteria will be used which consider data system quantization error and control system stability.

Flow ratio: Q_L/Q_H

- $Q_L/Q_H = 0$, no measurable loop flow permitted
- $Q_L/Q_H \geq 1$, acceptance tolerance ± 10% of target flow ratio
- $0 < Q_L/Q_H < 1$, acceptance tolerance larger of ± 10% of target ratio or loop and HPI flow variations of ± 10% of nominal.

Density difference: $\Delta\rho/\rho$

- $\Delta\rho/\rho = 0.124$, acceptable range $0.117 \leq \Delta\rho/\rho \leq 0.129$ considering temperature measurement accuracy and system control

- $\Delta\rho/\rho = 0.034$ acceptable range $0.031 \leq \Delta\rho/\rho \leq 0.039$

Froude number: F_{CL}

- at $\Delta\rho/\rho$ = 0.124 (nominal), acceptable tolerance for F_{CL} to be ±8% of target values for $F_{CL} > 0.025$ and ± 15% for $F_{CL} \leq 0.025$
- at $\Delta\rho/\rho$ = 0.034 (nominal), acceptable tolerance for F_{CL} to be ± 15% of target values of F_{CL}

These criteria will be applied to the average values of the computed test parameters over the duration of the test.

4.6.2 Initial Equilibrium Condition

In the pre-test heatup period, the test operator will examine the readings from certain instruments in order to judge that the fluid and test vessel have reached thermal equilibrium.

Fluid temperature:

- loop inlet and standpipe water temperature to agree within measurement error (±4°C) for several minutes prior to injection of HPI.
- lower plenum and hot well to be within ± 4°C of standpipe temperature prior to HPI injection.
- HPI flow temperature equilibrated prior to injection.

Metal temperature:

- temperature difference through metal wall thickness at selected locations (up to 6) to be less than ±4°C and inside wall temperature to be substantially in agreement with standpipe fluid temperature.

4.6.3 Test Duration Limits

The duration of a test is defined as that time period following initiation of HPI flow during which the inlet boundary conditions are within the acceptable tolerance limits and data are being acquired by the DAS. An acceptable test is one in which the fluid and metal temperatures in the downcomer vessel have reached a uniform distribution near the mixed mean temperature for the inlet flows and temperatures, within the test duration time.

As discussed in an earlier section, this condition is expected to be reached in a time equivalent to 3 times the characteristic mixing time as determined from the standpipe water temperature transient.

The downcomer wall temperatures also follow an exponential decay that is a function of thermal diffusion in the wall and the wall-to-fluid heat transfer coefficient. Although there is not sufficient experimental evidence available to develop an acceptance criterion

based on wall temperature only, the thermal penetration time for the wall can be used to provide a guide for establishing a minimum test duration. For the 70 mm (2.75 inch) thick wall in the facility, the thermal penetration time ($\Delta x^2/\pi\alpha$) with infinite heat transfer coefficient is 120 seconds. A test duration of 3 times the penetration time or 6 minutes seems to be a reasonable lower limit on duration and is consistent with the minimum test duration capability based on storage volume and flow rate for loop fluid.

A two-part test duration acceptance criterion results. The acceptable test duration will be the greater of:

1) 360 seconds, or
2) 3 times the characteristic mixing time based on stand pipe temperature, unless the operator terminates the test based on observations of thermal equilibrium in the fluid and walls.

4.6.4 Functioning Instrumentation

The test facility has over 300 instruments available in its present configuration. These include instruments for measuring the process parameters of flow rates, pressure, levels and fluid inlet temperatures, and instruments for detailed temperature and velocities in the cold leg and downcomer and downcomer wall temperatures and heat flux.

An acceptance criterion based on the test instruments should be in two parts. The first part requires that as a minimum the following measurements must be available for the duration of each test:

1. loop and HPI flow rates

2. loop and HPI temperatures at test facility inlet boundary

3. standpipe water temperature

These parameters are monitored by the test operators during the pre-test period in order to set test conditions within the specified tolerances. If any of the instruments are not functioning, that is cause for a "hold" on the test to take appropriate, corrective action. In the post-test data reduction, other instrument integrity checks are made by examining the average, minimum, maximum and fluctuations of the instrument readings over the test duration. A final judgement of test acceptance is made at that time.

The second part of the instrumentation criterion concerns the detailed measurements made throughout the test facility. The instruments used in this project were selected to be reasonably rugged and reliable. However, as a practical matter some random failures of instruments or data system components are expected, which may result in the loss of specific measurements for any test. In general, these losses may not be recognized until a test has been completed and the data reduction

is underway. Therefore, a practical instrumentation criterion has the objective of maximizing the number of detailed measurements available for each test and requires that certain minimum measurements must be available for all tests.

A minimum set of detailed measurements used for judging acceptability of the early tests from the 1/2-scale facility consists of the following:

Temperatures

Cold leg:	temperature profile at the nozzle (C5 location) comprised of at least five temperature measurements in any vertical array, with no more than two consecutive probes failed.
Downcomer:	2 fluid temperatures in first row of instruments below nozzle in plane of nozzle vertical centerline, 1 each from core and vessel sides; either center of gap or near-wall probes. Alternatively, equivalent locations on lower most thermocouple rake spanning width of downcomer below nozzle.
Standpipe:	1 temperature measurement either in the exit pipe from the lower plenum, or the central location within the lower plenum simulator volume.
Heat Flux	2 vessel wall heat flux locations, corresponding to the downcomer fluid temperature measurements cited above.

There are a larger set of detailed measurements that are desirable to maintain, and which can be accommodated by repair to or changing of instruments, albeit at the expense of test productivity. Indications of the desirability (but not necessity) for changing or fixing specific instruments are:

Cold Leg

- If temperature rakes at locations C1 or C2 develop gaps of 3 or more contiguous points (or 2 contiguous points at the top or bottom boundaries) the probes should be repaired or replaced with rakes from locations C3, C4 or C6.

Downcomer

- If fluid temperature profiles in first two rows of instruments below nozzle (vessel and core sides) experience gaps of 3 or more contiguous probes, repair or replace with similar instruments from less critical locations.

- If heat transfer coefficient data on vessel wall has gaps of 3 or more contiguous probes, or 2 or more near the vessel edges, repair or replace with similar instruments from less critical locations.

Standpipe

- The standpipe thermocouple should be repaired or replaced following any test in which it has failed.

4.6.5 Test Acceptance Ratings

The acceptance criteria outlined here establish quantitative guidelines which are used to rate the acceptability of a test for data analysis purposes. We use three different ratings depending on the overall success of meeting the general and specific criteria:

Rejected - This test was not good (major leak, failed to measure critical inlet condition, major error in procedure, etc.)

Accepted - Test meets all the tolerances and acceptance criteria described in Sections 4.6.1 through 4.6.4.

Accepted with Recommendation -

- The test data are valid and we have published data, but actual flows (or temperatures) were not within nominal tolerances established for that test - could include recommendation for a repeat, or not, depending on range of out-of-tolerance.

- More than usual instrument failures - we publish data but alert to deficiencies.

- Nominal test conditions are in tolerance, but large deviations - we publish data but alert to deficiencies.

5. DATA REDUCTION AND DISPLAY PROCEDURES

The principal outputs from the testing project are displays of the temperature, velocity and heat flux data for known test conditions and test geometry. That data will be made available in the form of Quick Look Reports (QLR) for each test that meets the acceptance criteria described in Section 4.6.

Details of the procedures used for data reduction and documentation of the analytical and numerical techniques are provided in the Design Record File.

Figure 5-1 provides a general overview of the data reduction process and the application of the test data to produce a QLR. The major steps in that process and the format of the Quick Look Reports are described in this section.

5.1 DATA REDUCTION

The voltage outputs from all the measuring instruments are recorded by the data acquisition computer for the full duration of a test including a test period of about 60 seconds prior to HPI injection. The data channel amplifier gain and offset voltages are also recorded by the computer and are stored in a calibration file for each test along with the file of transducer calibration and conversion constants. The process of data reduction involves two steps: first, conversion of these raw data to engineering units corresponding to the primary measurements of pressure and temperature, and second, calculation of derived parameters such as flow rates, velocities, and heat transfer data.

5.1.1 Primary Data Reduction

Temperature data are reduced from the raw voltages by the procedure outlined below:

1. The recorded voltages are converted to thermocouple emf using the amplifier offset voltages and gain factors.

2. The zone block temperature is converted to equivalent thermocouple emf for Type E (Chromel-Constantan) thermocouple and is added to the emf obtained in Step 1.

3. The thermocouple junction temperature is calculated from a 4th order polynomial:

$$T(V) = \sum_{i=0}^{4} (a_i V^i) \qquad (5.1)$$

where $T(V)$ = temperature for the computed thermoelectric voltage V

a = coefficient of each term in the polynomial, obtained from Reference 20

V = thermocouple voltage determined in Step 2.

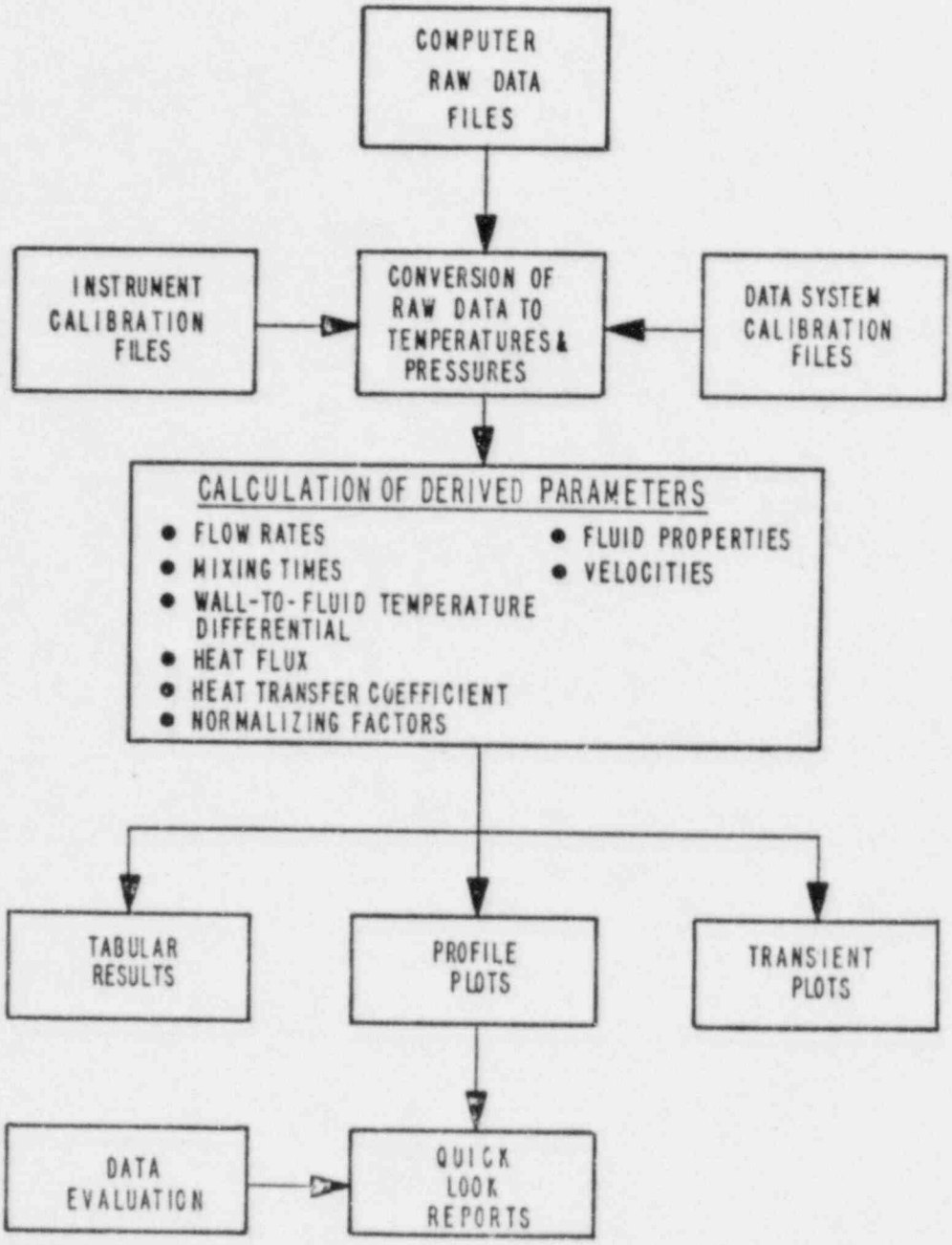

Figure 5-1. Overview of Data Reduction and Display Process

4. Temperatures are processed and used in other steps of data reduction in the English system of units (°F). Conversion to SI units is done only in the data printouts according to:

$$T(°C) = (5/9)\ [T(°F) - 32°F] \qquad (5.2)$$

Reduction of the pressure data from raw voltages is also accomplished in several stages:

1. The raw voltage recorded by the DAS is converted to transducer output by correcting for amplifier offset voltage and gain factor.

2. The transducer offset voltage recorded prior to the beginning of the test is calculated and is subtracted from the reading obtained in Step 1. This correction for offset voltage accounts for transducer zero shift due to factors such as ambient temperature changes and static pressure level effects.

3. The pressure or differential pressure is then calculated from the transducer calibration constants which consist of first order (linear) correlations of the calibration data.

The raw data from the direct-reading heat flux probes can also be reduced following similar procedures of correction for amplifier offsets and gains, and then conversion of the voltages thus obtained to units of heat flux (W/m^2) using the heat flux probe sensitivity factors. Following evaluations of the shakedown data, less emphasis is placed on the measurements from the direct-reading heat flux probes, and data from them is reduced only in special situations. The procedure for calculating heat flux from the wall temperature measurement is described in the next section.

5.1.2 Calculation of Derived Parameters

The primary measurements of pressure and temperature are used to calculate certain derived quantities that more completely describe the test conditions and that are used in preparation of the graphical and tabular displays of the Quick Look Reports.

FLUID PROPERTIES

Fluid properties that are used in data reduction are obtained from tables and curve fits based on data in Reference 21. The properties are determined at the average value of the fluid temperature measured over the test duration.

FLOW RATES

Inlet loop, HPI and vent flow rates (Q_L, Q_H, Q_V) are calculated from the measured differential pressures and temperatures at the orifice meters using the standard orifice equations (17). Flow rates are computed for each one second reading of the transducers and are averaged over the test duration.

TEMPERATURES

Loop, HPI and vent temperatures (T_L, T_H, T_V) are direct measurements. Reported values are averaged over the test duration.

The mixed mean temperature T_m is defined as the fluid temperature resulting from perfect, adiabatic mixing of the inlet flows. T_m is obtained from the correlation of fluid enthalpy as a function of temperature:

$$T_m = T(h_m) \tag{5.3}$$

where h_m = mixed mean enthalpy calculated from:

$$h_m = \frac{(\rho Q h)_L + (\rho Q h)_H + (\rho Q h)_V}{(\rho Q)_L + (\rho Q_H) + (\rho Q)_V} \tag{5.4}$$

where ρ = density (kg/m^3) at the average temperature
Q = average volumetric flow rate (m^3/s)
h = enthalpy (kJ/kg) at the average temperature

DIMENSIONLESS PARAMETERS

Several dimensionless parameters were defined to develop a possible test matrix based on scaling considerations. Those same dimensionless parameters are used to describe the nominal conditions of the tests. The cold leg Froude number is defined as:

$$F_{CL} = (Q_H/A_{CL}) / [g\, D_{CL}\, (\rho_H - \rho_L)/\rho_H]^{\frac{1}{2}} \tag{5.5}$$

where Q = HPI volume flow rate
A_{CL} = cold leg flow area
g = acceleration due to gravity
D_{CL} = cold leg diameter
ρ_H = density of HPI fluid
ρ_L = density of initial loop fluid

The density ratio $\Delta\rho/\rho$ appears in the Froude number, but is also an independent test variable:

$$\Delta\rho/\rho = \frac{\rho_H - \rho_L}{\rho_H} \tag{5.6}$$

Dimensionless flow ratios are also used to describe the test conditions:

$$Q_L/Q_H;\ Q_V/Q_H;\ Q_L+Q_V/Q_H$$

where Q_H = HPI flow rate
Q_L = loop flow rate
Q_V = vent flow rate

CHARACTERISTIC MIXING TIME

It is customary to evaluate the overall mixing characteristic of a flow system by analyzing the transient temperature (or composition) response at the system outlet - the standpipe temperature in our case. The results from the 1/5-scale experiments showed that the standpipe temperature follows closely an exponential decay, implying that the overall system response is similar to that of a "perfectly mixed" vessel:

$$T-T_s = (T_o - T_s) \exp(-t/\tau) \tag{5.7}$$

where: T_o = initial temperature
T_s = final temperature
t = time
τ = characteristic mixing time

The characteristic mixing time τ is a measure of how rapidly the system approaches equilibrium. For the thermal mixing facility we can define the characteristic mixing time by analogy to a "perfectly mixed" system.

The characteristic mixing time of a first-order system (perfectly mixed vessel) can be expressed in several ways:

(a) Initial Slope:

$$\tau = (T_o - T_s)/\left(-\frac{dT}{dt}\right)_{t=0} \tag{5.8}$$

(b) 1/e crossing:

$$T(\tau) - T_s = (1/e)(T_o - T_s) \tag{5.9}$$

τ = time at which $T = [T_s - (1/e)(T_o - T_s)]$

(c) Three point Fit:

$$\tau = \Delta t/\ln([T(\Delta t)-T(2\Delta t)]/[T(0) - T(\Delta t)]) \tag{5.10}$$

(d) Integral

$$\tau = \frac{1}{(T_o - T_1)} \int_0^{t_1} (T - T_1)dt + t_1/[\exp(t_1/\tau)-1] \tag{5.11}$$

Methods (a), (b), and (c) involve data at specific instants of time and hence are not suitable for this application, since the standpipe temperature transient has higher frequency oscillations superimposed on it. Methods (a) and (b) also require experiments which reach steady state. The integral method (d) requires more computation but can deal with both higher frequency oscillations and finite length tests.

The integral method is used in the computation of characteristic mixing times. Since τ appears on both sides of Equation 5.11 the computation involves iteration, but convergence is very fast; less than 5 iterations are required for 1% convergence if test duration is greater than 3τ. The integral in Equation 5.11 was evaluated from the measured data using Simpson's rule.

For the Quick Look Reports the mixing time is computed from temperature probes at two locations:

1. In the downcomer, 406 mm (16 in.) below the cold leg nozzle centerline elevation using a fluid thermocouple approximately 29 mm (1.16 in.) from the vessel wall.

2. In the standpipe, measuring fluid temperature exiting from the lower plenum.

LOCAL VELOCITY

Local fluid velocity is calculated from the differential pressure and temperature measured at the velocity probes in the facility. Velocity head H is calculated by Eq. 3.2 using the measured differential pressure ($p_T - p_s$) and fluid density ρ which is obtained from the local temperature. Then velocity V is calculated by Eq. 3.3, using an iteration procedure to find the pressure coefficient K at the computed value of V/ν (see Section 3.3.2).

The sign convention of the voltage from the velocity probe differential pressure transducers is used to assign positive (+) and negative (-) values to the computed velocity. In the convention adopted for this project, velocity is positive in the "normal" flow direction, i.e., flow in the cold leg toward the downcomer is positive and downward flow in the downcomer is positive.

SUPERFICIAL VELOCITIES

Superficial velocity is defined as the ratio of the total volumetric flow rate in a duct to the cross-sectional flow area of the duct. Superficial velocities are calculated at three locations in the facility:

1. Cold leg:

$$j_{CL} = (Q_L + Q_H)/A_{CL} \tag{5.12}$$

2. Downcomer above thermal shield:

$$j_{CL} = (Q_L + Q_H + Q_V)/A_{DC} \tag{5.13}$$

3. Downcomer in region of thermal shield:

$$j_{CL,TS} = (Q_L + Q_H + Q_V) \; / \; (A_{DC} - A_{TS}) \tag{5.14}$$

COLD LEG QUENCH FRONT VELOCITY

Quench front velocity is defined as:

$$V_{CL} = L_{CL}/t_{CL} \tag{5.15}$$

where the length L_{CL} is the distance between two thermocouple probes, one located in the cold leg near the HPI injector and the second at the cold leg nozzle and t_{CL} is the cold leg transit time. (The cold leg transit time is determined from the arrival times of the quench front at both locations.)

The procedure for determining quench front arrival time at a probe location is illustrated in the sketch below.

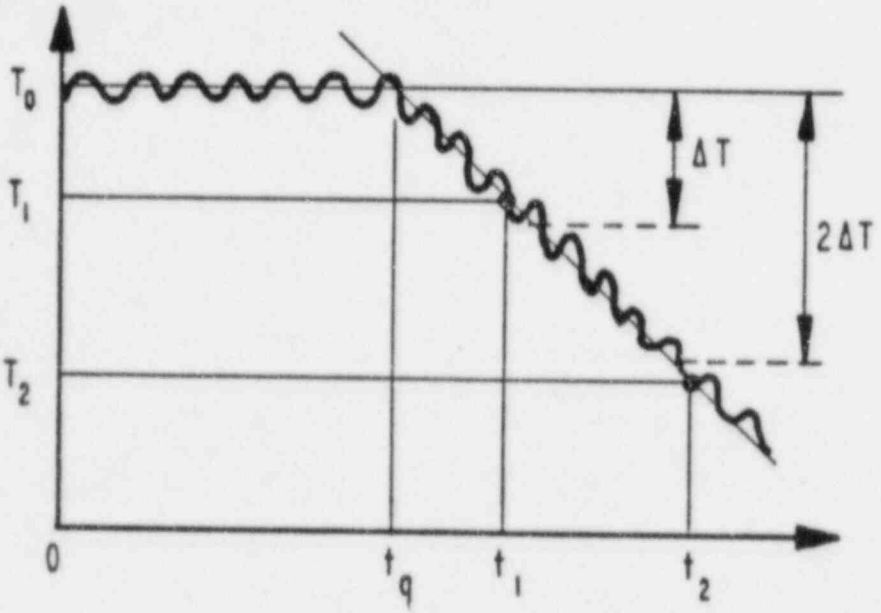

Determination of Quench Front Time

The quench arrival time at a probe location is given by:

$$t_q = t_1 - (t_2-t_1)(T_o-T_1)/(T_1-T_2) \tag{5.16}$$

where
- t_1 = time after HPI injection of the last temperature measurement higher than $T_o-\Delta T$
- t_2 = time after HPI injection of first temperature measurement lower than $T_o-2\Delta T$
- T_o = average temperature between test initiation and HPI injection
- T_1 = temperature at time t_1
- T_2 = temperature at time t_2
- ΔT = temperature change larger than random fluctuations (1°C).

The difference between quench arrival times is then the transit time t_{CL}. The distance L_{CL} separating the two probe locations is 2.31 m (7.59 ft) for the cold leg and instrument configuration used for the

tests reported in the companion Data Report (19). Data sampling rate introduces a maximum uncertainty of $\sqrt{2}$ seconds in measuring t_{CL}.

WALL HEAT FLUX

Heat flux values can be determined in three ways:

1. Performing an energy balance on the downcomer wall over the duration of the test, based on inner and outer surface temperature measurements.

2. Using the heat flux probe measurement of the temperature gradient near the wall surface.

3. Solving the one-dimensional heat conduction equation using the wall surface temperature measurement.

The energy balance method is quite precise (probably within ±5% considering departure from equilibrium, measurement uncertainty and heat loss to ambient) when averaged over the full test duration, but contains little transient information. The energy balance is used primarily as a check on the average accuracy of the transient methods. The heat flux meters follow the high frequency fluctuations closely and are most representative of the true transient. However, when the fluctuations are averaged they show a significant bias such that the average heat flux is greater than that computed from the wall energy balance. Therefore, the output of the heat flux probes is plotted selectively to illustrate the level of fluctuations and their correlation to the local temperature and velocity fluctuations. The one-dimensional conduction approach follows the main transient well and has uncertainty of the order of 10% to 25%. This is the primary means for heat flux data reduction.

Three assumptions were made in developing the data reduction procedure for wall heat flux:

1. one-dimensional heat conduction;
2. adiabatic boundary on the outside surface of the downcomer wall;
3. constant metal wall properties.

Under these assumptions the transient heat conduction equation for the downcomer wall can be solved in closed form using Duhamel's superposition integral (22). The heat flux is given by:

$$q''_s(t) = \frac{-2\,k}{L} \int_0^t \left(\sum_{n=0}^{\infty} \exp\left(-\alpha\,\lambda_n^2 (t-s)\right) \right) \frac{\partial T_W}{\partial s}\, ds \qquad (5.17)$$

where
- k = wall thermal conductivity
- L = wall thickness
- α = wall thermal diffusivity
- λ_n = eigen values = $\pi(2n+1)/(2L)$
- t^n = time after HPI injection
- T_W = wall surface temperature

Equation 5.17 is evaluated numerically to obtain the heat flux from the wall temperature transient.

The extent to which the actual situation deviates from the assumptions made in developing this data reduction procedure results in some uncertainty in the calculated heat flux. Additional contributions to heat flux uncertainty come from the reduced wall thickness at the probe locations and from errors in measuring the wall temperature. A detailed analysis of heat flux uncertainty was carried out using data from shakedown tests (Appendix A). Based on that analysis, the uncertainty in heat flux is estimated to be less than 20% at early times in a test (within one characteristic mixing time), increasing to about 25% late in the test when heat flux is much lower.

HEAT TRANSFER COEFFICIENT

The heat transfer coefficient is obtained from the wall surface heat flux and the wall to fluid temperature differential:

$$h = q_s''/(T_W - T_f) \tag{5.18}$$

where q_s'' surface flux determined from Eq. 5.17.

T_W = wall temperature

T_f = temperature of the downcomer fluid at a location adjacent to the wall temperature measurement

Wall surface temperature is obtained directly from the thermocouple probes located in the heat flux probes (Figure 3-15). Fluid temperature T_f can be taken from either the center of gap or the near-wall thermocouple probes. Both temperatures are nearly identical and result in essentially the same calculated heat transfer coefficient. This measurement redundancy provides some assurance against lost heat transfer data due to probe failures. In the normal data reduction the near-wall probe is used to form the differential with the wall temperature.

Prior to reducing the data to heat transfer coefficients, the wall and fluid temperatures are filtered to remove high frequency components which may introduce phase lag errors into the computation of h. A low-pass, zero phase shift digital filter is used for this purpose (23). The filter cutoff frequency was chosen as 0.05 Hz, corresponding to a cutoff period of 20 seconds. This time period is short relative to the characteristic mixing time, so the principal transient features of the heat transfer coefficient are retained. Yet, the period is long relative to the sampling and random noise frequencies and thus effectively reduces phase lag errors.

Errors in measuring T_W and T_f contribute some additional uncertainty to the calculation of h. The error sources we have identified are:

1. Thermocouple offset associated with the estimated random uncertainty ir measuring temperatures. This error is approximately 1°C.

2. Stem conduction error in the fluid thermocouple measurement which results from heat conduction along the metal probe between the warmer wall and the somewhat cooler fluid. This error is maximum for the near-wall thermocouple on the core side and is of the order of 2% of the wall to fluid temperature difference.

3. Wall temperature gradient error that is produced because the wall surface probe is located approximately 0.64 mm below the metal surface (see Figure 3-15). For a situation with high heat flux early in the transient cooldown this introduces an error of only about 0.4°C, becoming even less as the wall heat flux is reduced later in the cooldown.

4. Phase lag error which arises from the finite time interval between measurements of the wall and adjacent fluid temperatures. As mentioned earlier, the temperature data are filtered before computing (T_w-T_f) which greatly reduces the possible error. For example, data passed through a zero phase shift filter having a cutoff period equal to 1/10 of the characteristic mixing time will have a phase lag error of less than 0.35°C.

Figure 5-2 summarizes the uncertainty in calculating heat transfer coefficient from the heat flux and temperature measurements. The calculation in that plot is made for a probe location nearly on the vertical centerline of the nozzle and approximately midway between the nozzle elevation and the bottom of the downcomer.

Very early in the transient ($t/\tau<<1$) the uncertainty in h is approximately equally due to errors in determining q''_s and (T_w-T_f). As the transient proceeds and (T_w-T_f) increases the contribution of the relatively fixed errors in T_w and T_f become less significant, and heat transfer coefficient uncertainty is comprised mainly of uncertainty in the heat flux. Again, later in the transient as the wall cools and approaches equilibrium with the fluid the contribution of (T_w-T_f) begins to increase. However, at that time the heat transfer coefficient is lower and uncertainty in its computation is less important. This last point is illustrated in Figure 5-3 which shows the range of heat transfer coefficient over the period of the transient and the magnitude of the uncertainty. By the time the uncertainty has increased to 20% of h ($t/\tau>1$) the heat transfer coefficient has reduced to less than about half the peak value early in the test.

The uncertainty in heat transfer coefficient may vary somewhat with measurement location and flow condition. However, the differences are small since the major contribution to uncertainty is the probe geometry and that remains fixed.

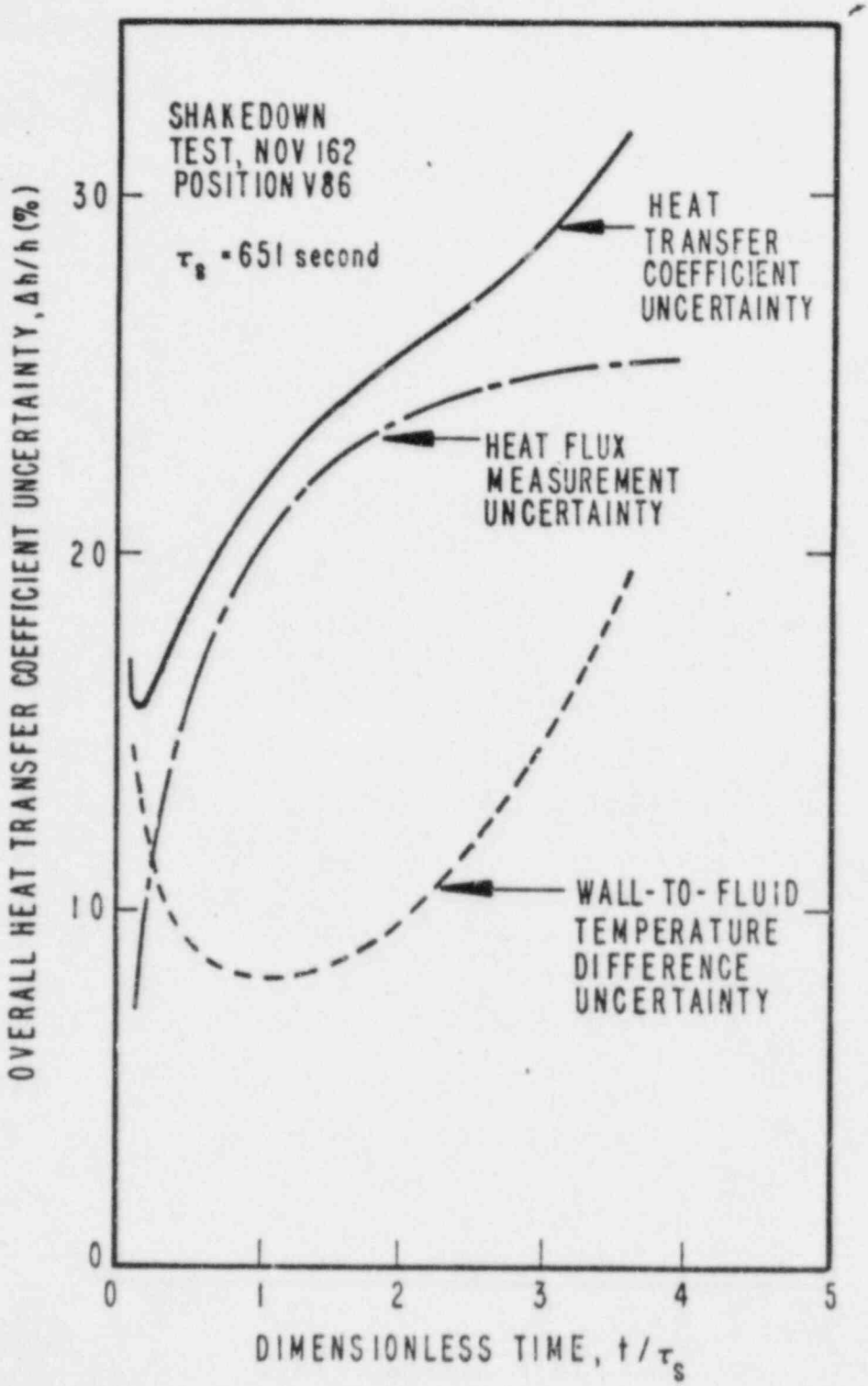

Figure 5-2. Heat Transfer Coefficient Uncertainty for Typical Shakedown Data

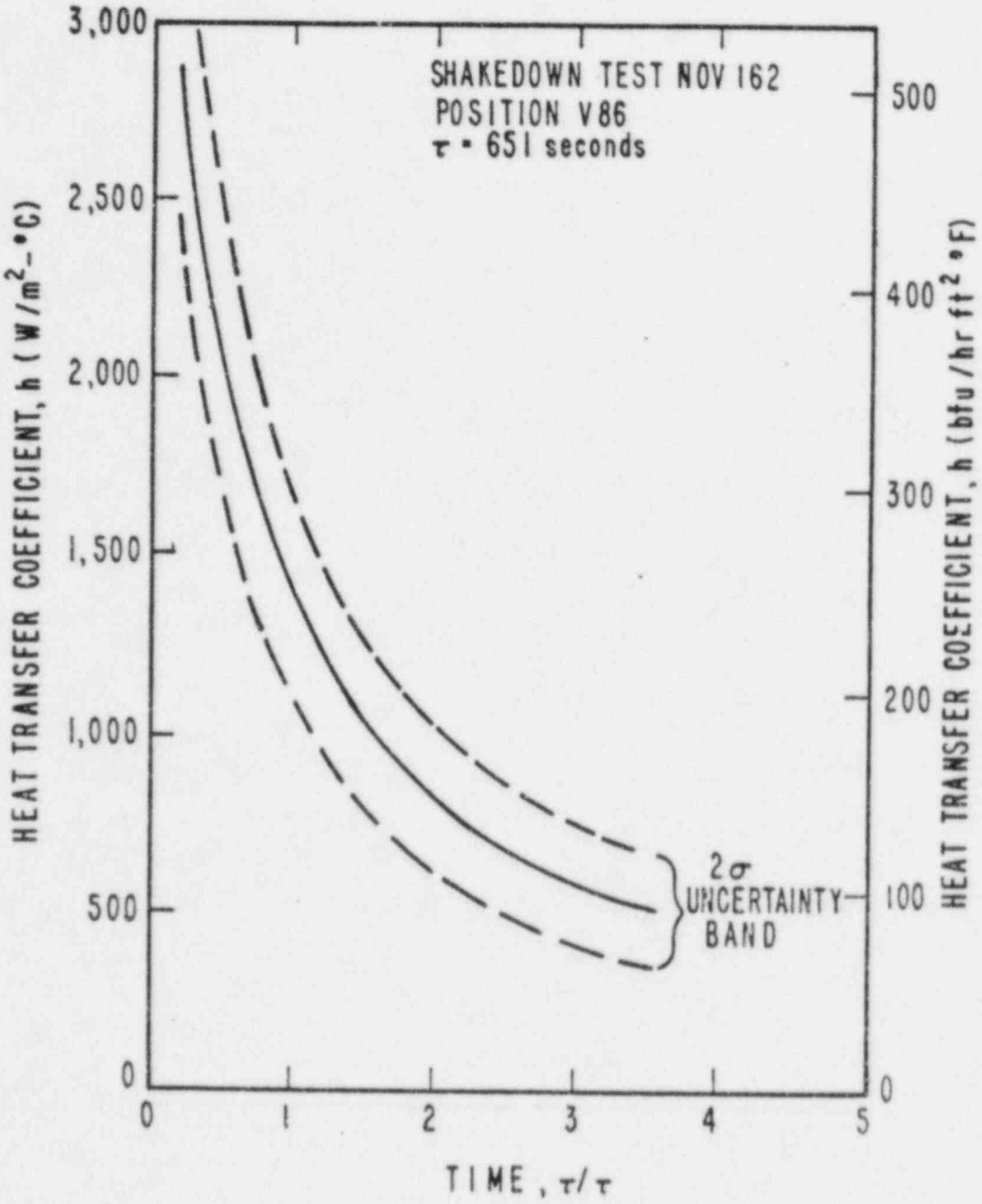

Figure 5-3. Heat Transfer Coefficient for Shakedown Test NOV162

MEAN AND STANDARD DEVIATION

The mean value and standard deviation of primary and derived parameters are calculated for presentation in the Quick Look Report data displays. These are calculated from the conventional definitions:

$$\text{MEAN} = 1/N \sum_{n=1}^{N} (X_n) \tag{5.19}$$

$$\text{STD. DEV.} = \left[\frac{\sum_{n=1}^{N} (X_n)^2 - \frac{\left(\sum_{n=1}^{N} X_n\right)^2}{N}}{N-1} \right]^{\frac{1}{2}} \tag{5.20}$$

where X_n = individual data measurement
N^n = total number of measurements included in the averaging period.

5.2 DATA DISPLAY

The results from each test are presented in a QLR following a standard format for data reduction and display. This section describes the types of data outputs in the QLR and how they are prepared, as a guide to users of the data provided with Reference 19.

5.2.1 Tabular Outputs

Five major tables are included in each QLR as a means of communicating some overall test conditions and test results. These tables are:

Table 1 Geometric Configuration: This table describes the specific geometry for which the QLR data apply. Actual, as-built dimensions and major volumes are listed in the tables along with notes regarding other hardware configurations, e.g. status of thermal shields, vent lines, flow skirt, etc. In addition, several figures are included in the QLR which provide a schematic view of the geometry and instrument locations.

Table 2 Test Conditions: This table lists the nominal and actual values of dimensional test parameters (flows and temperatures) and the dimensionless parameters (F_{CL}, $\Delta\rho/\rho$, flow ratios). The mean value of the measured and reduced parameters are reported along with the standard deviations which provide some measure of the steadiness of the process.

Table 3 Fluid Properties: This table lists the density, viscosity, enthalpy and thermal conductivity of water at the average values of the HPI, loop, vent and mixed mean temperatures.

Table 4 Global Results: Included in this table are the mixing times at the downcomer (below nozzle) and at the standpipe, cold leg quench front and superficial velocities, and downcomer superficial velocities above and within the thermal shield region.

Table 5 Initial and Final Values: This table lists each instrument in the test facility giving the operational status, initial and final values (means and standard deviations over a period equal to 0.1 of the standpipe time constant), minimum and maximum values recorded during the test, and number of times (if any) that the transducer output exceeded the measuring range of the DAS.

5.2.2 Graphical Outputs

Graphical data displays in the QLR take two forms: transient plots and profile plots. The transient plots are used for displaying the time history of primary and reduced data at key selected locations in the cold leg and downcomer, whereas profile plots provide a compact means for directly comparing data at many locations over the duration of the experiment. Each type of plot serves a special purpose, but because the profile plots are a much more efficient means for communicating the large amount of data produced from a test, the QLR emphasizes profile plots. Detailed data analysis is more readily accomplished using computer tapes of the reduced data, rather than point-by-point survey of transient plots.

NORMALIZING FACTORS

The local parameters to be plotted are temperature, velocity, heat flux, and heat transfer coefficient. All transient and profile plots are made dimensionless by use of normalizing factors which relate the plotted data to characteristic test facility dimensions or test conditions. The dimensionless groups thus formed simplify comparisons of data between tests, and may be of use in developing empirical correlations from a large body of experimental data. The normalizing factors used for the data displays are:

a. Time: $t^* = t/\tau_s$ (5.21)

where τ_s is the standpipe mixing time.

b. Temperature: $T^* = (T - T_H)/(T_H - T_L)$ (5.22)

where T_H and T_L are the HPI and loop flow mean temperatures.

c. Cold Leg Velocity: $V_{CL}^* = V/j_{CL}$ (5.23)

where j_{CL} is the cold leg superficial velocity (based on total cold leg flow): $Q_T = (Q_H + Q_L)$.

d. Downcomer Velocity: $V_{DC}^* = V/j_{DC}$ (5.24)

where j_{DC} is the downcomer superficial velocity (based on total downcomer flow): $Q_T = (Q_H + Q_L + Q_V)$.

e. Heat Flux: $q^* = q/[k_w(T_L - T_H)/W]$ (5.25)

where k_w is the metal wall thermal conductivity (50.1 W/m-°C) and W is the nominal metal wall thickness (50.8 mm).

f. Heat transfer coefficient: $Nu = h(2\ S)/k_f$ (5.26)

where k_f is the water thermal conductivity at the local film temperature, and S is the downcomer gap spacing: 0.059 m (0.192 ft) for probes on the vessel wall and 0.041 m (0.133 ft) for probes on the core barrel wall.

g. Distances - all distances are normalized with respect to cold leg diameter, except for the case of gap-wise temperature profiles where the downcomer gap width above the thermal shield, S = 0.137 m (0.45 ft), is used.

TRANSIENT PLOTS

Transient plots at key locations are made in pairs (a and b) which show the data in two time scales. Plot "a" covers the whole test duration and the time scale is normalized to the standpipe time constant. Plot "b" expands the time scale in the first 200 seconds after initiation of HPI, with the time axis plotted directly in seconds. All plots are made dimensionless by the normalizing factors described above.

The types of transient data and corresponding QLR figure numbers are described below:

Figures 3-1(a), 3-1(b) Cold Leg Temperature: Temperatures at the nozzle, injector, pump model and bottom of loop seal. Two thermocouples at each location to show quench front arrival.

Figures 3-2(a), 3-2(b) Cold Leg and Downcomer Velocities: Velocities in the cold leg, downstream of the injector at the top and bottom of the cold leg and at two locations in the downcomer, one on each side of the thermal shield below the nozzle.

Figures 3-3(a), 3-3(b) through 3-7(a), 3-7(b) Downcomer Data: These plots include center-of-gap temperature, dimensionless heat flux and Nusselt number for the vessel and core side measurements at the following downcomer wall locations.

Figure	Distance From Nozzle Centerline (m) Vertical	Horizontal
3-3a,b	-0.406	0
3-4a,b	-0.762	0
3-5a,b	-0.762	0.249
3-6a,b	-0.762	-0.374
3-7a,b	-1.12	0

PROFILE PLOTS

Plot Intervals - Profiles of test data are shown at five different times after HPI injection on a single plot. The time intervals selected include the initial and final profiles and three other profiles in between. The intermediate times are selected so that a well mixed transient having the standpipe time constant τ_s would show equal increments between data sets, as illustrated in the sketch below.

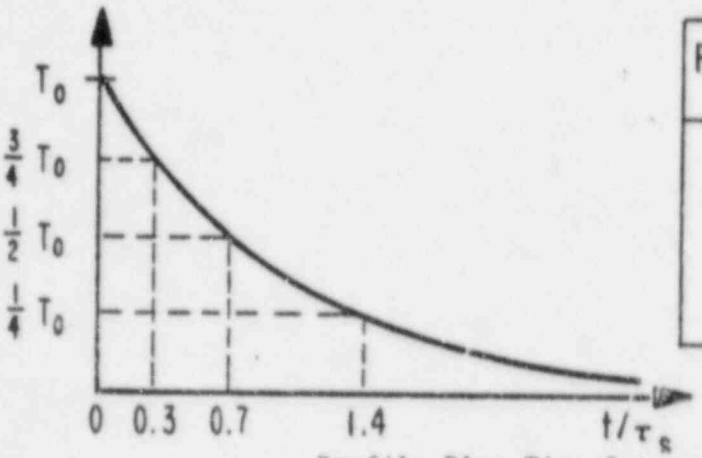

PROFILE	t/τ_s
1	0
2	0.288
3	0.693
4	1.386
5	FINAL

Profile Plot Time Intervals

Data Smoothing - Local data can have random fluctuations of the same order of magnitude as the gradients (differences) which are displayed. Therefore, instantaneous profiles at the selected time increments would be meaningless. For the profile plots, the data are averaged over a period short enough to preserve the main transient behavior yet sufficiently long to smooth out random fluctuations. The initial values (t=0) are obtained from all the data recorded prior to HPI injection (when the process is nominally steady), the intermediate values (t/τ_s=0.3, 0.7, 1.4) are averaged over a period $\pm 0.05\ \tau_s$, and the final values are obtained over the last $0.1\ \tau_s$ of the test.

The specific profile plots which are included in the QLR are described below.

Figure 4-1 Cold Leg Vertical Temperature Profiles: Temperature profiles at the cold leg instrument rakes, locations C1 through C6.

Figure 4-2 Nozzle Vertical Temperature Distribution: Vertical and horizontal temperature variations in the cold leg nozzle, measurement location C5.

Figure 4-3 Cold Leg Vertical Velocity Profile: Velocity profile in the cold leg at measurement location C2, downstream of injector.

Figure 4-4 Downcomer Gap Temperature Distribution: Temperature variations across gap width from vessel wall to core wall at three elevations in the vicinity of the nozzle.

Figures 4-5 through 4-10 Downcomer Horizontal Profiles: Plots of temperature (a), dimensionless heat flux (b) and Nusselt number (c) for both vessel side and core side data, at the 6 vertical locations listed below.

Figure	Vertical Distance Below Instrument Nozzle Centerline (m)	Row
4-5a,b,c	0.41	5
4-6a,b,c	0.77	6
4-7a,b,c	1.13	7
4-8a,b,c	1.50	8
4-9a,b,c	2.22	9
4-10a	3.05	10

Figures 4-11 Downcomer Vertical Profile: Plots of temperature (a), heat flux (b) and Nusselt number (c) in vertical row below nozzle centerline, vessel side and core side data.

5.3 DATA EVALUATION

As a final step in the data reduction process and before release of the final Quick Look Reports, the data are examined for overall consistency and for acceptability according to the acceptance criteria described in Section 4.6. Any instruments which have failed are noted and they are removed from the graphical and tabular outputs. If data from key locations are not available, alternate instrument locations may be used to complete certain data reductions, e.g. substitution of center-of-gap for near-wall temperature in calculation of h, or use of alternate nearby thermocouples for calculation of cold leg transit time.

Finally, test conditions which do not meet specified tolerances are noted and a decision made as to overall test acceptance.

6. REFERENCES

1. Chexal, B., Marston, T. and Sun, Bill K-H. Tackling the Pressurized Thermal Shock Issue. Nuclear Engrg. Int., 27(327), May 1982, pp. 38-42.

2. Rothe, P.H. and Marscher, W.D. Fluid and Thermal Mixing in a Model Cold Leg and Downcomer with Vent Valve Flow. NP-2227, EPRI, March 1982.

3. Rothe, P.H. and Ackerson, M.F. Fluid and Thermal Mixing in a Model Cold Leg and Downcomer with Loop Flow. NP-2312, EPRI, April 1982.

4. Rothe, P.H. and Fanning, M.W. Evaluation of Thermal Mixing Data from a Model Cold Leg and Downcomer. NP-2773, EPRI, Dec. 1982.

5. Rothe, P.H. and Fanning, M.W. Thermal Mixing in a Model Cold Leg and Downcomer at Low Flow Rates. NP-2935, EPRI, April 1983.

6. Fanning, M.W. and Rothe, P.H. Transient Cooldown in a Model Cold Leg and Downcomer. NP-3118, EPRI, May 1983.

7. Valenzuela, J.A. and Rothe, P.H. Flow Visualization During Transient Cooldown in a Model Cold Leg and Downcomer. NP- (Draft for review by EPRI), TM-936, Creare Inc., Aug. 1983.

8. Valenzuela, J.A. and Rothe, P.H. Film Scenario. Mixing of High Pressure Injection Coolant and Stagnant Loop Water in a Model PWR Cold Leg and Downcomer. TM-929, Creare Inc., Nov. 1983.

9. Theofanous, T.G. et.al. Decay of Bouyancy Driven Stratified Layers with Application to Thermal Shock (PTS). NUREG/CR-3700, U.S. NRC, May 1984.

10. Nourbakhsh, H.P. and Theofanous, T.G. Remix: Computer Program For Temperature Transients Due to High Pressure Injection In A Stagnant Loop. NUREG CR-3701, U.S. NRC, 1984.

11. Theofanous, T.G.et. al. Buoyancy Effects on Overcooling Transients Calculated for the USNRC Pressurized Thermal Shock Study. NUREG/CR-3702, U.S. NRC, 1984.

12. Daly, B. Three-Dimensional Calculations of Transient Fluid Thermal Mixing In the Downcomer of the Calvert Cliffs - 1 Plant Using SOLA - PTS. NUREG/CR-3704, U.S. NRC, April 1984.

13. Daly, B. and Torrey, M. SOLA PTS: A Transient 3 - D Algorithm For Fluid Thermal Mixing and Wall Heat Transfer in Complex Geometries NUREG/CR-3822, U.S. NRC, July 1984.

14. Sun, Bill K-H. et. al. The Thermal-Hydraulic Aspects of the Pressurized Thermal Shock Problem. EPRI Program Status. Presented at the U.S. NRC Advanced Code Review Group Meeting, Bethesda, MD, April 21-22, 1982.

15. Rothe, P.H. and Wallis, G.B. Scaling of Thermally Driven Fluid Mixing and Heat Transfer Associated with Pressurized Thermal Shock of Reactor Vessels. NRC/ANS Meeting on Basic Thermal Hydraulic Mechanisms in LWR Analysis, (Bethesda, MD, Sept. 1982), NUREG/CP-0043, U.S. NRC, April 1983, pp. 109-141.

16. Theofanous, T.G. and Nourbakhsh, H.P. PWR Downcomer Fluid Temperature Transients due to High Pressure Injection at Stagnated Loop Flow. NRC/ANS Meeting on Basic Thermal Hydraulic Mechanisms in LWR Analysis, (Bethesda, MD, Sept. 1982), NUREG/CP-0043, U.S. NRC, April 1983, pp. 583-613.

17. Fluid Meters - Their Theory and Application. 6th ed., ASME, 1971.

18. Kline, S.J. and McClintock, F.A. Describing Uncertainties in Single-Sample Experiments. Mechanical Engrg., Jan. 1953, pp. 3-8.

19. Valenzuela, J.A. and Dolan, F.X.; Fluid and Thermal Mixing in 1/2-Scale Test Facility. Vol.2. Data Report. EPRI NP-3802, NUREG/CR-3426 (to be published), TN-384, Creare Inc., Oct. 1984.

20. Powell, R.L. et. al. Thermocouple Reference Tables Based on the IPTS-68. NBS Monograph 125, National Bureau of Standards, March 1974.

21. Meyer, C.A. et. al., eds. ASME Steam Tables. Thermodynamic and Transport Properties of Steam Comprising Tables and Charts for Steam and Water. 4th ed., ASME, 1979.

22. Arpaci, V.S. Conduction Heat Transfer. Reading, MA: Addison-Wesley, 1966.

23. Stearns, S.D. Digital Signal Analysis. Rochelle Park, NJ: Hayden Publ. Co., 1975.

APPENDIX A

UNCERTAINTY IN THE MEASUREMENT OF THE HEAT TRANSFER COEFFICIENT

A.1 SUMMARY

This Appendix reviews the uncertainty in the calculation of the heat transfer coefficient h in the 1/2-scale thermal mixing facility. This uncertainty evaluation is based on the results of the tests NOV162 and NOV111 performed in November of 1983. Because of an unexpected energy addition to the lower plenum during those tests, the values of h given in this Appendix are preliminary. The uncertainty bounds on h developed here are expected to be representative for a test with similar inlet conditions but without the lower plenum energy addition.

The heat transfer coefficient is calculated from the ratio of the local heat flux to the fluid-to-wall temperature difference. As described in Section A.3, heat flux values can be determined with an uncertainty of the order 20% and temperature differences with an uncertainty of the order 10%. The total uncertainty in the heat transfer coefficient ranges from less than 20% early in the test (less than one characteristic mixing time) to 25% towards the end of the test (later than three characteristic mixing times).

In Section A.2 the definition of the heat transfer coefficient is discussed in the light of the available data on temperature distribution across the downcomer gap and high frequency fluctuations in the fluid and wall temperature transients. The uncertainty in the heat transfer coefficient measurement is evaluated in Section A.3.

A.2 DEFINITION OF "h"

The heat transfer coefficient is defined as:

$$h = q''_s / \Delta T_{wf} \qquad \text{(A1)}$$

$$\Delta T_{wf} = T_w - T_f \qquad \text{(A2)}$$

where T_w = wall surface temperature
T_f = fluid temperature
q_g = heat flux at the wall surface

While q''_s is a uniquely defined quantity, ΔT_{wf} is somewhat arbitrary. Not only does the fluid temperature vary with distance from the wall, but also at a given location it changes rapidly with time. Because of the incomplete mixing between the warmer fluid in the downcomer and the partially mixed HPI plume, the fluid temperature in the downcomer exhibits higher frequency fluctuations superimposed on the slower overall transient, as shown in Figure A-1.

The value of h measured in these tests will probably be used to compute the boundary conditions for some computer simulation of the flow in the downcomer. Hence one is interested in the temperature

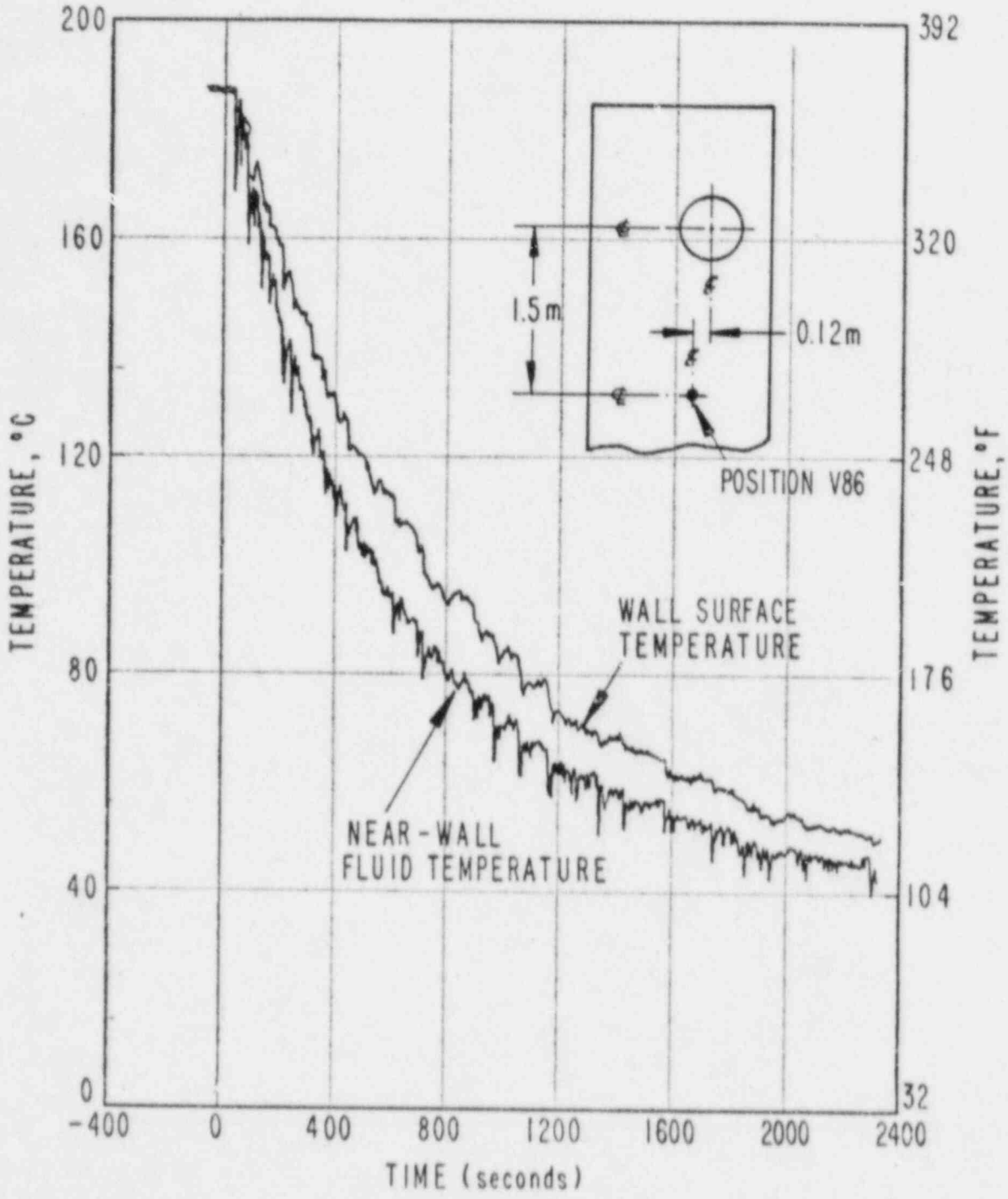

Figure A-1. Transient Data - Shakedown Test NOV162
Wall and Near-Wall Fluid Temperatures

difference averaged over a period of time that is short when compared to the mixing time of the facility, but long when compared to the turbulent fluctuations and the measuring instrument rise time. Fortunately, the characteristic mixing times are at least an order of magnitude longer than the period of the fluctuations and a meaningful time averaged temperature difference can be easily obtained by filtering the data through a zero phase shift, low-pass filter.

The flow in the downcomer is highly turbulent and the gap-wise temperature profile is expected to be flat. Indeed, temperature measurements made at the center of the gap (CTC) are practically indistinguishable from those made about one quarter of the gap width away from the wall (FTC). As shown in Figures A-1 and A-2, even the detailed structure of the transient is the same at both locations. Therefore, either temperature measurement can be used to compute the heat transfer coefficient. (The redundant temperature measurement reduces the probability of lost data due to instrument malfunction.)

A.3 MEASUREMENT UNCERTAINTIES

Since h is not a directly measured quantity, its uncertainty must be computed from the measurement uncertainties of q''_s and ΔT_{wf}. In general, the uncertainty in a parameter Y computed from a set N of independent measurements X_i is given by:

$$\frac{\Delta Y}{Y} = \left(\sum_{i=1}^{N} \left[\left(\frac{X_i}{Y} \right) \left(\frac{\partial Y}{\partial X_i} \right) \left(\frac{\Delta X_i}{X_i} \right) \right]^2 \right)^{1/2} \qquad \text{(A3)}$$

Hence, the uncertainty in the heat transfer coefficient can be expressed as:

$$\frac{\Delta h}{h} = \left[\left(\frac{\Delta q''_s}{q''_s} \right)^2 + \left(\frac{\Delta(\Delta T_{wf})}{\Delta T_{wf}} \right)^2 \right]^{1/2} \qquad \text{(A4)}$$

where $\Delta q''_s/q_s$ and $\Delta(\Delta T_{wf})/\Delta T_{wf}$ are the fractional uncertainties in the heat flux and temperature difference measurements.

A.3.1 Wall-to-Fluid Temperature Difference

Figure A-3 shows a sketch of the heat flux probe and the fluid and wall temperature measurement locations. The metal and fluid temperatures are measured independently and then subtracted in the data reduction process to obtain the temperature difference. Typical temperature differences range from 5 to 15°C, as shown in Figure A-4.

There are four sources of error in the temperature difference measurement:

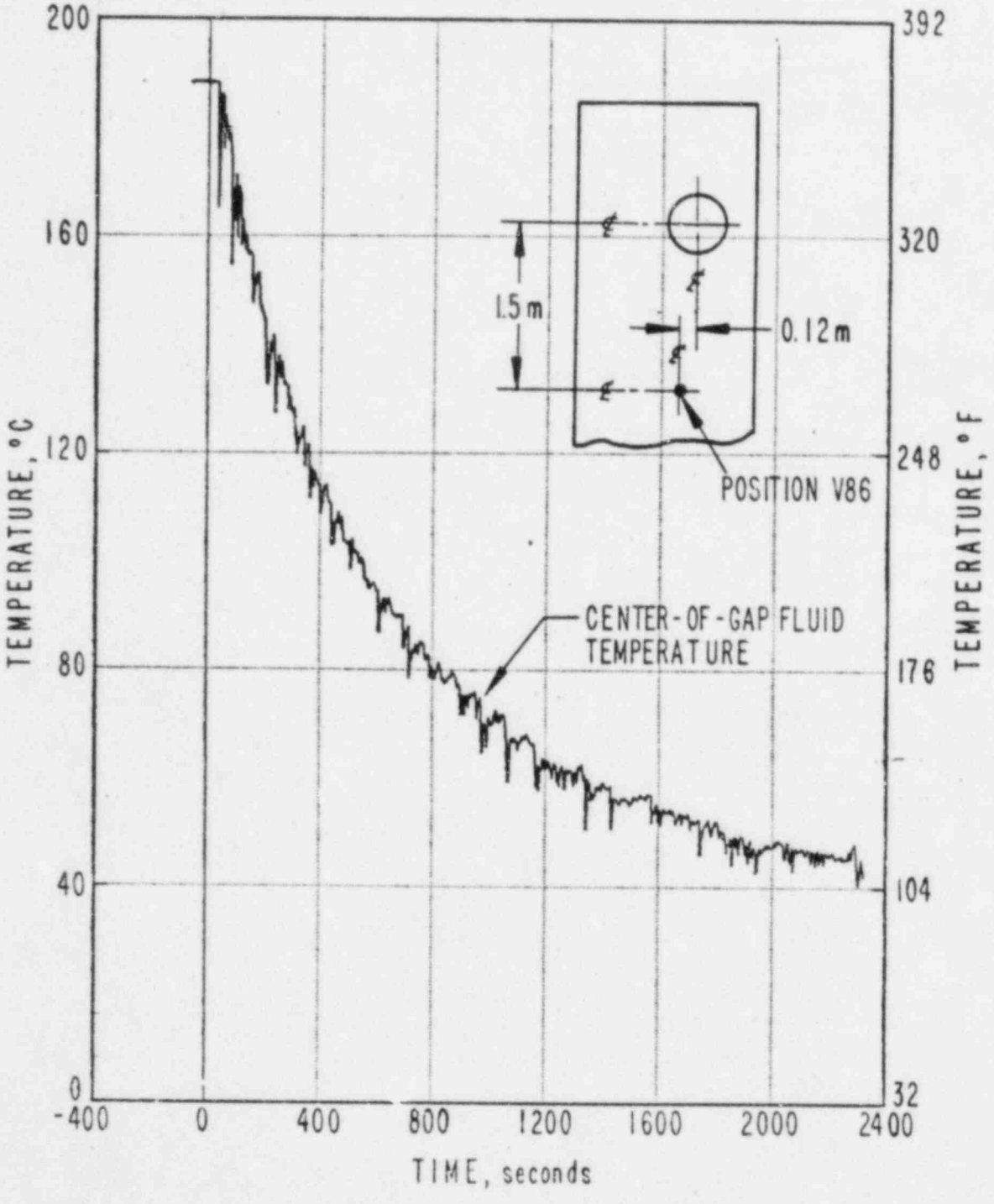

Figure A-2. Transient Data - Shakedown Test NCV162
Center-of-Gap Fluid Temperature

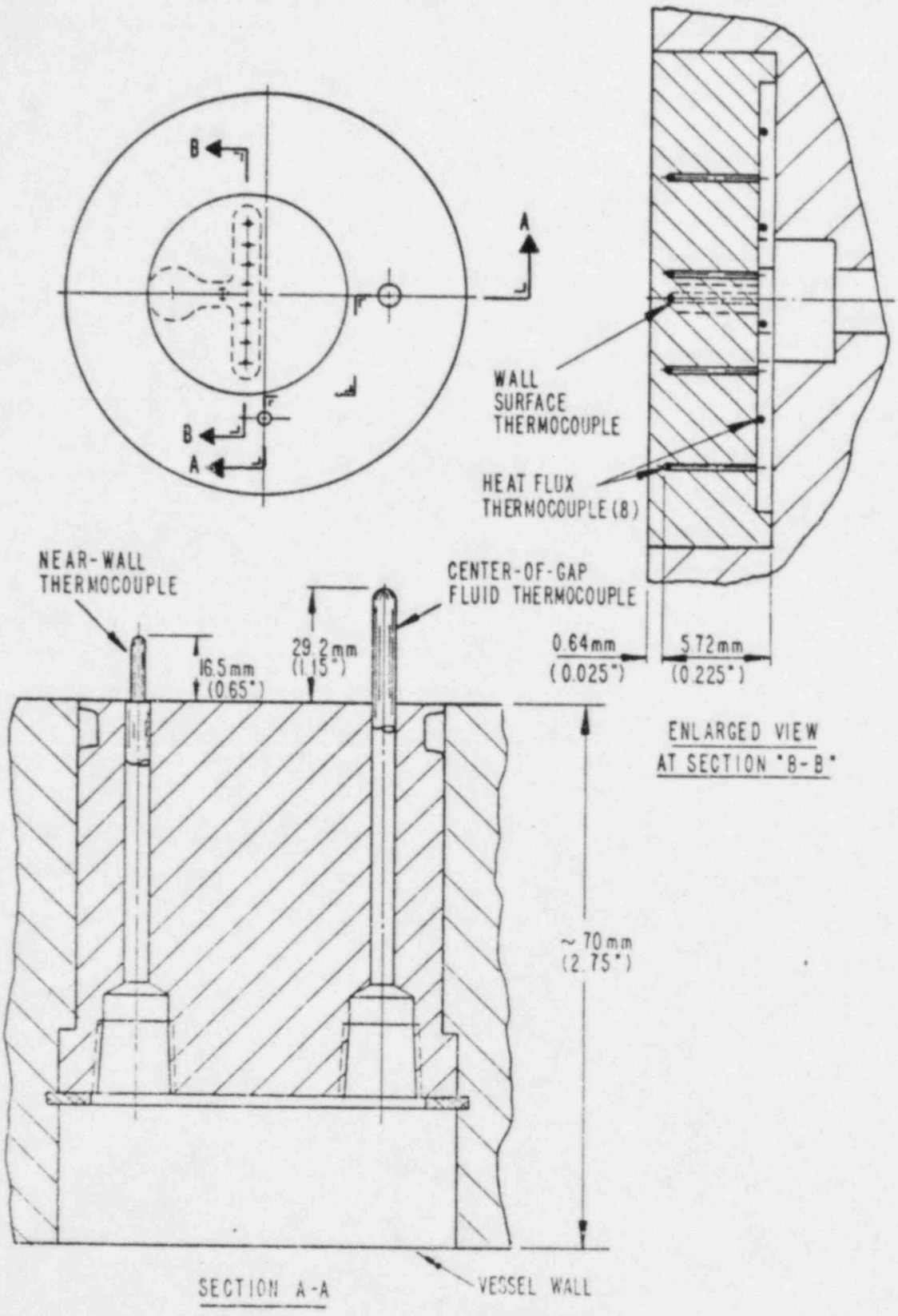

Figure A-3. Vessel Wall Heat Flux Probe
with Typical Fluid Temperature Probes

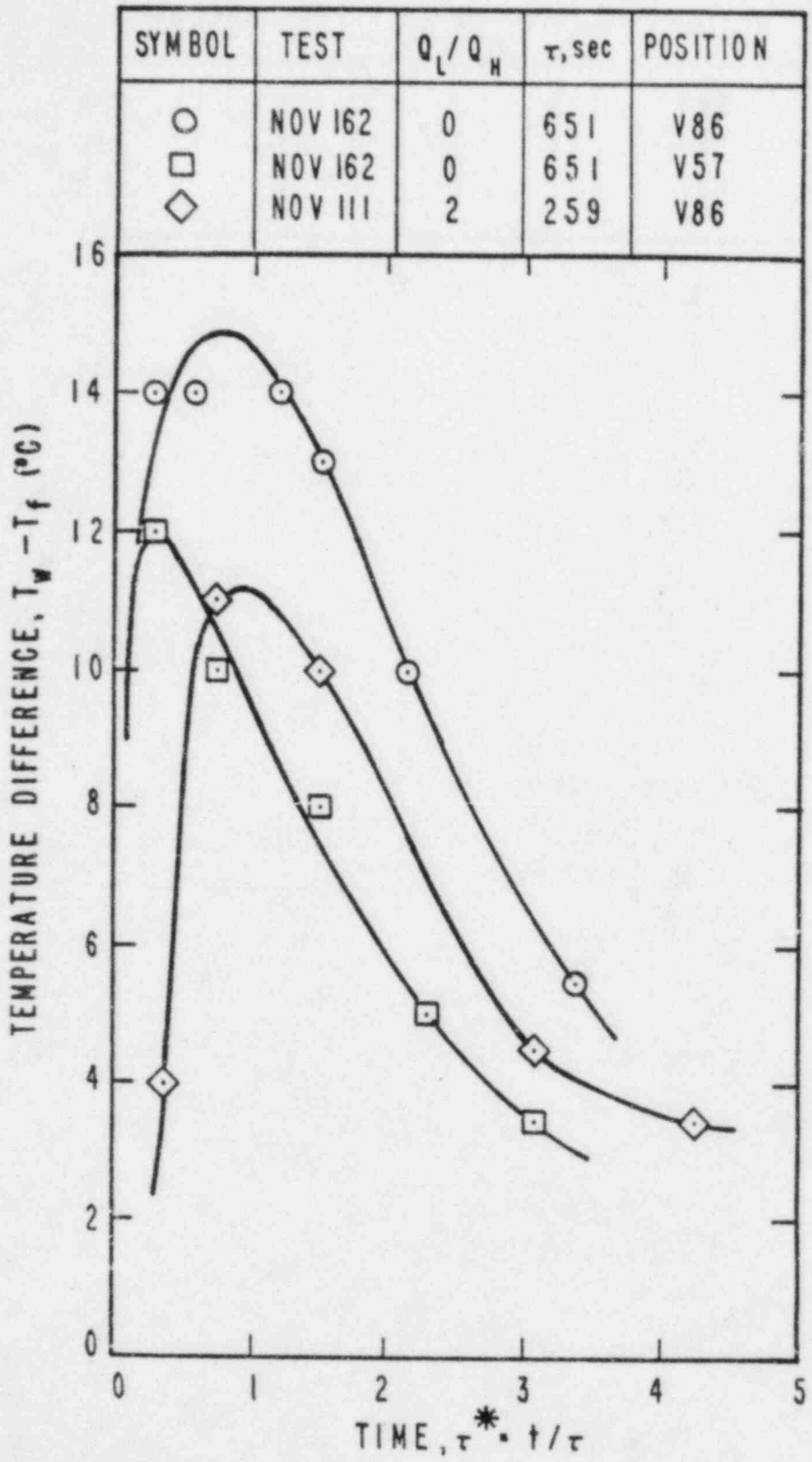

Figure A-4. Typical Wall-to-Fluid Temperature Difference

- metal and fluid thermocouple offset,
- stem conduction in fluid thermocouple,
- wall temperature gradient, and
- phase lag between fluid and metal temperature measurements.

The contribution of each type of error to the overall uncertainty in the temperature difference measurement is discussed in turn below.

Thermocouple Offset. Before starting each test, warm water is circulated through the facility until thermal equilibrium is reached. Data are recorded for approximately 60 seconds before HPI injection commences. During that pretest period, the facility is practically isothermal (within 1°C) and that provides an in-situ calibration point for the fluid and wall thermocouples. The observed 1°C deviation from equilibrium is in line with the estimated random uncertainty of the thermocouples.

In the data reduction, the wall-to-fluid temperature difference is set to zero at the beginning of the test. That introduces a small positive bias since the wall temperature should be slightly lower than the fluid temperature because of heat loss through the outer insulation. That bias, however, must be less than the observed initial scatter of 1°C.

Later in the test, the temperature level decreases and the random uncertainty associated with the thermocouple measurements decreases as well. Therefore an uncertainty of 1°C bounds the possible systematic bias as well as the random uncertainties in the thermocouple measurements.

Stem Conduction. The data reduction programs currently use the near wall thermocouple (FTC) to compute the temperature difference. That thermocouple is housed in a 1.6 mm (1/16 inch) stainless steel sheath which protrudes into the fluid 16.5 mm (0.65 inch) on the vessel side and 11.4 mm (0.45 inch) on the core side. Heat conduction through the stem introduces a systematic negative error on the temperature difference. This bias is small, of the order of 2% of the fluid-to-wall temperature difference.

Wall Gradient. As shown in Figure A-3, the metal thermocouple is 0.63 mm (0.025 inch) below the wall surface. On average, the thermocouple temperature will be slightly higher than the surface temperature since heat is flowing from the wall to the fluid. The magnitude of this systematic error can be computed (and a correction made if necessary) from the measured transient heat flux:

$$\Delta T_g = q''_s \, \delta / k \qquad \text{(A5)}$$

where δ is the distance to the surface (0.63 mm) and k is the wall thermal conductivity (50 W/m-°C).

Peak heat fluxes near the beginning of the test are of the order of 30,000 W/m^2 giving a peak error of about 0.4°C, while near the end of a test the wall gradient error will be less than 0.1°C.

Phase Lag Error. Measurements are recorded sequentially by the DAS with each channel being recorded once in each one second period. Therefore, for a given data scan the fluid and metal temperatures could be measured up to one second apart.

Since both the fluid and the metal temperatures are changing with time, this phase lag introduces a measurement error. The magnitude of the error is proportional to the rate of change of the temperatures.

The high frequency fluctuations shown in Figure A-1 have rates of change of about 10°C/s. The measurement lag can therefore introduce large errors into the temperature difference measurement. These errors are random and will not change the average value of the temperature difference. They will only introduce artificial scatter into the data.

However, as mentioned earlier, for the computation of h one is interested in the temperature difference averaged over a longer period of time. Therefore, if the temperature data are filtered with a zero phase shift filter having a cutoff period equal to a tenth of the characteristic mixing time, the phase lag error is reduced to less that 0.35°C.

Overall Measurement Uncertainty. The overall uncertainty in the temperature difference depends on the magnitude and sign of the errors and on the magnitude of the temperature difference. The fractional uncertainty is given by:

$$\frac{\Delta(\Delta T_{wf})}{\Delta T_{wf}} = \frac{1}{\Delta T_{wf}} \left[(\Delta T_o + \Delta T_g - \Delta T_s)^2 + (\Delta T_\ell)^2\right]^{1/2} \qquad \text{(A6)}$$

where: ΔT_o = offset error
ΔT^g = wall temperature gradient error
ΔT^s = stem conduction error
ΔT_ℓ = phase lag error

Typical wall-to-fluid temperature differences from tests NOV162 and NOV111 are shown in Figure A-4. They range between 5 and 15°C. The measurement uncertainty computed from Equation (A6) ranges between 10 and 20 percent throughout most of the test duration, as shown in Figure A-5. The key uncertainty source is the offset error, which is less significant than the heat flux uncertainty discussed below.

A.3.2 Heat Flux Measurement

Heat flux values can be determined in three ways:

1) performing an energy balance on the downcomer wall over the duration of the test, (based on inner and outer temperature measurements),

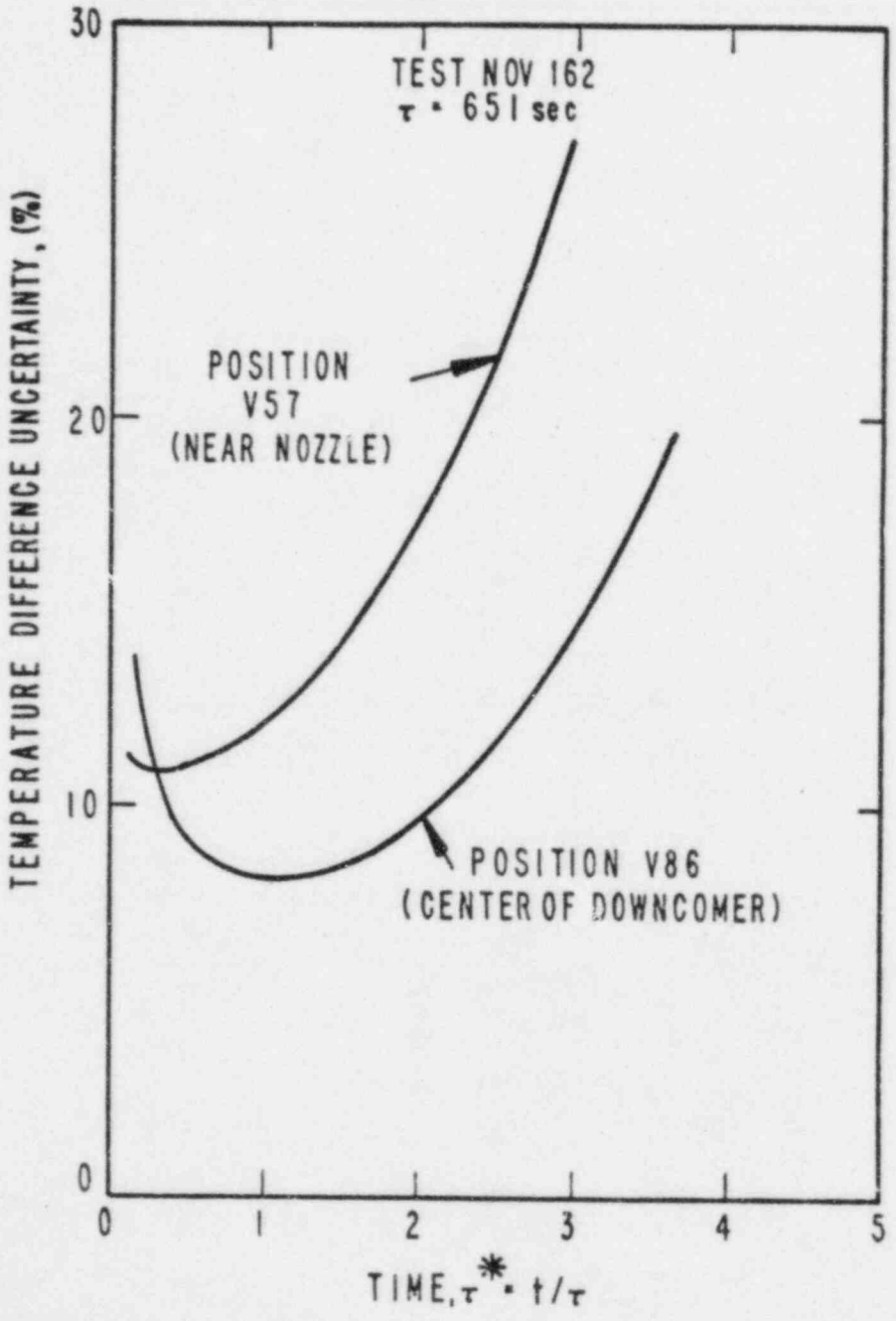

Figure A-5. Overall Uncertainty in Wall-to-Fluid Temperature Difference

2) solving the one-dimensional heat conduction equation using the wall surface temperature measurement, and

3) using the heat flux probe measurement of the temperature gradient near the wall surface.

The energy balance is quite precise (±5%) when averaged over the term of the test, but contains little transient information. It is used primarily as a check on the average accuracy of the other, transient methods. The one-dimensional conduction approach follows the main transient well and has uncertainty of the order of 20 to 30%. This method is the primary basis for the data reduction and display. The heat flux meters follow the high frequency fluctuations closely and are most characteristic of the true transient. However, when the fluctuations are averaged, they show a significant bias (average values greater than computed from the energy balance on the wall).

A.3.2.1 Heat Flux Data Reduction

The heat flux probes were developed to provide a more direct measure of the heat fluxes, without requiring elaborate data reduction procedures. It was recognized at the time that, if necessary, the heat flux could also be obtained by solving the transient heat conduction equation for the metal wall, using the measured wall surface temperature as a boundary condition. As described below, a relatively simple algorithm was developed to obtain the heat flux values from the wall temperature measurements with an overall uncertainty of about 25 percent.

Three assumptions were made in developing this data reduction procedure:

- one-dimensional heat conduction,
- adiabatic boundary condition on the outside surface of the downcomer wall, and
- constant metal properties.

As explained below, and detailed in later calculations, these assumptions do not introduce large uncertainties in the computed heat fluxes.

Under these assumptions, the transient heat conduction equation for the downcomer wall can be solved in closed form using Duhamel's superposition integral (A.1). Formally, the heat flux can be expressed in terms of the measured wall surface temperature as:

$$q_g(t) = \frac{-2k}{L} \int_0^t \left[\sum_{n=0}^{\infty} \exp\left[-\alpha \lambda_n^2 (t - s)\right] \right] \frac{\partial T_w(s)}{\partial s} ds \qquad (A7)$$

where: k = wall thermal conductivity
L = wall thickness
α = wall thermal diffusivity
λ_n = $\pi(2n+1)/2L$ eigen values
t^n = time after HPI injection
T_w = wall surface temperature

Equation A7 is evaluated by conventional numerical methods to obtain the wall surface heat flux q''_s. The heat transfer coefficient is obtained from the earlier definition

$$h = \frac{q''_s}{T_w - T_f} \tag{A8}$$

Prior to reducing the data, the wall and fluid temperature data are filtered to remove high frequency components which may introduce phase lag errors into the computation of h. A low pass, zero-phase-shift filter is used for this purpose (A.2). The filter selected for the data processing has a cutoff frequency of 0.05 Hz which corresponds to an averaging period of 20 seconds. This period is short relative to characteristic mixing times so the behavior of the main transient will be preserved, but phase lag errors will be greatly reduced.

A.3.2.2 Heat Flux Uncertainty

There are five main sources of uncertainty in the calculation of the heat flux:

- probe geometry (effective wall thickness),
- surface temperature measurement,
- two-dimensional heat conduction along the wall,
- energy loss from outer surface, and
- variations in metal properties.

In order to evaluate the relative magnitude of each source of uncertainty, we have analyzed in some detail the data from one location for the shakedown test NOV162. That test was a transient cooldown ($Q_L = 0$) with $F_{CL} = 0.0785$ and $\Delta\rho/\rho = 0.12$. We chose the measuring position V86, located on the vessel side, near the center of the downcomer. Because the temperature transients in the downcomer are fairly uniform, these results are believed to be representative of the conditions throughout most of the downcomer.

The heat flux at this location, computed from the surface temperature transient, was used in the evaluation of the five sources of uncertainty in the heat flux calculation. Each source of uncertainty is discussed in turn below.

Probe Geometry. Figure A-3 shows a sketch of the heat flux probe installed in the downcomer wall. There is a 19 mm difference in thickness between the heat flux probe and the surrounding downcomer wall. The probes were machined to the nominal wall thickness of 51 mm, while the downcomer walls were made from 76 mm plate and for

structural reasons had only enough metal removed to make them flat. Because of the local difference in wall thickness, the heat flux will be somewhat lower at the probe location then in the main body of the wall.

The effective wall thickness at the probe location will be somewhere between the two extremes of the probe thickness (51 mm) and the wall thickness (70 mm). By using the average value of 60 mm the uncertainty in the wall thickness is 16 percent. The resulting uncertainty in the heat flux calculation was computed by using the three thickness values (51, 60, and 70 mm) in Equation A7, and is shown in Figure A-6. Initially the uncertainty contribution is small since it takes some time for the transient to propagate to the outside wall. At times greater than one mixing time, the uncertainty in the heat flux calculation attributable to the probe geometry is of the order of 20 percent.

Surface Temperature Measurement. There are two errors associated with the surface temperature data. One is related to uncertainty in the measurement of the temperature itself (i.e. thermocouple calibration uncertainty and DAS measurement uncertainty) and the other is related to the position of the thermocouple bead relative to the wall surface. Both errors are small; the measurement uncertainty is less than 1°C and the error due to probe position (wall gradient) was shown earlier to be less than 0.4°C.

The average heat flux is proportional to the total temperature decrease of the wall over the test duration. Hence, the average uncertainty in heat flux calculation due to the error in the surface temperature measurement will be equal to the uncertainty in the measurement of the total temperature drop. That uncertainty is less than 1% for transient cooldown tests where the total temperature drop is about 150°C, and 1% to 3% for tests with loop flow (smaller total temperature drop). Since the wall temperature data is filtered to remove random fluctuations, the uncertainty in the instantaneous heat flux measurement associated with the surface temperature measurement error will be comparable to the average uncertainty. Two-Dimensional Effects. The instantaneous temperature distribution in the downcomer is not completely uniform. There is a somewhat colder region in the vicinity of the cold leg nozzle. Heat will be conducted into this region from the warmer surrounding regions. Therefore, near the nozzle heat conduction is not truly one-dimensional.

The magnitude of these two-dimensional effects can be estimated from the wall temperatures measured in the previous tests. Temperature nonuniformities are greatest during the early part of transient cooldown tests. Even in that situation, the net effect of conduction in the plane of the wall is only 700 W/m^2, less than 5% of the average heat flux during the test, and relevant mainly near the cold leg nozzle.

Heat Loss from Outer Surface. The energy loss through the insulation can be estimated as:

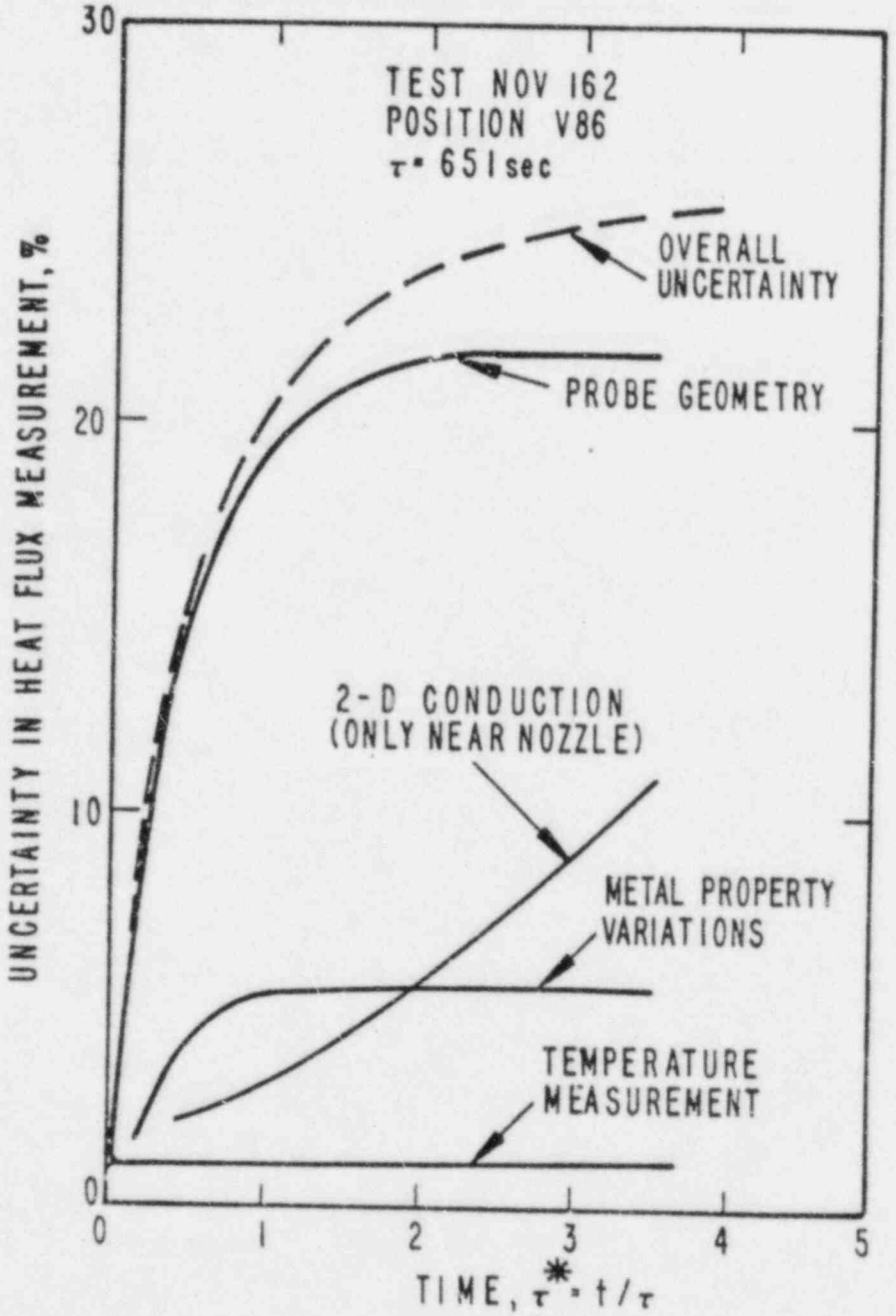

Figure A-6. Heat Flux Measurement Uncertainty Contribution

$$q''_i \leq \frac{k_i}{L_i} (T_w - T_a) \qquad (A9)$$

where k_i and L_i are the insulation thermal conductivity and thickness respectively, and T_a is the ambient temperature.

The maximum heat loss (at the beginning of the test) is less than 200 W/m^2. This loss is two orders of magnitude lower than the average heat flux on the inside wall and can be neglected.

Metal Properties. The data reduction algorithm assumes that the metal properties are uniform across the wall and do not change with temperature. This is a reasonable assumption for carbon steels. In the range of temperatures experienced by the facility (25 to 200°C), the thermal conductivity remains within 3.2 % of its average value and the specific heat within 4.8%. In order to estimate the uncertainty associated with the change in properties, the heat flux at location V86 was reduced three times using the properties at 25°C, 200°C, and the average properties. As shown in Figure A-6, the combined changes in properties introduce an uncertainty in the heat flux calculation of about 5 percent. This uncertainty is much smaller than that associated with the probe geometry and therefore it does not contribute significantly to the overall uncertainty.

Overall Measurement Uncertainty. The various sources of uncertainty in the heat flux calculation are independent and therefore the total uncertainty is given by:

$$\frac{\Delta q''_s}{q''_s} = \frac{1}{q''_s} \left(\Delta q_g^2 + \Delta q_t^2 + \Delta q_{2_{2-d}} + \Delta q_p^2 \right)^{1/2} \qquad (A10)$$

where Δq_g = heat flux uncertainty due to probe geometry
Δq_t = heat flux uncertainty due to surface temperature measurement
Δq_{2-d} = heat flux uncertainty due to two-dimensional heat conduction
Δq_p = heat flux uncertainty due to variable metal properties

The overall uncertainty in the heat flux measurement is also shown in Figure A-6. The total uncertainty is less than 20 percent during the early part of the test ($t/\tau<1$) and approaches 26 percent late in the test.

A.3.3 Heat Transfer Coefficient Uncertainty

Figure A-7 shows the estimated heat transfer coefficient uncertainty obtained from Equation A4. The uncertainty ranges from 16% early in the test to about 30% towards the end of the test (3.5 mixing times).

These results were obtained from the data at one location (V86) in a transient cooldown test (NOV162). The uncertainty may vary somewhat

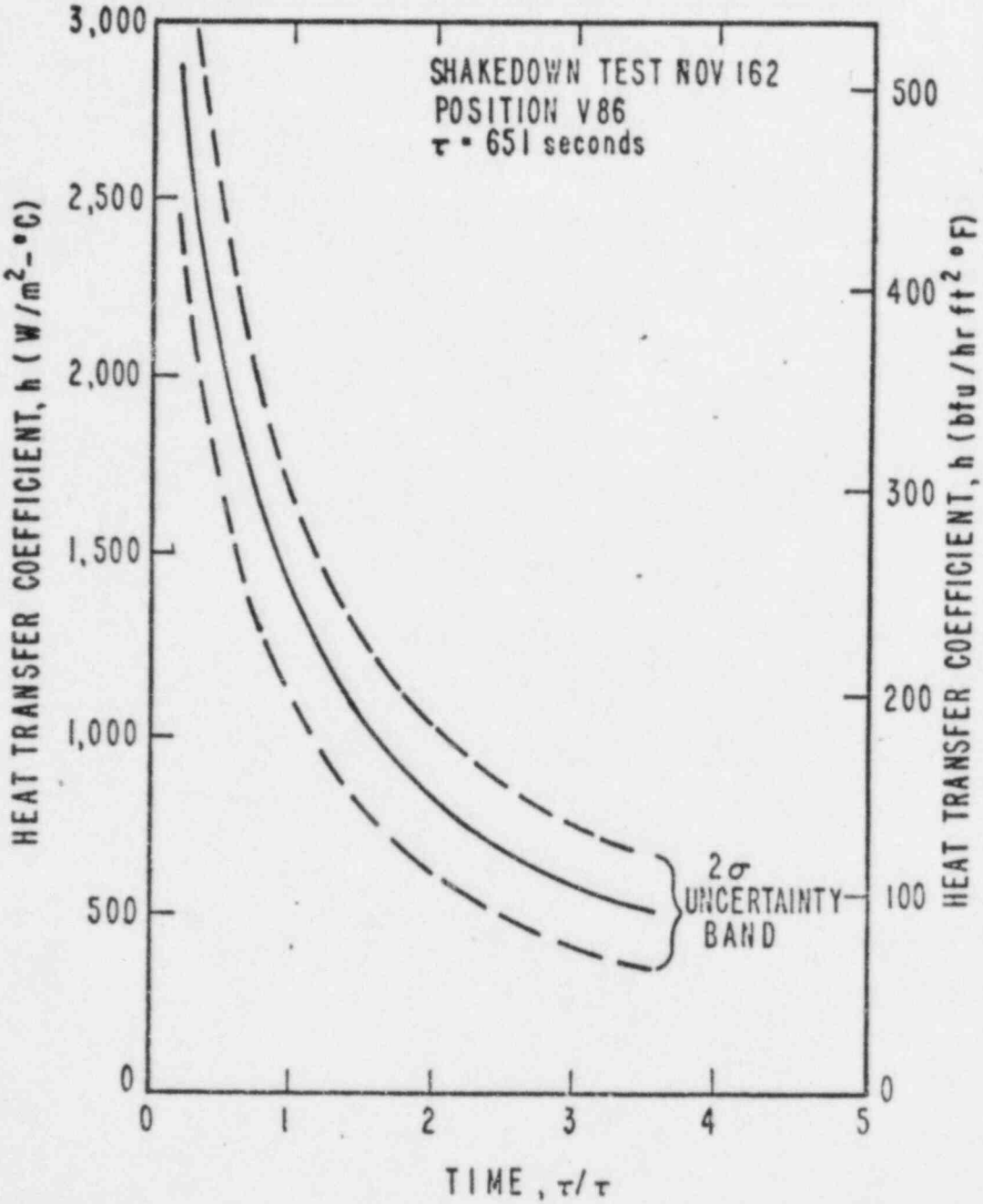

Figure A-7. Heat Transfer Coefficient for Shakedown Test NOV162

with location and flow conditions. However, the difference will be small. The major contributor to the uncertainty is the probe geometry and that remains fixed.

REFERENCES

A.1 Arpaci, V.S. Conduction Heat Transfer. Reading, MA: Addision-Wesley, 1966.

A.2 Stearns, S.D. Digital Signal Analysis. Rochelle Park, NJ: Hayden Publ. Co., 1975.

NRC FORM 335 (7-77)

U.S. NUCLEAR REGULATORY COMMISSION

BIBLIOGRAPHIC DATA SHEET

1. REPORT NUMBER (Assigned by DDC)
NUREG/CR-3426, Vol. 1
EPRI Nr-3802
Creare TN-384

4. TITLE AND SUBTITLE (Add Volume No., if appropriate)

Thermal and Fluid Mixing in 1/2-Scale Test Facility
(Facility and Test Design Report)

2. (Leave blank)

3. RECIPIENT'S ACCESSION NO.

7. AUTHOR(S)

F. X. Dolan, J. A. Valenzuela

5. DATE REPORT COMPLETED
MONTH: January YEAR: 1985

9. PERFORMING ORGANIZATION NAME AND MAILING ADDRESS (Include Zip Code)

Creare Incorporated
Etna Road
Hanover, NH 03755

DATE REPORT ISSUED
MONTH: September YEAR: 1985

6. (Leave blank)

8. (Leave blank)

12. SPONSORING ORGANIZATION NAME AND MAILING ADDRESS (Include Zip Code)

Division of Accident Evaluation
Office of Nuclear Regulatory Research
U.S. Nuclear Regulatory Commission
Washington, D.C. 20555

10. PROJECT/TASK/WORK UNIT NO.

11. CONTRACT NO.

A4070

13. TYPE OF REPORT

Technical

PERIOD COVERED (Inclusive dates)

September 1982 through October 1984

15. SUPPLEMENTARY NOTES

14. (Leave blank)

16. ABSTRACT (200 words or less)

This report describes the test facility and program designed to measure fluid mixing and heat transfer in a 1/2-scale model of the cold-leg downcomer and lower plenum of a pressurized water reactor under conditions of interest to the issues of pressurized thermal shock. Several cold-leg assemblies are modeled and the downcomer arrangement can be altered to match vendor-specific configurations. The facility can be operated to model flow rates based on Froude number of the injected flow in the cold-leg and with steady or transient inlet boundary conditions. Extensive instrumentation is provided to measure flow rates, temperatures and pressure at the facility boundaries and for detailed measurements of temperature, velocity and heat transfer data in the cold-leg and downcomer models. The test data are monitored and recorded by a computer data acquisition system that is also used for post-test data reduction and plotting.

The planned test matrix includes 75 tests with variations in cold-leg and downcomer geometries, loop and HPI flow rates, cold-leg Froude number and loop to HPI density difference. Test results will be reported in a series of Quick-Look Reports.

17. KEY WORDS AND DOCUMENT ANALYSIS

17a. DESCRIPTORS

Froude Number
Thermal Fluid Mixing
HPI Jet
Buoyant Plumes

17b. IDENTIFIERS/OPEN-ENDED TERMS

18. AVAILABILITY STATEMENT

Unlimited

19. SECURITY CLASS (This report)
Unclassified

21. NO. OF PAGES

20. SECURITY CLASS (This page)
Unclassified

22. PRICE
$

UNITED STATES
NUCLEAR REGULATORY COMMISSION
WASHINGTON, D.C. 20555

cover 4